Probabilistic estimation of fatigue loads on monopile-based offshore wind turbines

- Application to sensitivity assessment & clustering optimization for support structure cost reduction -

Master of Science Thesis

Author:	Lisa Ziegler	
Supervisors:	Prof. Dr. A.V. Metrikine	TU Delft - Chairman
	Dr. E. Lourens	TU Delft
	Prof. Dr. M. Muskulus	NTNU
	S. Schafhirt	NTNU
	Dr. S.N. Voormeeren	Siemens Wind Power
	R. Haghi	Siemens Wind Power
	E. Smid	Siemens Wind Power

May 12, 2015

NTNU – Trondheim
Norwegian University of Science and Technology

SIEMENS

TU Delft Delft University of Technology

Abstract

Offshore wind energy faces three important trends: (1) wind farms grow in size, (2) monopiles are installed in deeper water, and (3) cost reduction remains the most important challenge. With wind farm size, the importance of variations in environmental site conditions across the wind farm increases. These site variations, e.g. water depth and soil conditions, can lead to significant differences of loads on support structures.
For monopiles in deeper water, design is dominated by wave-induced fatigue loads. Since full fatigue load calculations are computationally demanding, they can typically not be performed for each turbine within large wind farms. Therefore, turbines must be grouped into clusters in early project phases, making time-efficient approaches essential. Optimization of design clustering is necessary to reduce design conservatism and the cost of offshore wind energy.
Hence, the goal of this thesis is to investigate load site variations and clustering. Therefore, a probabilistic fatigue load estimation method is developed and verified with aeroelastic simulations in the time domain. Subsequently, the developed method is applied for an exemplary wind farm of 150 turbines in 30-40m water depth to perform

- sensitivity studies of loads to changes in MSL, soil stiffness, and wave parameters,
- probabilistic assessments of data, statistical and model uncertainties, and
- deterministic and probabilistic design clustering.

The estimation method is based on frequency domain analysis to calculate wave-induced fatigue loads, a scaling approach for wind loads, combination of wind-wave loads with quadratic superposition, and Monte-Carlo simulations to assess uncertainties. Verification confirms an accuracy of 95% for lifetime equivalent fatigue loads compared to time domain simulations. The computational speed is in the order of 100 times faster than typical time domain tools. Sensitivity studies show a significant influence of water depth and wave period on EFLs. The influence of soil on EFLs is minor for high soil stiffness but can increase significant for soils with low stiffness. Normal distributed input parameters in a probabilistic assessment yield a positively skewed probability distribution of EFLs. Design clustering is optimized based on site-specific fatigue loads using brute-force and discrete optimization algorithms. Results for the exemplary wind farm show a design load reduction of up to 13% compared to standardized design. Probabilistic clustering proved to be only relevant at cluster borders leading to a difference in allocation for 12 out of 150 turbines.
Project results show that it is essential to account for load differences in large wind farms due to varying site conditions. This study improves clustering and provides a basis for design optimization and uncertainty analysis in large wind farms. Further work is needed to extend tool verification and formulate design clustering for cost optimization.

Acknowledgements

Many people have contributed to the success of this project with their experiences, ideas and recommendations. In particular, I want to thank:

Prof. Michael Muskulus for the guidance on this project from NTNU. Thanks for making it possible for me to attend the DeepWind'2015 R&D conference and to submit two scientific papers. I can honestly say that your support had a big impact on the success of this thesis - and on my decision to stay with research in the coming years. Thanks also to **Sebastian Schafhirt** from NTNU for your great help with computations and reporting. It's a pleasure to come back to Trondheim and the offshore wind group soon.

Prof. Andrei Metrikine and **Eliz-Mari Lourens** who supervised my thesis from TU Delft's end. Thanks for your advice and always pushing the "physical meaning" in focus. And who knows, we may have some interesting discussions about Structural Health Monitoring in the future.

My supervisors from Siemens Wind Power for their support. Thanks to **Sven Voormeeren** who initiated this project. I appreciate our discussions, feedback and the big chunk of time you invested in my thesis. I want to thank **Rad Haghi** who not only supervised my work, but also set up many BHawC simulations so that I could verify my estimation tool. Thanks a lot also to **Erik Smid** for sharing your extensive experiences in load analysis with me and answering all my questions. Thank you, all three, for reading and correcting my report - that cannot be taken for granted! Finally, thanks to all my **Siemens and study colleagues** for always helping when needed. The offshore wind community is small - I am looking forward to meet you guys again in the future.

My parents who are just awesome. Danke, dass ihr immer da seid, egal wie viele Kilometer zwischen uns liegen.

Contents

List of Figures

List of Tables

Nomenclature

Latin symbols

b	wind amplitude	m/s
c	airfoil chord length	m
C	structural damping	Ns/m
C_D	drag coefficient	$-$
C_L	lift coefficient	$-$
C_M	inertia coefficient	$-$
d	water depth	m
dt	time step	s
D	damage	$-$
D	diameter	m
D_i	Dirlik's constant	$-$
e	average Monte-Carlo error	$-$
E	expected value	$-$
EFL	equivalent fatigue load	N, Nm
f	frequency	Hz
f_{drag}	drag force	N/m
$f_{inertia}$	inertia force	N/m
f_p	wave peak frequency	Hz
F	areo- or hydrodynamic force	N
F_D	drag force	N
F_L	lift force	N
g	gravitational acceleration	m/s^2
H	transfer function	$m/N, m/Nm$
H_S	significant wave height	m
k	wave number	rad/m
K	structural stiffness	N/m
L	length scale	m
L	load range	N, Nm
m	Woehler slope	$-$
m_n	n$^{\text{th}}$ spectral moment	$[unit]^2/s^n$

M	structural mass	kg
n	number of seeds or load ranges	$-$
N	number of cycles	$-$
N	number of Monte-Carlo simulations	$-$
p	probability density function	$-$
Q	Dirlik's constants	$-$
R	Dirlik's constants	$-$
S	power spectrum	$[unit]^2/Hz$
STD	standard deviation	$unit$
t	time	s
T_C	mean time between peaks	s
TI	turbulence intensity	$-$
T_{life}	lifetime	s
T_P	wave spectrum peak period	s
T_{sime}	simulation time	s
T_Z	zero-crossing period	s
u	water particle velocity	m/s
$\dot{u}$	water particle acceleration	m/s^2
U_{rel}	relative wind speed at blade section	m/s
V_W	wind speed	m/s
Z	normalized load range	$-$

Greek symbols

γ	peak enhancement factor	$-$
γ	irregularity factor	$-$
ϵ	random phase	rad
ζ	damping ratio	$-$
λ	wave length	m
ϕ	inflow angle	$degree$
ϕ	mode shape	$-$
ρ	water density	kg/m^3
ρ_a	air density	kg/m^3
ω	angular frequency	rad/s

Abbreviations

ALS	Accidental Limit State
BEM	Blade Element Momentum
BHawC	Bonus Energy Horizontal axis wind turbine Code
DLC	Design Load Case

DNV	Det Norske Veritas
EFL	Equivalent Fatigue Loads
FDM	Frequency Domain Method
IEC	International Electrotechnical Commission
(I)FFT	(Inverse) Fast Fourier Transform
FLS	Fatigue Limit State
JONSWAP	JOint North Sea WAve Project
MSL	Mean Sea Level
MCS	Monte-Carlo Simulation
PDF	Probability Density Function
PSD	Power Spectral Density
RNA	Rotor Nacelle Assembly
SLS	Serviceability Limit State
ULS	Ultimate Limit State
OWT	Offshore Wind Turbine

Chapter 1

Importance of load estimates in the offshore wind industry

Offshore wind energy is a growing industry vital for successful transition from fossil fuels to renewable energy. Compared to onshore technology, offshore turbines benefit from higher mean wind speeds, more steady wind conditions and greater availability of potential sites. Nevertheless, costs of offshore wind energy are still too high due to more expensive support structures, grid connections and offshore installations [1]. In order to make offshore wind energy economically viable, the wind industry has committed to 40% cost reduction in 2020 with respect to the 2012 cost level [2].
Part of this cost reduction is realized from support structures, where a recent study shows a potential of approximately one sixth of the total cost reduction [2]. Predominating support structures are monopiles as they cover 75% of the offshore wind market in 2013 [3]. According to the European Wind Energy Association [3], the trend of increasing size of offhore wind farms is expected to continue in the next years. Large offshore wind farms are predominantly located in deeper water (25-40m), for which monopile designs are typically governed by fatigue loads with significant contributions from wave excitation [4].
Large offshore wind farms cover areas of several square kilometer, in which considerable variations in environmental site conditions, for instance water depth, soil properties, and turbulence can exist. These variations lead to divergent design loads on support structures across the wind farm. Full load calculations are computationally demanding and can typically not be performed for each turbine [5]. In industry projects, offshore wind turbines (OWTs) are therefore often grouped into design clusters, where loads are only evaluated for a limited number of design positions. Allocating of OWT to design clusters must be performed in an early project phase, making time-efficient approaches essential. Hence fatigue load estimates are of highest relevance for a systematic concept of design optimization of offshore support structures and thus for the reduction of offshore wind energy costs.

Review of literature

Several approaches exist in literature to decrease computational costs of load analysis on OWT [6–17]. Approaches either use integrated analysis or suggest wind-wave separate assessment. In separate assessments, wave fatigue loads are mainly estimated with frequency domain analysis [6–9, 12, 13], which has also been applied to wind

loads [7, 9, 13–15]. Other authors suggest simplified rotor load models or parametric models for fatigue damage estimation [10, 15]. For integrated methods, proposal exists for reducing the number of environmental conditions, load cases, number of seeds or simulations length [6, 11, 17].
Since fatigue load calculation processes contain significant uncertainties, a number of researchers performed probabilistic fatigue assessment. A brief overview of existing publications is given by Yeter [18] and Veldkamp [19]. Sensitivity studies investigated the influence of site parameters and foundation configuration on the natural frequency, and emphasized the need for further work regarding sensitivity of fatigue damage [20, 21].
Nowadays, industry practices base clustering decisions on variations of mean sea level (MSL) or eigenfrequency of the support structures [22]. Recently, Seidel suggested an improved approach of clustering using a site parameter that takes structural and hydrodynamic properties into account [22]. This site parameter is, however, only suitable for wave-load dominated designs. Thus, further work is needed to formulate turbine clustering as an optimization problem incorporating all important site-specific information.

Research objectives and methodology

Based on the problem statement and review of existing publications, there is the need for research to obtain a better understanding of how fatigue loads behave in large offshore wind farms due to varying and uncertain site conditions. Thus, a link between fatigue estimation methods and probabilistic assessments is necessary that can be applied for sensitivity study of loads and optimization of turbine clustering in large offshore wind farms.
Given this research motivation, the main research question of the thesis is:

How can probabilistic fatigue load estimation improve turbine clustering in large offshore wind farms to reduce costs of offshore wind energy?

From this question the following three research objectives were derived:

1. Insight into load sensitivity to varying site conditions,

2. Analysis of effects of uncertainties in data, statistics and models, and

3. Optimization of turbine clustering.

In order to approach the research objectives, a probabilistic fatigue estimation method was developed in the computing environment MATLAB®. A verification study is performed with aero-elastic simulations for a 4MW OWT in approximately 35m water depth. The developed method is applied in local and global sensitivity studies to assess effects of site variations of the parameters MSL, soil stiffness, wave height, and wave period on fatigue loads. Furthermore, a probabilistic assessment is carried out with Monte-Carlo simulations (MCS) to analyze impacts of uncertainties on fatigue loads. Finally, the previous results are used to optimize turbine clustering based on site-specific fatigue load estimates.

Outline of report

The thesis consists of two research papers and a summary report. The main research work is presented in the papers. The summary report adds theoretical background and work that has not been published. The remaining report is structured as follows:

Chapter 2	In Chapter 2 relevant theoretical fundamentals of load analysis on OWT support structures are described. The focus is on types of loads, state-of-the-art of load modeling, and uncertainties in fatigue load calculation. Furthermore, parameters affecting the load level are outlined according to present scientific and industrial knowledge.
Chapter 3	Chapter 3 describes the implementation of the developed method for probabilistic fatigue load estimation on monopiles using frequency domain calculations for wave loads, scaling methods for wind loads and MCS. Next to the program structure, the objective of the model, assumptions, and limitations are discussed.
Chapter 4	In the fourth chapter the developed fatigue estimation method is verified with time domain aero-elastic simulations. Verification is performed for wave-only, wind-only and wind-wave combined loads. Finally, results and limitations of the verification study are discussed.
Chapter 5	Wave-induced fatigue loads for three simulation cases are presented in Chapter 5. Special emphasis is placed on the effect of aerodynamic damping and wind-wave misalignment. Statistical uncertainty in wave loads is analyzed using resampling methods. Finally, an overview of the content of the appended papers about wave load sensitivity and design clustering is given.
Chapter 6	Chapter 6 assesses the probabilistic fatigue estimation method and its applications for sensitivity assessment and clustering optimization. Limitations are discussed followed by an evaluation of scientific value and potential applications of method and results in industry.
Chapter 7	The last chapter summarizes the performed study and results. The report closes with recommendations for future research.
Appendix	Paper A deals with the sensitivity of wave fatigue loads under varying side conditions. Design clustering using deterministic and probabilistic fatigue estimates is topic of paper B.

Papers and authorship

The main work of the papers regarding programming, analysis and post-processing was carried out by the author of this thesis. Forming of the research idea, approaches, result discussion and minor parts of programming (time domain simulations, finite element model, discrete optimization solver) was a collaboration of the thesis supervisors from NTNU, Prof. Michael Muskulus and Sebastian Schafhirt, and the industry supervisor, Sven Voormeeren and his colleagues. In the following, the integration of the papers in the thesis scope is outlined.

Paper 1: Lisa Ziegler, Sven Voormeeren, Sebastian Schafhirt and Michael Muskulus. *"Sensitivity of Wave Fatigue Loads on Offshore Wind Turbines under varying Site Conditions"*, accepted for publication in Energy Procedia (Elsevier).
This paper presents the sensitivity analysis of wave-induced fatigue loads to varying site conditions using frequency domain analysis. An probabilistic assessment is performed with MCS. This paper addresses the first two research objectives and lays the groundwork for optimization of turbine clustering.

Paper 2: Lisa Ziegler, Sven Voormeeren, Sebastian Schafhirt and Michael Muskulus. *"Design clustering of offshore wind turbines using probabilistic fatigue load estimation"*, submitted to Renewable Energy (Elsevier).
Design clustering of OWTs in large wind farms is the subject of this paper using deterministic and probabilistic fatigue load estimates. Therefore, the paper presents an application of the in this thesis developed fatigue estimation method and answers the central research question about turbine clustering.

Chapter 2

Loads on offshore wind turbines

The relevant theoretical fundamentals of load analysis on offshore wind turbine support structures are described in this chapter. The focus is hereby on types of loads, state-of-the-art of load modeling and uncertainties in fatigue load calculations. Furthermore, parameters affecting the load level are outlined according to present scientific and industrial knowledge. For theoretical background on offshore wind turbines, aerodynamics and hydrodynamic loads, reference is made to relevant literature [23–25].

2.1 Loads and load cases

OWT are subjected to various load sources. The design of OWTs has to withstand all loads during anticipated lifetime of the structure while being cost-effective. Therefore, knowledge of expected loads during lifetime is crucial for a successful design. Loads can be categorized either through load origin or according to the affected limit state. In order to ensure a reliable design, a large number of load cases need to be analyzed [26]. Several engineering standards from classification societies as well as international standards exist for the design of OWTs. Mainly the standards "Design requirements for offshore wind turbines" by International Electrotechnical Commission (IEC 61400-3) [26] and "Design of offshore wind turbine support structures" by Det Norske Veritas (DNV-OS-J101) [27] are considered for this study.

Functional and environmental loads

Loads on OWTs originate from the operation of wind turbines itself or from environmental impacts. Functional loads can be permanent or variable for which examples are given in Table 2.1 [27].

Permanent loads	**Variable loads**
Mass of structure	Actuation loads
Mass of permanent equipment	Ship impacts
Hydrostatic pressure	Loads from installation

Table 2.1: Permanent and variable loads [27].

Permanent loads stay constant during lifetime of the structure, while variable loads depend on operation, and therefore change in time. Environmental loads acting on the structure are site-specific and vary in size and point of application during lifetime. Examples of environmental influences causing loads on OWTs are

- wind,
- wave and current,
- tides,
- ice (floating and on blades),
- marine growth, and
- earthquakes if applicable.

Depending on the impact characteristic these influences either affect the maximum load carrying capacity, being ultimate loads, or the fatigue resistance of the materials, being fatigue loads, as described in the following section.

Ultimate and fatigue loads

In the design standards for OWTs several limit states are defined, which state the margin of the structure of still being able to satisfy design requirements [26, 27]. These are the criteria

- Ultimate Limit State (ULS),
- Fatigue Limit State (FLS),
- Accidental Limit State (ALS), and
- Serviceability Limit State (SLS).

In this thesis, ULS and FLS are further examined, since these are typically design driving. ULS describes the capacity to withstand maximum extreme loads, while cumulative damage due to cyclic loading is covered in FLS [27].
Examples of typical extreme loads in the design practice are combinations of 1-year, 5-year, and 50-year maximum wind or wave extremes. Fatigue loads are cyclic loads with lower amplitude than extreme loads occurring continuously during the entire lifetime of the structure, for example wind and wave loads in wind turbine operation.
For monopile support structures in deeper water locations, fatigue loads are typically design driving [28]. Furthermore, in these locations the contribution of wave loads plays a major role in fatigue analysis [12]. A recent study of a monopile support structure for a 6MW wind turbine in 40m water depth shows that the combined wind-wave fatigue loads are clearly dominated by wave contributions [4]. Accordingly, the influence of wind loads on total fatigue loads is minor. Additionally, wind loads can be predicted with good accuracy and are less sensitive to site variations. Therefore, this study focuses on detailed estimation of wave-induced fatigue loads, while wind loads are approximated with a simple scaling method.

Load cases

In order to represent the most important load contributing events occurring during life of the OWT, various design situations with several load cases are considered in its design. IEC 61400-3 defines eight design situations, namely

- power production,
- power production plus occurrence of fault,
- start up,
- normal/ extreme shut down,
- emergency shut down,
- parked (standstill or idling),
- parked and fault conditions, and
- transport, assembly, maintenance, repair [26].

Load cases are set up as further specification of these design situations, for example stating appropriate normal or extreme condition for wind, waves, directionality, currents, water levels, and other factors. Each load case then either contributes to fatigue or ultimate load analysis for which a specific safety factor is defined [26]. All load cases with a reasonable probability of occurrence should be considered which leads to a total number of more than thirty cases to analyze according to IEC 61400-3 [26]. For each of the cases multiple time domain simulations with three to twelve seeds and simulation length of typically ten minutes need to be set up. Next to the general load cases defined in the standard, specific situations might need to be analyzed additionally. Altogether, for one position within a wind farm the total number of performed load simulations are typically in the range of 2000 to 10000 for one iteration [29]. Due to this enormous effort, it is often not possible to perform time domain load analyses for every turbine position within the wind farm.

This condensed outline of the various loads and load cases illustrates the complexity of load analysis. In order to decrease the design effort by implementing valid simplifications, a better understanding of the influence of various parameters on the load level is needed. Parameters effecting the load level are examined in the following section.

2.2 Parameters effecting the load level

Parameters influencing the load level of OWTs can be categorized into internal system conditions and external influences. Internal parameters are structural or turbine properties, for instance mass or mode shapes, while external parameters are related to environmental influences, for example water depth or soil conditions. All parameters are evaluated according their

- importance for load level, and
- availability and uncertainty at project start.

The criteria availability and uncertainty are important since the fatigue estimation method is mainly for use in early project phases. In these phases, not all site conditions are given for every turbine location and interpolation between available site

measurements introduces uncertainties.
For the following parameter study, reference is made to design standards, relevant articles and reports as well as project experience within Siemens Wind Power [4, 6, 12, 26, 27, 30, 31]. Table 2.2 gives an overview of categorization of load influencing parameters.

Category	**Parameter**	**Importance [- to ++]**	**Availability [- to +]**
Structural Parameter	Eigenfrequency	++	0
	Mode shape	++	0
	Mass	+	+
	Damping ratio	++	0
Environmental Parameter	Water depth	++	+
	Wind	++	+
	Wave climate	++	0
	Current	0	0
	Directionality	+	0
	Ice	0	0
	Soil	++	0
	Earthquake	0	0
	Scour and erosion	-	+
	Marine growth	-	+
Turbine Parameter	Rated power	0	+
	Actuation loads	0	+
	Yaw misalignment	0	+
	Operation mode	+	+
	Wakes	0	-

Table 2.2: Categorization of load influencing parameters.

The analysis identified the parameters from which a high importance for the load level is expected as the following:

- water depth,
- soil,
- wind and wave climate,
- directionality,
- eigenfrequency, and
- damping ratio.

Results for sensitivities of fatigue loads to changes and uncertainties in these parameters are presented in section 5.2 and the scientific papers in Appendix B.

2.3 State-of-the-art of load calculation process

The load influencing parameters vary between different offshore sites which leads to divergent loads on support structures. Consequently, support structures are custom engineered for every offshore wind farm. This custom engineering includes the following iterative steps:

1. load evaluation based on site-specific conditions and
2. subsequent structural design of tower and foundation using site-specific loads.

One loop in this iterative process typically takes four to six weeks [32].

2.3.1 Design positions

Larger offshore wind farms nowadays consist of sixty or more turbines which cover a wide area of several square kilometers. This large area leads to considerable variations of environmental site conditions within the farm. Ideally, support structures for each individual wind turbine should be custom engineered. However, this is not feasible in practice since time for the development phase of the project is limited.
In practice, loads are evaluated for a limited number of design positions within the wind farm. A design position is chosen in order to perform the engineering only once. The resulting load levels and structural design need to hold for all assigned positions within the wind farm. Consequently, the design position must be the position where highest loads occur [32]. This position can be either physical or virtual. A virtual design position combines worst-case properties of several physical positions. After the design positions are selected, the remaining turbines are allocated to clusters.
Nowadays, clustering and selection of design position in the wind turbine industry is often performed based on previous project experiences using criteria such as approximate first eigenfrequency and water depth. These parameters indeed have an important influence on the load level as shown in section 2.2. However, latest studies have shown that the interpolation accuracy is not sufficient for design purposes [12]. Recently, an alternative approach was published which states a “site parameter” that can be used to interpolate loads between different turbine positions [12]. Optimization of design positions and clustering will decrease design conservatism and therefore contribute to the cost reduction of offshore wind energy.

2.3.2 Design split versus integrated methods

In industry practice, a design split usually exists between wind turbine manufacturers and foundation designers. This split evolved from the history of wind energy, where wind turbine manufacturer benefited from their experiences from onshore wind energy, while foundation designers build on expertise from the offshore oil and gas industry [6]. Wind loads are typically calculated by a wind turbine manufacturer which is also responsible for the design of wind turbine towers. Foundation designers take care of wave loads and the foundation design. However, the support structure acts as one system with foundation and tower influencing the response behavior. Therefore, extensive communication is needed at the interface leading to slow design progress and conservative design since different models and safety factors are applied [33].

Several researchers conclude that an integrated design method can lead to an optimized design while reducing engineering efforts [4, 6, 33–36]. Accordingly, this study uses an integrated model incorporating foundation and tower in a single system.

2.3.3 Deterministic versus probabilistic design

The design of OWT support structures contains high numbers of stochastic variables that influence loads and material strength. These stochastic variables lead to uncertainty in design procedures. Design approaches treat this uncertainty either deterministic, where all uncertain variables are represented with one characteristic value, or probabilistic, where structural reliability is defined through an accepted probability of failure in time [27].
The design standards for OWTs recommend deterministic design based on the partial safety factor method [26, 27]. In this method, load and resistance factors are applied in calculations in order to achieve a target safety value. The target safety value for OWT foundations as unmanned structures should match a probability of failure of 10^{-4} according to [27]. The only standard considering probability-based design is DNV-OS-J101, which recommends it for calibration of load and material factors in deterministic analysis, specific design problems, and novel designs with limited experience available [27].
In daily engineering practice, deterministic approaches are convenient due to limited time and resources. Research results from probabilistic analysis can be used to improve deterministic approaches and to assess the chances that results differ significant from deterministically calculated ones. The main gain from probabilistic approaches is improved knowledge of structural reliability. This is important for

- reduction of design conservatism through exact matching of target safety values [19],
- better financing conditions from security of economic planning [37, 38],
- planning of operation and maintenance [18], and
- decision on remaining structural reliability at the end of OWTs design lifetime.

A brief overview of previous work on probabilistic design of OWTs is given by Veldkamp [19] and Yeter et al. [18]. Veldkamp focused on probabilistic analysis of fatigue design considering also randomness of wave loads for OWTs [19]. In his work, he calibrates partial safety factors from annual failure probabilities derived with First Order Reliability Methods and MCS. Later, uncertainty modeling, reliability assessment and use of test results through Maximum Likelihood Methods and Bayesian statistics is described by Sorensen and Toft [39]. A current research project by ForWind on probabilistic safety assessment of OWTs tries to answer the overall question of probability of failures in current OWT design [40]. Recently, Yeter et al. [18] published a fatigue reliability assessment of a tripod OWT support structure using a stochastic spectral approach for wind and wave loading [18].
The briefly summarized publications above assess the frame of reliability-based design for OWTs. Additionally, several studies examine the importance of specific uncertainties in load calculations [17, 41–44]. As an example, Zwick and Muskulus [17] state

a maximum error of 35% for substructure fatigue loading caused by input loading variability due to a single 10min simulation.
The main novelty of this work is to apply probabilistic load estimates for sensitivity assessment of fatigue loads to varying site conditions, which provides a basis for design clustering in large offshore wind farms. Beyond the scope of this thesis, further work is needed to combine the here obtained probabilistic loads with uncertainties in structural resistance.

2.3.4 Time versus frequency domain calculations

In current engineering practice, fatigue loads on OWTs are mainly assessed by extensive time domain simulations of various load cases described in section 2.1. Time domain simulations are used since they enable non-linear analysis with coupled simulations of wind, wave and control system [45]. The results of time domain analysis are treated as most accurate and are therefore commonly used for certification purpose. Results with high accuracy are important especially for checking Rotor Nacelle Assemblies (RNA) against type certification loads. However, for support structure design less sophisticated models might be sufficient, which will be further investigated in this study. Especially for preliminary design and clustering optimization, time domain simulations are not suitable due to high computational costs.
Frequency domain methods, as an alternative, have the potential to heavily decrease computational costs. Since frequency domain analysis is linearized and treats wind and waves as decoupled, the method is considered less accurate than time domain approaches. Nevertheless, frequency domain methods have been preferably applied historically in the offshore oil and gas industry, when computationally resources were limited, and are also recommended in offshore guidelines [46]. Frequency domain methods also have been transferred to OWTs by several researchers [6, 7, 12].
Kuehn [6] suggested a simplified method for fatigue analysis by superimposing time domain simulations of aerodynamic loads with frequency domain results of wave loads on the support structure. Later, van der Tempel [7] applied frequency domain analysis to complete support structure design, where a comparison to time domain results showed reasonable accuracy. Both researchers treat wind and wave loads separately, but emphasize the importance of accounting for aerodynamic damping due to its large effect on support structure dynamics. Seidel [12] recently published a highly simplified approach to calculate wave-induced fatigue loads on monopiles only considering the first mode of structural response, while not accounting for aerodynamic damping. Furthermore, Seidel [4] suggests methods to use this approach for lumping of scatter diagrams and fatigue load interpolation.
The above mentioned studies developed, applied and verified frequency domain methods and stated the potential of it to be used for design optimization due to its calculation speed. The model developed in this study combines elements of the existing works describes above and uses these in sensitivity and uncertainty studies.

2.4 Load modeling

For a detailed description of hydrodynamic and aerodynamic load modeling on OWTs, reference is made to standard literature [23–25, 47–49]. In the following a brief summary of the for this study relevant concepts is given.

2.4.1 Wave load modeling

Nowadays, Morison equation is the most widely used concept to calculate wave loads on OWT monopiles [31]. It is an empirical formula valid for slender structures since it assumes that the structure does not affect the wave kinematics [50]. The wave force is computed as a superposition of drag and inertia forces per unit length (cf. Equation 2.1-2.2). The velocity of the structure is commonly neglected for OWT monopiles since it is small compared to the water particle velocity.

$$dF = f_{drag} + f_{inertia} \tag{2.1}$$

$$dF = \frac{1}{2} \cdot C_D \cdot \rho \cdot D \cdot |u| \cdot u + \frac{\pi}{4} \cdot C_M \cdot \rho \cdot D^2 \cdot \dot{u} \tag{2.2}$$

with

dF	hydrodynamic load	[N/m]
f_{drag}	drag force	[N/m]
$f_{inertia}$	inertia force	[N/m]
C_D	drag coefficient	[-]
C_M	inertia coefficient	[-]
ρ	water density	[kg/m^3]
u	water particle velocity	[m/s]
$\dot{u}$	water particle acceleration	[m/s^2]
D	diameter of cylinder section	[m]

Figure 2.1 depicts the dominant wave forces on a cylindrical offshore structure [51]. Morison equation is applicable if the criterion $\pi D/\lambda < 0.5$ is valid. D represents the diameter of the structure and λ the wave length. This is indicated in Figure 2.1, where Morison equation is appropriate left of the boundary line at $\pi D/\lambda = 0.5$ [51]. Moreover, Figure 2.1 shows the importance of drag and inertia forces depending on wave height and structure diameter. For lower wave heights with respect to the structure diameter, inertia loads are dominating, while for higher wave heights drag loads become more important.
In this study, Morison equation was applied with a linearized drag force, since the contribution of drag forces is minor for a larger monopile in fatigue relevant sea states (section I in Figure 2.1). Linearization of the drag force is necessary because this term is proportional to water particle velocities squared. However, in the frequency domain calculations used in this study, only linear relations are representable.
Industry moves towards larger turbines in deeper water supported by XL-monopiles with diameters above 6m. This increase in monopile diameter makes diffraction effects more dominant in wave forces as shown in Figure 2.1. Since Morison equation is not capable of including diffraction effects, an external diffraction correction was applied on the inertia coefficient C_m in this thesis [52]. Methods capable of including diffraction effects are pressure integration from potential flow or diffraction theory [49].

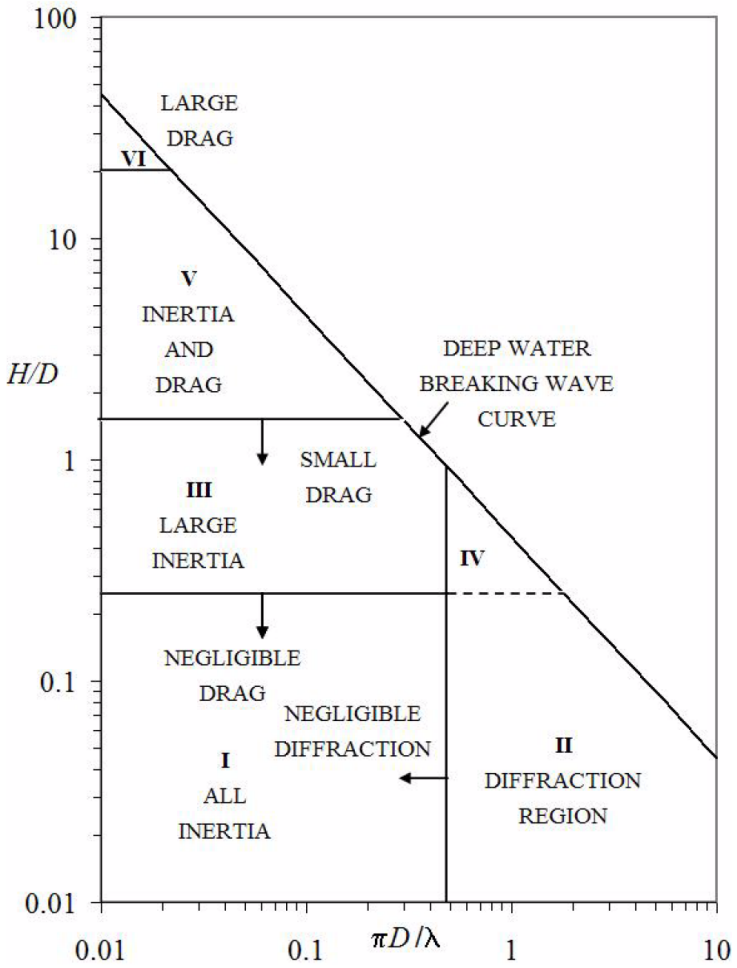

Figure 2.1: Dominant wave forces on a cylindrical offshore structures [51]. H represents the wave height [m], D the diameter of the structure [m] and λ the wave length [m].

2.4.2 Wind load modeling

The predominant concept used for calculating aerodynamic loads on OWTs is Blade Element Momentum (BEM) Theory which is extensively described in [24, 47]. The change in momentum of a wind flow through the rotor, which is seen as an actuator disk, is calculated using momentum conservation assuming that the horizontal flow is incompressible. Blade element theory is then applied to calculate the forces on the blade, depending on the relative velocity that each blade section experiences (cf. Figure 2.2).
Lift and drag forces occurring on each blade element are calculated with Equations 2.3-2.5. The relative wind speed U_{rel} at a blade section is found from the ambient wind velocity at the blade U, the rotational speed Ωr and the axial and tangential induction factors a and a'. The induction factors have to be calculated iteratively from coupling momentum theory with blade element theory.

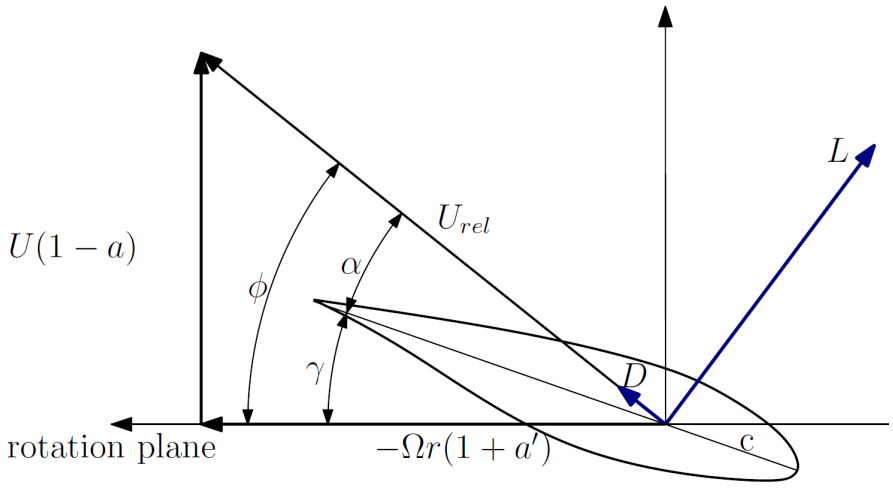

Figure 2.2: Local forces on an airfoil [45]. L represents the lift force, D the drag force, U_{rel} the relative wind speed, a the induction factor and c the chord length.

$$dF = dF_L \cdot cos\phi + dF_D \cdot sin\phi \tag{2.3}$$

$$dF_L = \frac{1}{2} \cdot \rho_a \cdot C_L \cdot U_{rel}^2 \cdot c \tag{2.4}$$

$$dF_D = \frac{1}{2} \cdot \rho_a \cdot C_D \cdot U_{rel}^2 \cdot c \tag{2.5}$$

with

dF	aerodynamic blade load	[N/m]
ϕ	inflow angle	[degree]
dF_L	lift force	[N/m]
dF_D	drag force	[N/m]
C_L	aerodynamic lift coefficient	[-]
C_D	aerodynamic drag coefficient	[-]
ρ_a	air density	[kg/m^3]
c	airfoil chord length	[m]
U_{rel}	relative wind speed at a blade section	[m/s]

In this thesis, BHawC, which abbreviates Bonus Horizontal axis wind turbine Code, is used for calculation of aerodynamic loads. BHawC is a non-linear aero-elastic tool for global dynamic analysis of wind turbines developed in-house by Bonus Energy, a Danish wind turbine manufacturer that has been acquired by Siemens in 2004. BHawC uses BEM theory to calculate aerodynamic loads with an expansion for skewed and unsteady inflows. Additionally, corrections for high induction values, dynamic stall and Prandtl's tip loss correction, which accounts for the assumption of infinite number of blades, are implemented [53].

2.5 Uncertainty in fatigue loads

Uncertainties in fatigue loads can be categorized into aleatory and epistemic uncertainty. Aleatory uncertainty is inherent due to the random nature of processes, for example randomness of sea states. Epistemic uncertainty is knowledge based and can be reduced if more information is gathered [54]. Sources of epistemic uncertainties are [39, 55]:

1. *Data uncertainty* due to measurement imperfection, for example soil or MSL data.
2. *Statistical uncertainty* due to estimation of parameters from a limited number of observations, for example wave characteristics in scatter diagrams.
3. *Model uncertainty* due to simplification of physical phenomena in model formulations, for example use of linear wave theory, wake modeling or input probability distributions.

According to Sorensen and Toft [39], the most important uncertainties are natural fluctuations and model uncertainties. It is important to notice that the level of uncertainties change during different phases of the offshore wind project. In an early project stage, e.g. preliminary design, not all input data exists for every turbine location within the wind farm. Therefore, uncertainties increase due to interpolation of existing data. In the subsequent detailed design phase, more data is typically available reducing input uncertainty. Additionally, in an initial design phase, simplified load models are applied due to time constraints leading to higher model uncertainty.

Chapter 3

Probabilistic fatigue load estimation method

This chapter describes the developed method for probabilistic fatigue load estimation on monopiles using frequency domain calculations for wave loads and a scaling method for wind loads. Probabilistic assessment is performed with Monte-Carlo simulations. The tool is realized in the computing environment MATLAB®. Next to the structure of the tool, objectives of the model, assumptions, and limitations are discussed.

3.1 Model objective and tool structure

The aim of the developed method for fatigue load estimation is to obtain loads in short computation time, while being accurate enough to be used for probabilistic assessments and to differentiate effect of site variations.
Site variations can have a major effect on fatigue loads. Table 3.1 presents fatigue load differences of four existing wind farm projects for bending moments at tower bottom [56]. The results state the differences in fore-aft or side-side bending moments depending on which one is the highest. The studied site variations incorporate water depth differences from 6m to 22m. Soil properties also change over the site, however soil differences were not quantified in [56]. In order to be meaningful for studies of load site variations, the error of the fatigue load estimation method must be well below load site differences.

Water depth	Max. fatigue difference
27-35m	14%
5-27m	41%
19-25m	27%
18-26m	21%

Table 3.1: Maximum fatigue load differences for bending moments at tower bottom of four wind farms due to site variations [56].

Regarding the model efficiency, the defined objective is to obtaining lifetime equivalent fatigue loads (EFLs) of one simulation case within seconds. In comparison, the time domain simulation for one case takes approximately two hours consisting of about six seeds of 10-minute-simulations that have around twenty minutes simulation time each depending on the chosen model and complexity of the problem [29].
The basic structure of the developed fatigue load estimation method is shown in Figure 3.1. It is based on three core elements: calculation of wave loads in the frequency domain, scaling of wind loads from a reference case and combination of wind-wave loads through direct quadratic superposition [6]. The inputs into the model are environmental conditions, on which basis an initial design of the support structure is set up. After calculating the combined wind-wave EFLs, the validity of the initial design has to be checked and updated in an iterative process. This thesis project assumes that fatigue loads are design driving for monopiles in deeper water. In practice, a check should be performed that the initial design withstands all extreme loads during design lifetime.

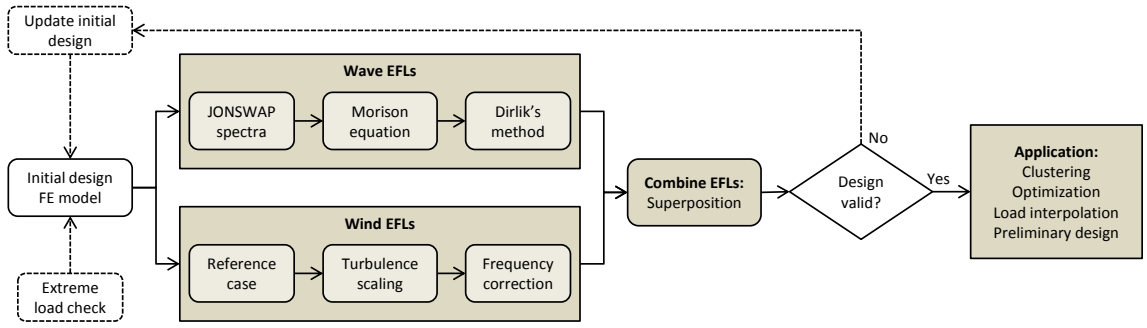

Figure 3.1: Flowchart of fatigue load estimation method.

To calculate wave fatigue loads, frequency domain analysis was chosen due to the benefits of computational efficiency and simplicity of setup. Furthermore, successful implementation of frequency domain methods for OWTs already exists as explained in Chapter 2.3.4. The three major components of the frequency domain analysis are, firstly, calculation of generalized wave loads on the monopile using Morison equation. The term generalized hereby expresses that the loads are external loads on the monopile. Secondly, internal responses in terms of displacement, shear forces and bending moments are computed using transfer functions from a finite element model of the support structure. Finally, an expected value of EFLs is obtained based on spectral analysis using Dirlik's method [57].
Since wind loads are less important in the anticipated application field, the first priority in the choice of wind load estimation is computational efficiency, while simplifications of physical phenomena and losses in accuracy are acceptable. Wind loads are calculated with a scaling approach from a reference case. This reference case for wind loads consists of EFLs from time domain aero-elastic simulations using BHawC. This reference case is turbine type specific, but generic regarding environmental conditions and support structure dimensions. Location-specific EFLs are obtained by a linear scaling of turbulence intensity and a correction for the first natural frequency of the support structure.

Finally, wind and wave EFLs are combined using direct quadratic superposition [6]. The output of the method is EFLs for a specified number of cycles. This information can further be used to compute the lifetime damage of the structure. Each component of the tool is described in detail in the following sections.

3.2 Assumptions for proposed method

In order to create a fast computational model for fatigue load estimation, several assumptions have been implemented to simplify full load calculations. These simplifications might have an influence on the accuracy of the obtained EFLs. The effect of some of the assumptions is analysed further in the verification study (cf. Chapter 4).

Assumptions for environmental data:

- Wind-wave scatter diagrams are lumped into 20 simulation cases consisting of mean wind speeds V_W, significant wave heights H_S, and wave peak periods T_P. The lumping is performed in a damage equivalent way using a method suggested by Kuehn [6]. For each simulation case wind-wave directionality is simplified into fully aligned or fully misaligned. For this purpose, wind and wave roses are lumped in bins of 30degree. Fully aligned wind and waves occur in the same bin. All other combination of wind and wave directions are treated as fully misaligned.
- Soil is modeled with distributed linear springs according to the Winkler model [58, 59].
- Further effects like currents and sea ice are neglected since the effects on the load level are expected to be minor (cf. Chapter 2.2). In general, it has to be noted that sea ice can have a major impact on loads, but is assumed to not occur for the considered sites e.g. North Sea. It is assumed that scour protection is installed, so that erosion and scour effects are not considered.

Reduction of scatter diagrams and the chosen soil model are conform with latest industry practices. These simplifications are not expected to cause any differences compared to simulation results of time domain models. Expected to be more critical is the assumption regarding directionality, for which results are presented in Chapter 5.1.3.

Assumptions for structural model:

The structural model in the wind load calculation has the setup used in BHawC with a full representation of the RNA. For a detailed description about the structural formulation in BHawC reference is made to [53].
The following assumptions concern the structural model used in the frequency domain analysis for wave loads.

- The foundation and tower are described with a linear finite element model of Timoshenko beam elements. It is based on a realistic reference design, where outer diameter, wall thickness and elastic properties change over height of the support structure.

- The first ten modes of the structure are taken into account according to ten eigenfrequencies.

- The RNA is modeled as an equivalent concentrated mass on top of the tower.

- Damping consists of a contribution from combined structural, hydrodynamic and soil damping (critical damping ratio ca. 1%) and a contribution from aerodynamic damping (critical damping ratio ca. 1.5 - 8%). The latter is a function of wind speed, rotor speed, and mode shape and is superimposed to structural damping. It is determined turbine specific with modal analysis from a non-linear aero-elastic model. Aerodynamic damping for the first mode (fore-aft) is increased for aligned wind and waves, while it is decreased for higher structure modes as well as for wind-wave misalignment.

- The term interface refers to the node at tower bottom.

Through the finite element model an accurate description of the modal properties of the support structure is achieved. The first ten eigenfrequencies cover the frequency range of wave excitation broadly. Simplifying the RNA as concentrated mass will effect the response of the support structure, for instance influences of blade eigenfrequencies cannot be depicted.

Assumptions for calculation method:

- Only fatigue relevant design load cases of the design situations power production and idling are taken into account, since these are the predominantly occuring events and therefore are expected to contribute most to fatigue damage.

- The wind estimation approach only accounts for turbulence intensity and first natural frequency. Differences in air density, wind shear, structural geometry or mode shapes are neglected, since the effects on the load level are expected to either be minor or represented through the natural frequency correction.

- Applying a turbulence and natural frequency scaling on a wind-only reference case assumes that both effects are independent. The natural frequency correction has not been checked for different turbulence intensities. However, the dependency of both effects is expected to be minor and neglected in the following analysis.

- Turbulence scaling assumes that wind loads can be approximated by taking turbulence intensity as a linear factor out of the calculation.

- The absolute formulation of Morisons equation is used, since structural velocity is low compared to wave velocity. The drag term is linearized with a method developed by Borgman [60].

- Constant stretching is used to stretch the wave kinematics from MSL to wave crest [61]. Diffraction is accounted for by use of the empirical MacCamy-Fuchs diffraction correction [52].

- Instead of using distributed transfer functions of the finite element model along the monopile wave-action zone, only transfer functions for equivalent wave loads at MSL are generated. This is done in order to minimize the computational effort for creating transfer functions.
- Dirlik's approximation is used as spectral method to obtain expected number of cycles and load ranges from load power spectra [57].
- Direct quadratic superposition of wind and wave response assumes that (i) the behaviour of the structure is linear and (ii) the zero-crossing period of wind and wave responses are identical [6]. Linear behaviour is commonly valid for the environmental conditions contributing most to fatigue damage. Zero-crossing periods are not equal in general, however detailed verification studies by Kuehn [6] proofed good performance of the method.

The largest effect on the accuracy of the results is expected to be caused by the application of Dirlik's method. Previous studies using Dirlik's method for OWTs have shown that result accuracies are fluctuating with the problem statement [7, 14]. Ragan & Manuel showed that Dirlik's method performed well for estimation of equivalent fatigue tower bending moments on onshore wind turbines, while only poor results are obtained for blade edge bending moments [14]. Neglecting the velocity of the structure in Morison equation is a common industry practice for monopile design for OWTs. Furthermore, the effect of linearizing the drag term in Morison equation is expected to be negligible, since wave loads are inertia dominated for this problem (cf. Chapter 2.4.1). Simplifying the use of transfer functions on only a single interaction point is expected to introduce result inaccuracies, since the structural response is also influenced by the mode shape of the structure at the point of force application. Direct quadratic superposition of separately calculated wind and wave loads is commonly referred to as conservative, since it neglects the interference term, which is assumed to be negative [62]. The influence of the interference term is expected lower when the problem is majorly dominated by one load component. For the considered application for monopiles in deeper water, wave loads are exceeding wind loads majorly for environmental conditions around rated wind speed, while for lower and higher wind speeds the contributions converge more.

3.3 Frequency domain method for wave fatigue loads

The concept behind each component of the developed method is explained in the following section in detail. Explicit values of chosen coefficients, discretization and other input parameters are given in Appendix A.

3.3.1 Generalized wave loads

The first component of the frequency domain method for wave-induced fatigue loads is the computation of generalized wave loads. A flowchart of the generalized wave load calculation is presented in Figure 3.2.
The first step in the flowchart is to discretize the frequency space and depth vector. It is advisable to cut-off the frequency vector at higher frequencies, where the energy of the

wave spectrum is minimal and therefore the contribution to the sea surface elevation is negligible. In this study, the cut-off frequency is 1Hz. Accordingly, in the structural model all modes that can possibly be excited by the wave loading need to be included. For discretization of the depth vector maximum size elements of 0.5m are used while a finer definition around MSL might be beneficial due to rapid change of the wave kinematics in this area. The explicit values chosen for the discretization in this model are stated in Appendix A.

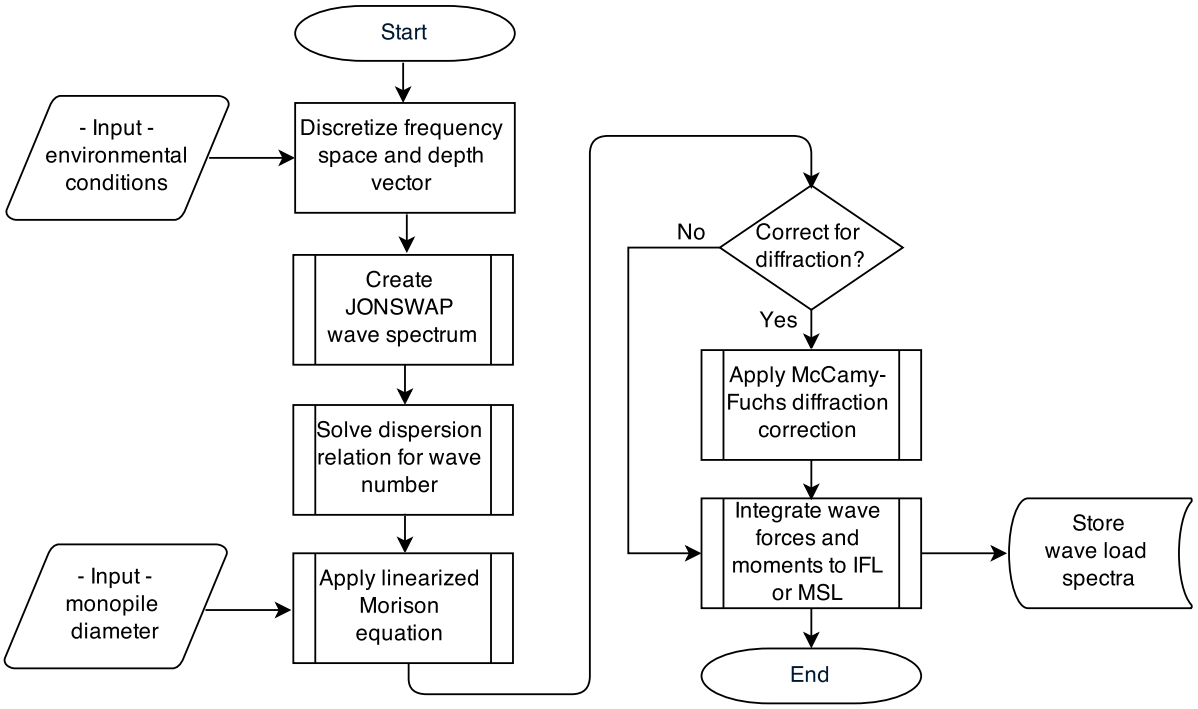

Figure 3.2: Flowchart of generalized wave load calculation.

Afterwards, a JONSWAP wave spectrum is created based on environmental input conditions of H_S and T_P which are obtained from lumped scatter diagrams (cf. Equation 3.1-3.4) [63].

$$S_{JW}(f) = C(\gamma) \cdot 0.3125 \cdot H_S^2 \cdot f_p^5 \cdot f^{-5} \cdot exp\left[-\frac{5}{4}\left(\frac{f_p}{f}\right)^4\right] \cdot \gamma^{exp(\alpha)} \tag{3.1}$$

$$\sigma = \begin{cases} 0.07 & \text{for} \quad f \leq f_p \\ 0.09 & \text{for} \quad f > f_p \end{cases} \tag{3.2}$$

$$C(\gamma) = 1 - 0.287 \cdot ln\gamma \tag{3.3}$$

$$\alpha = -\frac{(f - f_p)^2}{2 \cdot \sigma^2 \cdot f_p^2} \tag{3.4}$$

with

S_{JW}	JONSWAP wave spectrum	[m^{2}s]
γ	peak enhancement factor	[-]
H_S	significant wave height	[m]
f_p	wave peak frequency	[Hz]
f	frequency	[Hz]
C(γ)	normalizing factor	[-]

Next to setting up the wave spectrum, the dispersion relation, as stated in Equation 3.5, needs to be solved in order to obtain the wave numbers k.

$$\omega^2 = g \cdot k \cdot tanh(kd) \tag{3.5}$$

with

ω	angular frequency	[rad/s]
g	gravitational acceleration	[m/s^2]
k	wave number	[rad/m]
d	water depth	[m]

Afterwards, Morison equation is applied to generate wave loads on the monopile. Input herefore is the monopile diameter in the water column. In order to treat Morison equation in the frequency domain, the drag term has to be linearized since it is proportional to the water particle velocity squared (cf. Chapter 2.4.1). The linearization method suggested by Borgmann [60] is implemented which approximates the drag term by the first term of the Fourier series expansion (cf. Equation 3.6-3.11).

$$S_{VV}(f,z) = \left[\frac{(2 \cdot \pi \cdot f)^2 \cdot cosh^2(k \cdot z)}{sinh^2(k \cdot d)}\right] \cdot S_{JW}(f) \tag{3.6}$$

$$S_{AA}(f,z) = \left[\frac{(2 \cdot \pi \cdot f)^4 \cdot cosh^2(k \cdot z)}{sinh^2(k \cdot d)}\right] \cdot S_{JW}(f) \tag{3.7}$$

$$S_f(f,z) = \frac{8 \cdot c_{mor}^2 \cdot \sigma^2}{\pi} \cdot S_{VV}(f) + k_{mor}^2 \cdot S_{AA}(f) \tag{3.8}$$

$$c_{mor} = \frac{1}{2} \cdot C_D \cdot \rho \cdot D \tag{3.9}$$

$$k_{mor} = C_M \cdot \rho \cdot \frac{\pi}{4} \cdot D^2 \tag{3.10}$$

$$\sigma^2 = \int_0^\infty S_{JW}(f)\,\mathrm{d}f \tag{3.11}$$

with

S_{VV}	velocity spectrum	[m^2/s]
S_{AA}	acceleration spectrum	[m^2/s^3]
ρ	water density	[kg/m^3]
f	frequency vector	[Hz]
z	depth vector	[m]
k	wave number	[rad/m]
d	water depth	[m]
S_{JW}	JONSWAP wave spectrum	[m^{2}s]
C_M	inertia coefficient	[-]
C_D	drag coefficient	[-]
D	monopile diameter	[m]
σ^2	variance	[m]

The choice of inertia and drag coefficients have major influence on the size of wave loads. It is crucial to determine which load part is dominating and to choose this coefficient carefully.
If diffraction is relevant for the problem, a McCamy-Fuchs diffraction correction for the inertia coefficient of Morison equation is implemented [7, 52]. As described in Chapter 2.4.1 diffraction is relevant for increasing ratios of monopile diameter D over wave length λ. Consequently, the McCamy-Fuchs diffraction correction is implemented in the model as a function of diameter and wave length. The correction algorithm reduces the magnitude of the inertia coefficient as shown in Figure 3.3.

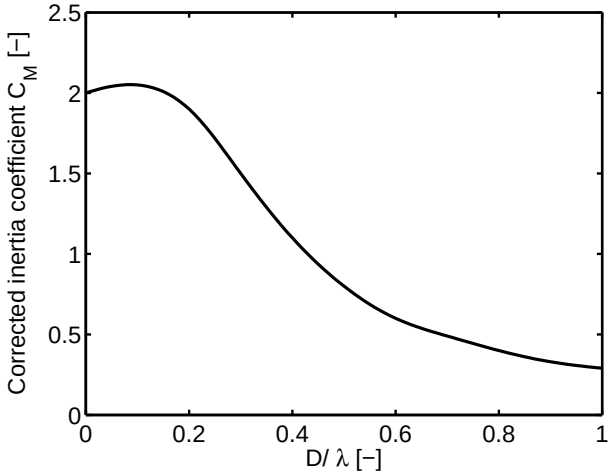

Figure 3.3: McCamy-Fuchs diffraction correction for inertia coefficient C_M. D represents the diameter of the structure [m] and λ the wave length [m].

Finally, the wave loads obtained from Morison equation as a function of depth and frequency are integrated over depth to obtain equivalent wave loads either at interface or MSL. The choice of integration point depends on which structural response transfer function is used as further explained in Section 3.3.2.
The output of the generalized wave load calculation are equivalent wave load spectra. An example case of a JONSWAP wave spectrum for a typical fatigue sea state and the

resulting equivalent wave load spectrum at MSL are shown in Figure 3.4.

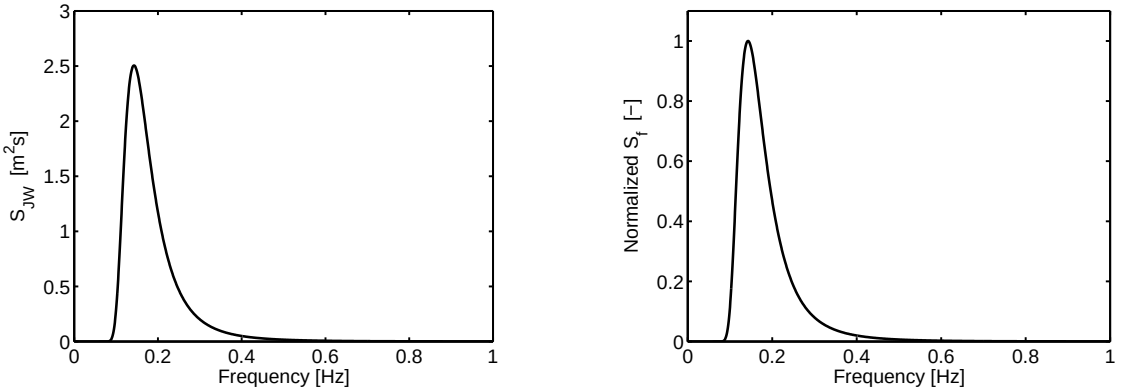

(a) JONSWAP wave spectrum **(b)** Wave load spectrum

Figure 3.4: (a) JONSWAP wave spectrum and (b) equivalent wave load spectrum for example of $H_s = 2m$, $T_p = 7s$, $\gamma = 1$ and the reference structure. The wave load spectrum is obtained for integration to MSL.

Figure 3.4a shows that the JONSWAP spectrum has the highest energy distribution around wave peak frequency. Through Morison equation this energy is passed on to the wave loads spectrum covering the same frequency range as the input wave spectrum. The wave load frequency range is important for support structure design since ideally the first natural frequency of the support structure is located outside the major range of wave excitation.

3.3.2 Structural response

After the equivalent wave loads on the structure are calculated, the structural response is determined in the frequency domain by use of transfer functions. The transfer functions are generated with a finite element model of the support structure using modal synthesis. The finite element model is created in MATLAB® from the input of an initial design of the support structure using an existing tool written by Voormeeren [64], which has been modified for the purpose of this study. Further explanation on the finite element model is not given here since it is not focus of the project. Instead, reference is made to standard literature for theoretical background on structural dynamics and finite elements [65–67].
Transfer functions describe the relation between load input and structural response in terms of displacements or internal loads of the system (cf. Equation 3.12-3.13). Equation 3.13 states exemplarily the transfer function linking input on degree of freedom 1 to output on degree of freedom of the structure. Finally, the power spectral densities (PSD) of the structural responses are calculated with Equation 3.14. The obtained load spectra are stored as outputs of this tool component.

$$H(\omega) = \frac{Output}{Input} = \frac{Displacement}{Force} \tag{3.12}$$

$$H_{11}(\omega) = \sum_{j=1}^{n} \frac{\phi_{j,1} \cdot \phi_{j,1}^{T}}{(\omega_j^2 - \omega^2) + 2 \cdot i \cdot \zeta_j \cdot \omega_j \cdot \omega} \tag{3.13}$$

$$S_R(f) = |H(f)|^2 \cdot S_f(f) \tag{3.14}$$

with

H	transfer function	[m/N]
ω	angular frequency	[rad/s]
f	frequency	[Hz]
ω_j	jth natural frequency	[rad/s]
ϕ	mode shape	[-]
ζ	damping ratio	[-]
S_R	structural response PSD	[m^2/Hz], [N^2/Hz], [(Nm)^2/Hz]
S_f	wave load PSD	[N^2/Hz], [(Nm)^2/Hz]

The transfer functions in the developed method lead from wave load input at interface level or MSL to displacement or internal loads output at the nodes at mudline or interface level. Figure 3.5a depicts a transfer function linking external forces on a node at interface level to internal shear forces at the same node. An example power spectrum for shear forces at mudline is presented in Figure 3.5b.

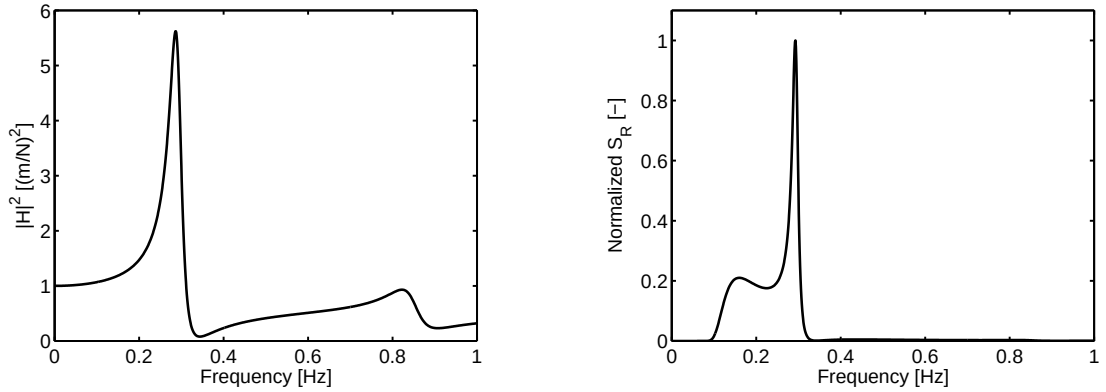

(a) Transfer function **(b)** Shear force response spectrum

Figure 3.5: (a) Transfer function and (b) shear force response spectrum at mudline node for example of $H_s = 2m$, $T_p = 7s$, wind-waves misaligned, $\gamma = 1$ and the reference structure.

Figure 3.5a shows the transfer function giving the expected relation that a static unit force at 0Hz leads to a unit internal response force. The internal force response spectrum has a peak at the first eigenfrequency of the structure as well as at wave peak frequency (cf. Figure 3.5b). This example illustrates that the response spectrum cannot be considered narrow-banded which influences the spectral methods applicable to obtain fatigue load estimates as described in the following section.

3.3.3 Fatigue load estimates with Dirlik's method

Fatigue loads are cyclic loads on the support structure as explained in Chapter 2.1. In this tool component, fatigue load estimates are deduced from the internal load power spectra given out in the previous step.
The common method to consider fatigue loads during the design of OWTs is to compare long-term stress distributions with a material response model, for example S-N curves. S-N curves are created based on laboratory tests of materials and state the number of cycles N a material can withstand for a specific stress range S before failure [68]. In the design standard DNV-OS-J101 [27] suitable S-N curves are given for support structure design. The cumulative fatigue damage is then calculated based on S-N-curves using Palmgren-Miners rule as stated in Equation 3.15 [69]. The cumulative damage $D_{fatigue}$ needs to be smaller than one for the entire lifetime so that the structure does not fail due to fatigue.

$$D_{fatigue} = \sum_i \frac{n_i}{N_i} \tag{3.15}$$

with

$D_{fatigue}$	cumulative fatigue damage	[-]
n	number of cycles from stress history	[-]
N	number of cycles from S-N curve	[-]

In this study, the concept of EFLs is used since it allows a quantitative comparison of structural response loads due to different environmental input. EFLs are defined as the constant-amplitude load range that causes the same amount of fatigue damage as all variable-amplitude load ranges L from the load time history for a specified number of load cycles N_k (cf. Equation 3.16) [19].

$$EFL = \sum_i \left(\frac{n_i \cdot L_i^m}{N_k} \right)^{\frac{1}{m}} \tag{3.16}$$

with

EFL	equivalent fatigue load	[N], [Nm]
L	load range	[N], [Nm]
n	number of cycles	[-]
N_k	specified number of cycles	[-]
m	Woehler slope	[-]

In order to calculate EFLs, information about the number of cycles and load ranges occuring during the entire lifetime of the structure is needed. For time domain simulations, this information is typically obtained by performing cycle-counting algorithms, e.g. rainflow-counting, on the computed load history. For further explanation on rainflow-counting reference is made to the developers Endo & Matsuishi [70].
In the frequency domain, equivalent results to rainflow-counting on time histories need to be obtained from the load power spectrum. For narrow-band spectra, load

peaks are Rayleigh distributed for which an analytical solution for the damage is then given. Applying a Rayleigh distribution to broad-band spectra leads to overestimation of probabilities of large stress ranges, since this method does not account for negative peaks and positive troughs in the time signal. This will lead to a conservative damage estimation [6].
First results of the wave load calculation have shown that response spectra cannot always be considered narrow-banded in this study (cf. Figure 3.5). In the literature, an empirical approach developed by Dirlik [57] is treated as the most accurate method for broad-band load spectra to match the result of rainflow-counting for OWTs [7, 14]. Dirlik combined and weighted one exponential and two Rayleigh distribution to determine the probability density of stress ranges [57]. The definition of the Dirlik's constants to weight these distributions is purely empirical based on evaluation of a large data set, where Dirlik fitted spectral results to results from rainflow-counting on time series [7].
Accordingly, Dirlik's method is applied on the load spectra obtained from the previous computation step in the developed tool. The steps of the computation method to calculate fatigue load estimates using Dirlik's method is visualized in Figure 3.6.

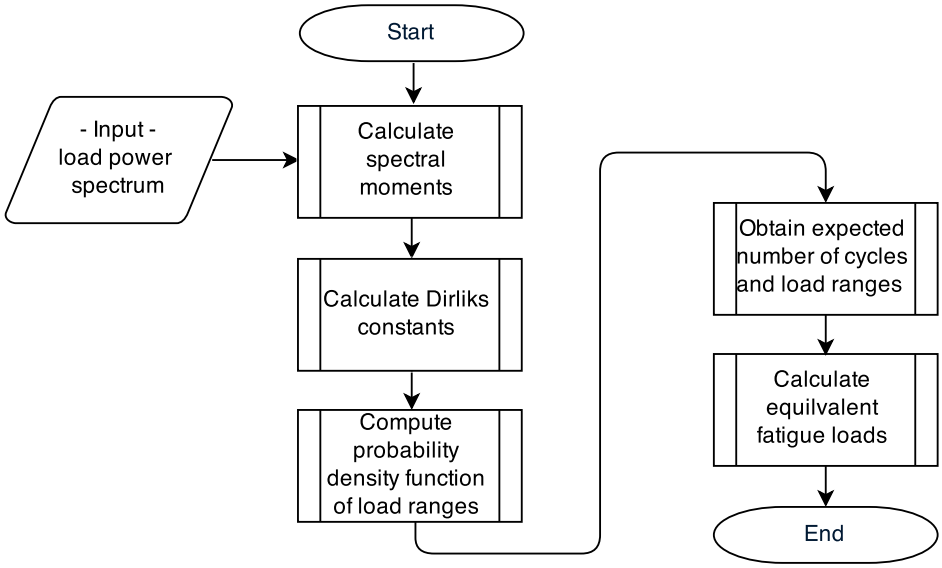

Figure 3.6: Flowchart for obtaining fatigue load estimates with Dirlik's method.

The first step is to compute spectral moments of the load power spectrum according to Equation 3.17 [14]. The formulas 3.18-3.19, to calculate the mean zero-crossing period T_Z and the mean time between signal peaks T_C based on spectral moments, are derived with extreme value statistics. This derivation is explained in detail by Newland [71].

$$m_n = \int_0^\infty f^n \cdot S_l(f)\,\mathrm{d}f \tag{3.17}$$

$$T_Z = \sqrt{\frac{m_0}{m_2}} \tag{3.18}$$

$$T_C = \sqrt{\frac{m_2}{m_4}} \tag{3.19}$$

with

m_n	n$^{\text{th}}$ spectral moment	[(unit)^2/s$^{\text{n}}$]
S_l	load power spectral density	[N^2/Hz],[(Nm)^2/Hz]
f	frequency	[Hz]
T_Z	zero-crossing period	[s]
T_C	mean time between peaks	[s]

The irregularity factor γ, defined as the ratio of time between peaks T_C to zero-crossings T_Z, is a measure of the bandwidth of a signal (cf. Equation 3.20). For γ being one, T_C equals T_Z which means that here is only one dominant frequency in the signal, and thus the spectrum is narrow-banded. If γ equals zero, then the signal contains an equal amount of energy at all frequencies [48]. A broad-band signal is defined by $0 \leq \gamma < 1$ which is reflected in the time signal with a higher number of peaks than zero-crossings in a defined time interval.

$$\gamma = \frac{T_C}{T_Z} = \frac{m_2}{\sqrt{m_0 \cdot m_4}} \tag{3.20}$$

with

γ	irregularity factor	[-]
m_n	n$^{\text{th}}$ spectral moment	[(unit)^2/s$^{\text{n}}$]
T_Z	zero-crossing period	[s]
T_C	mean time between peaks	[s]

Based on the previous parameters, Dirlik's constants are calculated with Equation 3.21-3.26.

$$x_m = \frac{m_1}{m_0} \cdot \sqrt{\frac{m_2}{m_4}} \tag{3.21}$$

$$D_1 = \frac{2 \cdot (x_m - \gamma^2)}{1 + \gamma^2} \tag{3.22}$$

$$R = \frac{\gamma - x_m - D_1^2}{1 - \gamma - D_1 + D_1^2} \tag{3.23}$$

$$D_2 = \frac{1 - \gamma - D_1 + D_1^2}{1 - R} \tag{3.24}$$

$$D_3 = 1 - D_1 - D_2 \tag{3.25}$$

$$Q = \frac{1.25 \cdot (\gamma - D_3 - D_2 \cdot R)}{D_1} \tag{3.26}$$

with

m_n	n$^{\text{th}}$ spectral moment	[(unit)^2/s$^{\text{n}}$]
γ	irregularity factor	[-]
x_m	Dirlik's parameter	[-]
D_i, R, Q	Dirlik's constants	[-]

Subsequently, the probability density function (PDF) of the load ranges is defined by Dirlik [57] with Equation 3.27-3.28. The expected value of the constant amplitude load

range $E[L]$ for n number of cycles is obtained by integrating load ranges weighted with the PDF as shown in Equation 3.29. The expected number of cycles $E[n]$ is given by dividing the lifetime of the structure T with the mean time between peaks T_C.

$$p(L) = \frac{1}{2 \cdot \sqrt{m_0}} \cdot \left[\frac{D_1}{Q} \cdot e^{\frac{-Z}{Q}} + \frac{D_2 \cdot Z}{R^2} \cdot e^{-\frac{Z^2}{2 \cdot R^2}} + D_3 \cdot Z \cdot e^{-\frac{Z^2}{2}} \right] \tag{3.27}$$

$$Z = \frac{L}{2 \cdot \sqrt{m_0}} \tag{3.28}$$

$$E[L] = \left[\int_0^\infty L^m \cdot p(L) \, \mathrm{d}L \right]^{1/m} \tag{3.29}$$

$$E[n] = \frac{T}{T_C} = T \cdot \sqrt{\frac{m_4}{m_2}} \tag{3.30}$$

with

$p(L)$	load range PDF	[-]
D_i, R, Q	Dirlik's constants	[-]
m_n	n$^{\text{th}}$ spectral moment	[(unit)^2/s$^{\text{n}}$]
Z	normalized load range	[-]
L	load ranges	[N],[Nm]
$E[L]$	expected value of load range	[N],[Nm]
m	Woehler slope	[-]
$E[n]$	expected value of cycles	[-]
T	lifetime of structure	[s]
T_C	mean time between peaks	[s]

Figure 3.7 shows an example case of a computed PDF using Dirlik's method. A brief check in the model confirms that the area under the constructed PDF equals one.

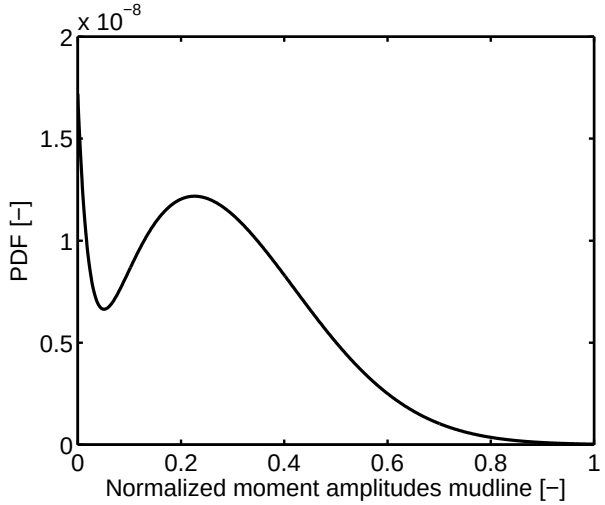

Figure 3.7: Probability density function of load ranges for internal bending moment at mudline obtained with Dirlik's method for an example sea state of $H_s = 2.22m$, $T_p = 7s$ and wind-waves misaligned.

3.4 Scaling method for wind loads

To estimate wind-induced EFLs, a scaling approach of wind loads from a reference case to the new location based on linear turbulence scaling and a correction for the first natural frequencies of the support structure is suggested. This approach was initiated by Smid [72] and was successfully used for initial design in several projects by Siemens Wind Power. The following sections describe the turbulence scaling and natural frequency correction in detail.

3.4.1 Turbulence intensity scaling

The first component of the scaling method for wind loads is the selection of a reference case of wind-only EFLs consisting of time domain, aero-elastic simulations with BHawC. This reference case is turbine type specific but generic regarding environmental conditions and support structure dimensions. The reference cases are in general available from an existing database of the wind turbine manufacturer for each turbine type. The reference cases for offshore situations consists typically of a complete set of wind load simulations for Class C turbulence intensity.
After the reference case is selected, location-specific design turbulences for each turbine position in the wind farm have to be defined. These are computed from the measured, ambient turbulence intensity with the Frandsen wake model to include wake effects from neighboring turbines [73]. The Frandsen wake model takes into account the thrust curve of the turbine, mean wind speeds, wind directions and spacing ratio to calculate an effective design turbulence for every turbine. A detailed description about the model and equations is given in [73].
Figure 3.8 presents the turbulence intensity Class C used in the reference case, the ambient turbulence intensity for an example wind farm and the calculated design turbulence for one turbine location within the wind farm. Class C turbulence is in general conservative compared to the design turbulence intensity. The design turbulence is usually significantly higher than free turbulences because of wake effects.

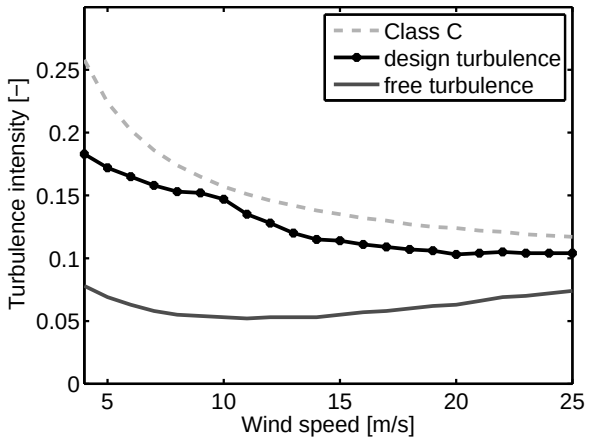

Figure 3.8: Class C, ambient and location-specific turbulence intensity based on Frandsen wake model.

Location-specific wind loads are then approximated applying linear scaling of the turbulence intensity as shown in Equation 3.31. It should be noted that this scaling method is an approximation assuming that the effect of turbulence intensity can be taken as linear factor out of the fatigue load calculation.
Physically, the turbulence intensity goes squared in the Kaimal spectrum which is an often used turbulence model for design load calculation (cf. Equation 3.32) [74]. Later, the square root of the Kaimal spectrum is taken for calculating local wind velocity fluctuations (cf. Equation 3.33-3.34). This makes wind-only EFLs approximately linear dependent on turbulence intensity. However, wind-only loads are also influenced by other effects, for example the controller behavior, which is not captured by the turbulence intensity scaling.

$$EFL_{ls}(V_W) \approx EFL_{ref}(V_W) \cdot \frac{TI_{ls}(V_W)}{TI_{ref}(V_W)} \tag{3.31}$$

$$S_K(f) = \frac{4 \cdot TI^2 \cdot L \cdot V_W}{(1 + 6 \cdot \frac{f \cdot L}{V_W})^{\frac{5}{3}}} \tag{3.32}$$

$$V(t) = V_W + \sum_{p=1}^{m} b_p \cdot cos(\omega_p \cdot t + \epsilon_p) \tag{3.33}$$

$$b(f) = \sqrt{2 \cdot S_k(f) \cdot \Delta f} \tag{3.34}$$

with

EFL_{ls}	location-specific wind EFL	[Nm]
EFL_{ref}	reference case wind EFL	[Nm]
TI_{ls}	location-specific turbulence intensity	[-]
TI_{ref}	reference case turbulence intensity	[-]
S_K	Kaimal spectrum	[(m/s)^{2}s]
L	integral length scale	[m]
V_W	mean wind speed	[m/s]
V	wind speed	[m/s]
f	frequency	[Hz]
m	number of wind components	[-]
b	wind amplitudes	[m/s]
t	time	[s]
ω	angular frequency	[rad/s]
ϵ	random phase	[rad]

3.4.2 Natural frequency correction

After the wind-only EFLs are calculated for location-specific turbulences, EFLs are corrected for the location-specific first natural frequency of the support structure. The location-specific first natural frequency is obtained from the finite element model of the support structure during the wave-load computation (cf. Section 3.3.2).
The natural frequency correction was derived by analyzing results of aero-elastic time

domain simulations for three different turbines types with three to seven frequency sets each as shown in Figure 3.9. The analyzed turbines are the Siemens 3.6MW turbine with 120m rotor diameter, the 4.0MW turbine with 130m rotor diameter and the 6.0MW turbine with 154m rotor diameter. In Figure 3.9, EFLs are normalized to the turbine specific EFL value of the designs first natural frequency. The first natural frequency of the support structure is normalized to the turbine specific 1P-3P range with P being the turbine's nominal rotational frequency: zero equals the 1P value, while one equals 3P. After this normalization, all turbine types show a similar trend of EFL sensitivity in the range of 0.1-0.3 normalized frequency. This frequency range covers typical variations of first natural frequencies in offshore wind farms broadly. A turbine-generalized correction factor for the first natural frequency could be derived by cubic spline data interpolation (cf. Figure 3.9).

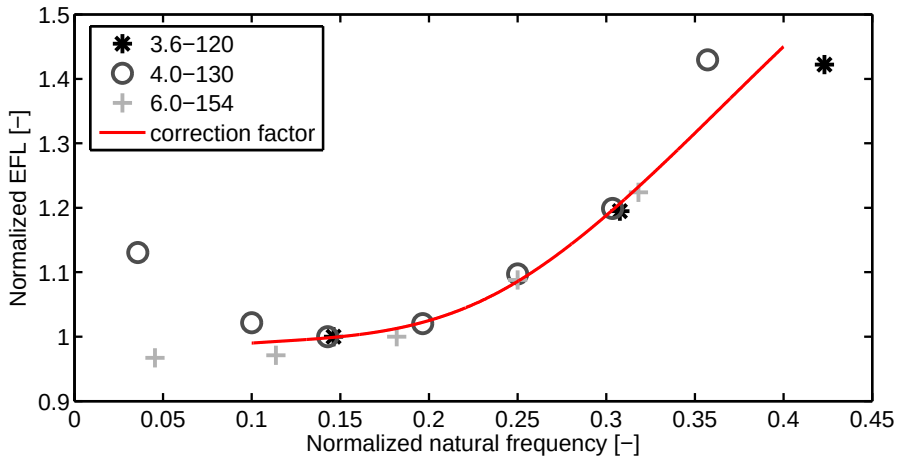

Figure 3.9: Natural frequency correction for wind-only loads for three turbine types. The correction factor is derived with cubic spline data interpolation.

The correction factor is influenced by the 1P-3P rotational frequency band since more dynamic excitation and accordingly higher load ranges occur when the first natural frequency of the turbine moves closer to 1P/3P. Additionally, higher first natural frequencies cause more load cycles which increases fatigue loads.
This correction factor is only valid for turbines with comparable size and rotational frequencies. Larger turbines with bigger rotors in general have lower 1P frequencies due to tip speed restriction. This is expected to lower the sensitivity of EFLs to higher normalized first natural frequencies since the relative increase of load cycles is less.

3.5 Combining wind and wave loads

Several approaches exist to combine separately calculated wind and wave loads, for example superposition of time series, response spectra or EFLs [6]. The main reason for choosing direct quadratic superposition of EFLs for this tool was that EFLs are the most convenient result obtained from wave load computation in the frequency domain, as well as wind load computation in the time domain [6]. The advantage of quadratic superposition over in-phase superposition is the reduction of conservatism due to

accounting for the random phase between wind and wave loads [6].
Wind and wave EFLs are combined using direct quadratic superposition according to Equation 3.35 [6].

$$EFL_{tot} \approx \sqrt{EFL_{wind}^2 + EFL_{wave}^2} \tag{3.35}$$

with

EFL_{tot}	wind-wave combined EFL	[Nm]
EFL_{wind}	wind-induced EFL	[Nm]
EFL_{wave}	wave-induced EFL	[Nm]

It must be emphasized that this approach is only an approximation with no theoretical proof since it also neglects the interference term between wind and wave loads. The validity of this approximation is confirmed for the problem setting of this thesis in the verification study (cf. Chapter 4).

3.6 Probabilistic load assessment

The computational efficiency of the proposed fatigue load estimation method allows probabilistic assessment through MCS. MCS repeat random sampling to discover the solution space of a problem numerically [71].
In the probabilistic load assessment, all uncertain input parameters are represented with a probability distribution. In each MCS, random samples from all independent parameter distributions are drawn simultaneously. EFLs are then calculated based on these data samples. The MCS are repeated a large number of times leading to a numerical set of EFLs. For this set of EFLs statistical properties like mean, standard deviation, skewness and kurtosis are calculated. These statistical properties characterize what probability distribution EFLs have due to the specified input uncertainty. In detail, kurtosis describes how peaked the probability distribution is, while skewness indicates the symmetry.
The accuracy of MC estimates depend on the number of simulations. The average MC errors of mean and standard deviation scale roughly with Equation 3.36-3.37 [75].

$$e_{mean} \approx \frac{1}{\sqrt{N}} \tag{3.36}$$

$$e_{STD} \approx \frac{STD}{\sqrt{N}} \tag{3.37}$$

with

e	average MC error	[-]
N	number of MCS	[-]
STD	output standard deviation	[-]

The advantage of MCS is simplicity of use making it a powerful tool when analytical solutions are complex. On the other hand, many simulations are needed for a good MC

estimate resulting in possibly long computation times. Table 3.2 gives an overview of the total computation times spend on problems in this thesis using a standard computer. For turbine clustering, 1000 MCS are run individually for each of the 150 turbines in the wind farm.

Problem	**MCS**	**Time**
EFL uncertainty	10000	10h
Turbine clustering	1000	48h

Table 3.2: MC computation times for problem statements in this thesis using a standard computer.

3.6.1 Input distributions

A main bottleneck of the probabilistic assessment is the definition of suitable probability distributions of variables with data and model uncertainty. Since usually no explicit measurement data is available for this, assumptions have to be made based on available wind farm data, existing publications of sensitivity studies, and expert opinion. A detailed analysis of suitable distribution for (offshore) wind turbine environments was published by Veldkamp [19]. Other sensitivity studies suggest variability ranges with focus on soil [76] or structural parameters [21].
In this study, uncertain input parameters are modeled with a normal probability distribution based on their mean value and the standard deviations stated in Table 3.3. Soil variations are represented by scaling of the soil stiffness which is obtained from nominal p-y curves with a factor that is constant over the full depth. The mean values of MSL, soil stiffness and TI are location-specific for each turbine within the wind farm. The model parameters γ and C_M are a function of the wave parameters as stated in Appendix A. The standard deviations are thus given for normalized mean values.

Parameter	**MSL**	**Soil**	**TI**	γ	C_M
STD [-]	0.05	0.2	0.1	0.1	0.1

Table 3.3: Normalized standard deviation of input parameters in probabilistic assessment.

Soil properties typically contain high uncertainties due to difficult measurement while the water depth is known with high accuracy. The standard deviation of MSL is chosen based on tide variation for an example wind farm. Figure 3.10 presents the input distributions of MSL and soil used in this study.

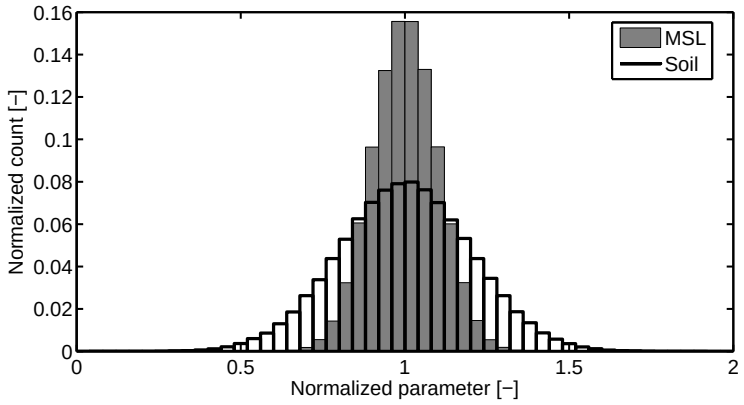

Figure 3.10: Normal distributions of input parameters MSL and soil used in this study.

3.6.2 Bootstrapping

The unknown distribution of variables with statistical uncertainty can be estimated with resampling methods. These methods are purely based on existing statistical data, thus no assumptions regarding the variability of the statistical input variable have to be made. The "Bootstrapping" method suggested by Efron [77] resamples data with replacement. Sampling with replacement means that an element of the original sample can appear multiple times in the new sample. From the relation between resampled data and original sample, conclusions are drawn about the properties of the underlying distribution linking original sample and unknown population. The bootstrapping method states that the inference resampled data to original sample is identical to the inference original sample to unknown population.
Bootstrapping was applied to estimate the variability within scatter diagrams.

Explanation of bootstrapping for scatter diagrams:
The goal is to find out how well a scatter diagram describes the real sea environment based on only a limited measurement time. Thus, the scatter diagram is handled as it would be the real sea environment. From this scatter diagram the sea states are "measured" that occur in a time interval identical to the "original measurement time". The "measurement" here is the resampling with replacement and the "original measurement time" is the identical number of total observations in the scatter diagram. The number of resamples than defines, how often the full set of "measurements" is repeated. For example, 1000 resamples means that there are 1000 scatter diagrams measured from the real sea environment. Since there is now a large set of resamples available, the variability that emerges due to only a limited measurement time can be calculated from it, for instance by calculating the standard deviation of the data set of resamples. Finally, it is assumed that this variability is identical to the variability obtained for the real sea environment.

The underlying assumption in bootstrapping is the independence of samples. It is important to note that bootstrapping is a data-driven method, so it cannot increase the information given in the original data. For example, H_S-T_P bins that do not occur in

the original scatter diagram can never occur in one of the resampled scatter diagrams. Bootstrapping is implemented for scatter diagrams with the following procedure:

1. Calculate the cumulative sum of occurrence for all H_S-T_P bins in the original scatter diagram.
2. Generate N uniformly distributed random numbers between 0 and 1, with N being the number of observations within the original scatter diagram.
3. Select the H_S-T_P bin that just exceeds the drawn random number and assign the count 1 to this bin.
4. Obtain the resampled scatter diagram by normalizing the occurrence of each H_S-T_P bin with the total number of observations. This gives each new scatter diagram a total probability of 100%.

This procedure is repeated a sufficient large number of times, which defines the number of resamples. In this thesis 10000 resamples are used.

Chapter 4

Verification of developed fatigue estimation method

In this chapter, the developed fatigue estimation method is verified with aero-elastic simulations in the time domain. Verification is performed for wave-only, wind-only and wind-wave combined loads. After description of the reference case, setup and post-processing of time domain simulations is outlined. Finally, verification results are presented followed by a discussion of the verification study and detected limitations.

4.1 Reference case

The purpose of the verification study is to confirm that the developed fatigue estimation method is appropriate for study of site variations and probabilistic assessments as defined in Chapter 3.1. Additionally, the verification study provides insight on differences in results between time and frequency domain calculations.
In order to compare time and frequency domain methods as close as possible, a simple set up of a reference case is used with a 4MW OWT in a water depth of approximately 35m. The reference case consists of various simulations with

- an identical structural model in terms of structural dimensions, damping and modal properties,
- several fatigue relevant sea states with various V_W, H_S, and T_P values, and
- simplified wind and wave directionalities for each sea state, namely fully aligned and fully misaligned.

The structural dimensions of the monopile are presented in Figure 4.1. The axes are normalized due to confidentiality. The diameter of the pile is decreased before MSL in order to lower wave loads. At interface level the monopile is connected to the tower via a transition piece.

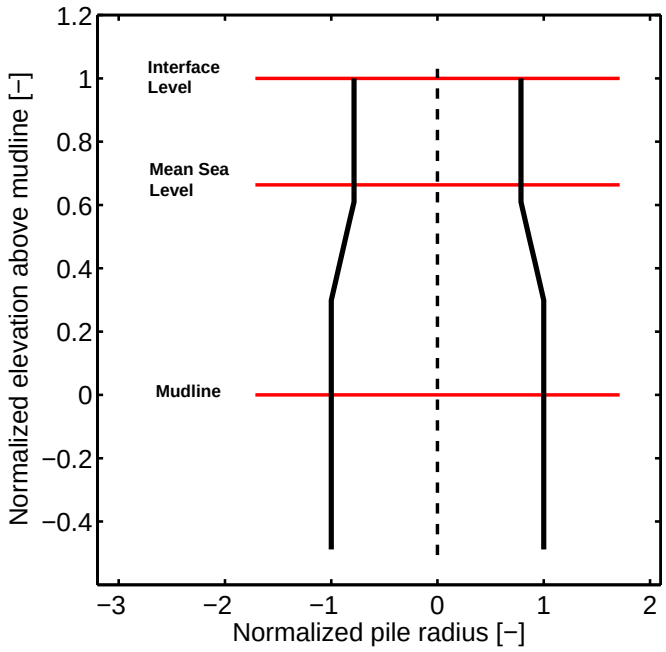

Figure 4.1: Structural dimensions of the foundation structure used in the reference case.

For the verification study three set of simulations are run:

1. **Wave-only** simulations with aerodynamics turned off.
2. **Wind-only** simulations represented through flat sea surface without waves and current.
3. **Wind-wave** combined simulations similar to standard practice in design projects.

4.2 Time domain simulations using aero-elastic code BHawC

Setup of time domain simulations

Non-linear aero-elastic simulations from BHawC are used for the verification study. In BHawC, the support structure is modeled with finite elements using Timoshenko beam elements. This is identical to the setup in the developed frequency domain method except that the model is linearized in the frequency domain. During normal simulations aerodynamic loads are modeled using BEM Theory with dynamic inflow [53]. Wave load files are generated outside BHawC by the foundation designer based on JONSWAP wave spectra with distributed loads along the monopile (cf. Chapter 2.3.2).
For the verification study, a simulation length of 600s after transients, time step of 0.04s and five different wave and turbulence seeds (random realizations) are chosen in the simulation. Multiple seeds are necessary in order to minimize statistical errors in the results because of use of random numbers for generating wind and surface elevation time series from the Kaimal wind and JONSWAP wave spectra. The simulation

parameters used for the verification study are summarized in Table 4.1.

Parameter	Description	Value
t	length of time series	600s
dt	time step	0.04s
n_s	number of seeds	5

Table 4.1: BHawC simulation parameters.

Post-processing of time domain simulations

Load time series from the time domain simulations are post-processed with rainflow-counting to calculate EFLs. These results are then compared quantitatively to EFLs obtained from each component of the load estimation tool to assess accuracies of the method.
For the rainflow-counting algorithm, a MATLAB® toolbox developed by Nieslony is used [78]. The output is number of cycles per load range from which the equivalent lifetime fatigue load for a specified number of cycles is computed with Equation 4.1.

$$EFL = \left(\sum_i \frac{n_i}{N_k} \cdot \frac{T_{life}}{T_{sim}} \cdot L_i^m \right)^{1/m} \tag{4.1}$$

with

n_i	counted number of cycles	[-]
N_k	specified number of cycles	[-]
T_{life}	lifetime	[s]
T_{sim}	simulation time	[s]
L_i	load range	[N], [Nm]
m	Woehler slope	[-]
EFL	equivalent fatigue loads	[N],[Nm]

For an in-depth evaluation of the wave load tool, load time series are additionally transferred to the frequency domain using Fourier transform. This enables evaluation of the wave load tool in three different progress stages: qualitative comparison of (i) internal load PSDs, (ii) PDFs from rainflow-count and Dirlik's method, and (iii) quantitative comparison of EFLs.
PSDs are estimated from the time series by applying Welch's method. This method uses periodogram spectrum estimates to reduce noise in the estimated spectrum due to limited length of the time series. The signal is split into windowed sections with specified overlap. Finally, the periodogram is calculated using fast fourier transform [79]. Table 4.2 presents the choices made for the parameters of Welch's method which proved to give the good results. The resulting PSD of sea surface elevation as well as internal shear forces and bending moments at interface level and mudline are compared qualitatively to resulting PSDs of the developed frequency domain method.

Choice	Value
Window type	Hamming
Number of sections	10
Overlap	50%

Table 4.2: Choices for Welch's method.

4.3 Comparison of wave-only fatigue loads

In the wave-only verification study, estimation results for three sea states with lower and higher fatigue relevant waves, according to Table 4.3, are compared qualitatively and quantitatively to time domain simulation.

Sea state	H_S [m]	T_P [s]
1	0.78	4.02
2	2.22	7.00
3	4.43	9.64

Table 4.3: Sea states used for verification study.

Figure 4.2 shows the time series of sea surface elevation and response bending moment at mudline for an example sea state of $H_s = 2.22m$, $T_p = 7.0s$, and the reference structural model defined in Section 4.1. The y-axis of the bending moment are normalized to the maximum load value.

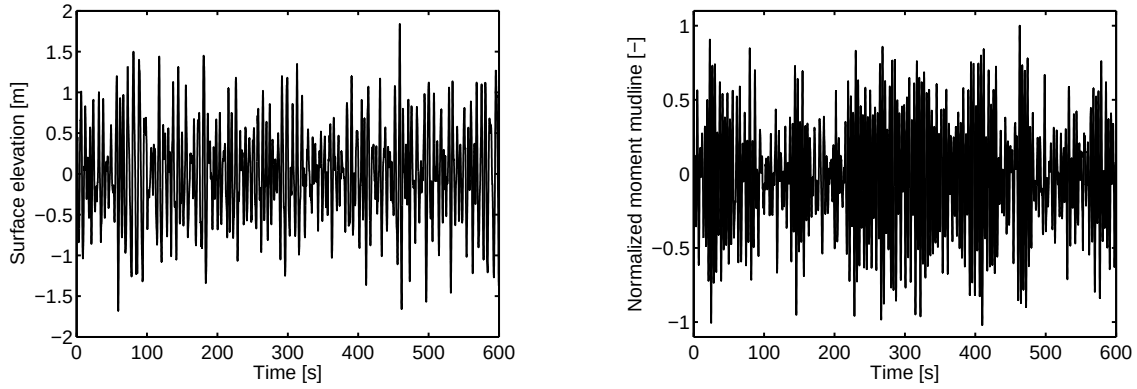

(a) Sea surface elevation. **(b)** Mudline bending moment.

Figure 4.2: Time series of (a) sea surface elevation and (b) mudline bending moment for an example sea state of $H_s = 2.22m$, $T_p = 7.0s$ using BHawC.

4.3.1 Qualitative analysis using power spectra

In the qualitative analysis it is initially investigated whether the PSD of the sea surface elevation is identical to the JONSWAP wave spectrum of the setup in the model. For a qualitative statement only one time series for comparison with JONSWAP spectra is used. Figure 4.3 presents the comparison for the example sea state of $H_s = 2.22m$, $T_p = 7.0s$. The JONSWAP spectrum is created with a peak enhancement factor of $\gamma = 1$, which is typical for fatigue analysis since it represents a fully developed sea state [27].

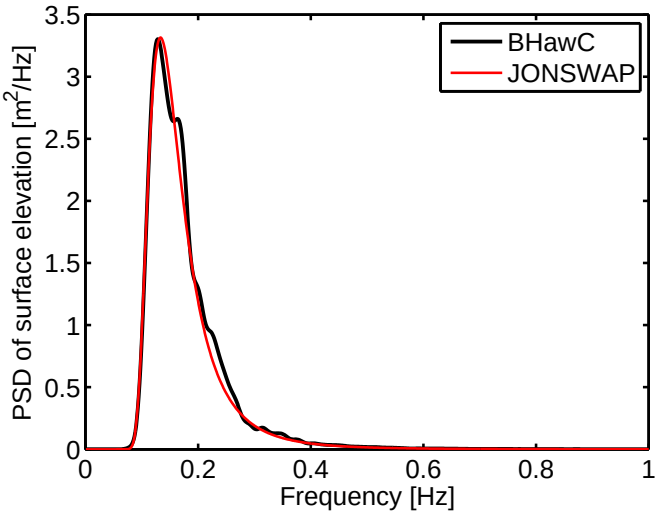

Figure 4.3: Comparison of PSD of sea surface simulation and JONSWAP wave spectra used in frequency domain method for an example sea state of $H_s = 2.22m$, $T_p = 7.0s$, and $\gamma = 1$.

Figure 4.3 shows that one time series is not fully sufficient to create a smooth spectrum since for stronger smoothing, for example by increasing the number of section in Welch's method, information can be lost. Furthermore, it has to be noted that for more smoothing applied with Welch's method, the peak height of the spectrum reduces while the peak width increases slightly. An improvement of the PSD could be obtained by either using a longer time series or adding multiple time series.
A possible source of error for setting up the JONSWAP wave spectrum is the choice of the peak enhancement factor γ since it has a high influence on the energy distribution over the frequency range in a sea state. The quality of the comparison to the PSD of the sea surface elevation also depends on how the sea surface elevation was constructed from the wave spectrum since the number of wave components used for setting up the time series as well as the chosen cut-off frequency of the spectrum have a high influence on the energy distribution.
Figure 4.4 presents a comparison of the internal responses at mudline from frequency and time domain simulations. The y-axis are normalized to the maximum PSD. It can be observed that the developed method gives a very good estimate of the PSD of internal bending moments at mudline (cf. Figure 4.4a). A response at wave peak frequency $f_p = 0.14Hz$ as well as a response at the first eigenfrequency $f_1 = 0.29Hz$ due to dynamic amplification is modeled appropriately. However, the response of the model at the eigenfrequency is slightly shifted to a higher frequency compared to the

BHawC result which is due to the modeling of added mass in the finite element model. The frequency domain method represents accurately that no response is visible in the frequency range around the second eigenmode of the structure $f_2 = 0.85Hz$ for this example case.

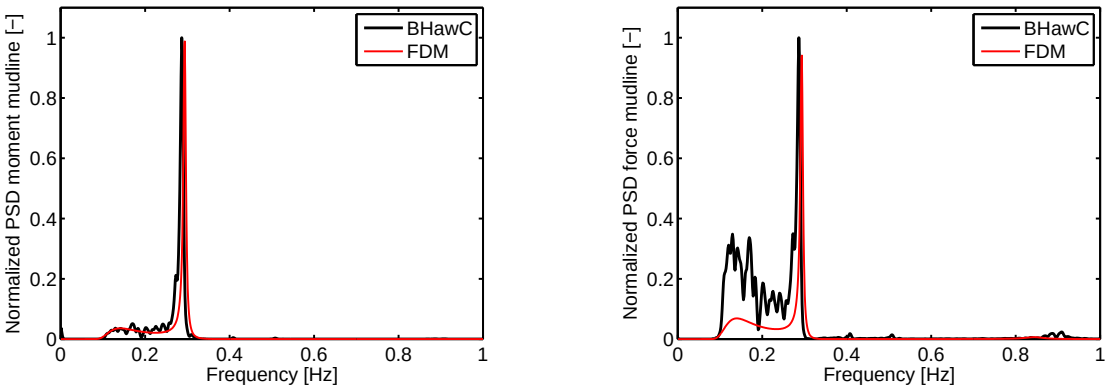

(a) PSD response moment mudline.

(b) PSD response force mudline.

Figure 4.4: Comparison of normalized PSDs of (a) response bending moment and (b) response shear force at mudline for an example sea state of $H_s = 2.22m$, $T_p = 7.0s$.

In the PSD of the internal forces from BHawC small peaks next to the wave frequencies and natural frequency are visible (cf. Figure 4.4b). These responses originate from the rotor blades which cannot be represented with the frequency domain method, since the RNA is simplified as a lumped mass. Furthermore, a small peak at 0.9Hz belongs to the second bending mode of the support structure which is weakly represented by the frequency domain method at a lower frequency of 0.85Hz. The shift of the eigenfrequencies is again due to added mass effects. Unlike the internal bending moment PSD, the force PSD underestimates the response around wave peak frequency which is expected to lead to an underestimation of the equivalent fatigue shear forces for the mudline location. This effect is analyzed quantitatively in the following chapter. It can be seen that the bending moment calculated in the time domain is represented accurately by the frequency domain method. However, the force spectrum obtained by frequency domain calculation overestimates the response at wave peak frequency. The PSDs of the responses at interface level are shown in Figure 4.5. The inaccuracy of the estimation of the shear forces at mudline and interface level is judged less significant since design driving parameter are internal bending moments. A hypothesis is that this inaccuracy originates from the fact that the distributed wave loads along the monopile are integrated to interface level in order to save computation time by generating only a single transfer functions. If internal forces are of interest in applications, generating distributed transfer functions along the monopile is recommended.

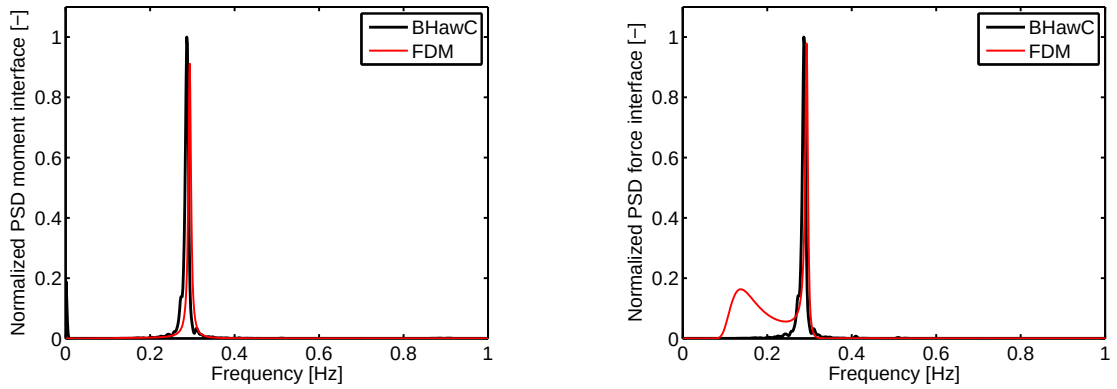

(a) PSD response moment interface level.

(b) PSD response force interface level.

Figure 4.5: Comparison of normalized PSDs of (a) response bending moment and (b) response shear force at interface level for an example sea state of $H_s = 2.22m$, $T_p = 7.0s$.

4.3.2 Quantitative analysis of equivalent fatigue loads

In this section, the errors of the developed wave load estimation are quantified through comparison of EFLs with time domain simulation using BHawC. Figure 4.6 presents the results of rainflow-counting compared to PDFs from Dirlik's method for the bending moment at mudline in an example sea state of $H_s = 2.22m$ and $T_p = 7.0s$.

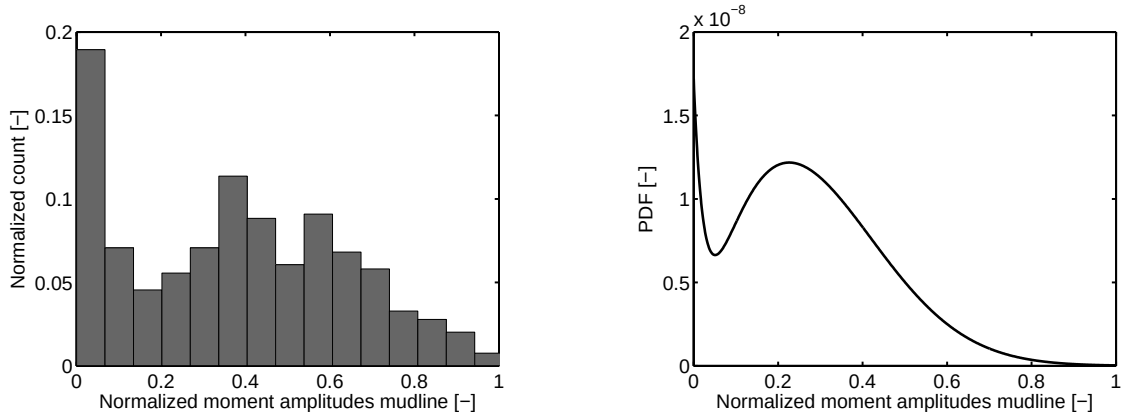

(a) Histogram of rainflow counts for mudline moment.

(b) Dirlik's PDF for mudline moment.

Figure 4.6: Comparison of (a) histogram of rainflow counts and (b) Dirlik's PDF for an example sea state of $H_s = 2.22m$, $T_p = 7.0s$. The bending moment ranges are normalized to the maximum value.

From a qualitative perspective, the Dirlik's PDF describes the results of rainflow-counting quite well. This is likewise the case for internal shear forces at mudline as well as responses at interface level (cf. Figure 4.7). The three different slopes of the PDF in both figures show the contribution of the exponential and two Rayleigh distributions combined and weighted in Dirlik's formula (cf. Equation 3.27). Consequently, the closer the rainflow count can be approximated by a weighted combination of these

three distributions, the better will be the results obtained by Dirlik's method compared to rainflow-counting.

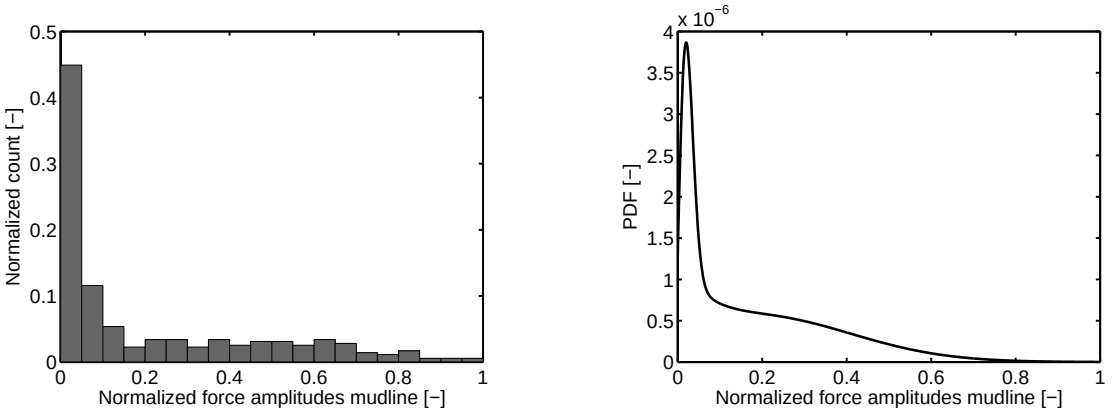

(a) Histogram of rainflow counts for mudline force.

(b) Dirlik's PDF for mudline force.

Figure 4.7: Comparison of (a) histogram of rainflow counts and (b) Dirlik's PDF for an example sea state of $H_s = 2.22m$, $T_p = 7.0s$. The force ranges are normalized to the maximum value.

The resulting EFL from rainflow-counting (cf. BHawC) and Dirlik's method (cf. FDM) are given in Table 4.4. The EFLs are normalized with the results of the time domain simulation.

Sea State	Load	Mudline		Interface	
		BHawC	FDM	BHawC	FDM
1	Force	1.0	0.79	1.0	0.03
	Moment	1.0	0.97	1.0	0.99
2	Force	1.0	0.67	1.0	0.59
	Moment	1.0	0.96	1.0	0.96
3	Force	1.0	0.74	1.0	0.88
	Moment	1.0	1.08	1.0	0.94

Table 4.4: Normalized EFLs in terms of shear forces and bending moments of time domain simulations (BHawC) and the developed frequency domain method (FDM).

Regarding the response bending moment estimation, the frequency domain method leads to the closest results for sea states with lower wave heights where an accuracy of more than 95% is achieved. Nevertheless, even for higher fatigue relevant wave heights, e.g. in sea state 3, the calculated equivalent fatigue bending moments differ less than 10% from the time domain result. The estimation of shear forces is less accurate which is in agreement with the expectation from the qualitative spectral analysis.

4.4 Comparison of wind-only fatigue loads

The wind-load estimation tool consists of a turbulence intensity scaling and a natural frequency correction. This verification study only tests the turbulence scaling part. The natural frequency correction is derived from BHawC simulations, thus comparing it to new BHawC simulations does not add value. Instead, future work should verify results with other codes or ideally measurement data.
For the verification of turbulence scaling, a complete set of BHawC simulations for wind speeds from 4m/s to 30m/s in bins of 1m/s with location-specific turbulence intensities was set up. All model and simulation parameters apart from the turbulence intensity were kept identical in the verification simulation compared to the reference case. EFLs per wind speed are combined to a lifetime fatigue value by weighting each wind speed with a wind farm specific Weibull distribution.
Figure 4.8a shows turbulence intensities for the reference case (Class C) and the location-specific turbulence intensities used in the verification study. Location-specific turbulences were calculated with the Frandsen model to account for wake effects from neighboring turbines. The Weibull distribution of wind speeds is presented in Figure 4.8b.

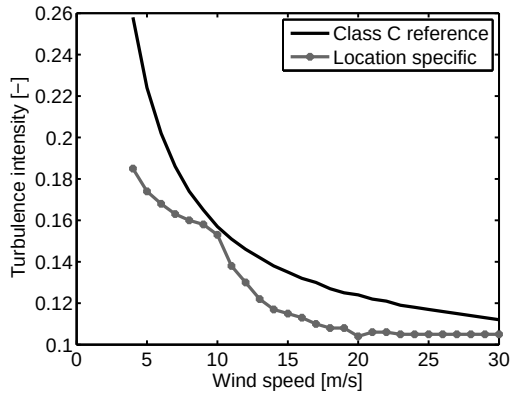

(a) Class C and location-specific turbulence intensities.

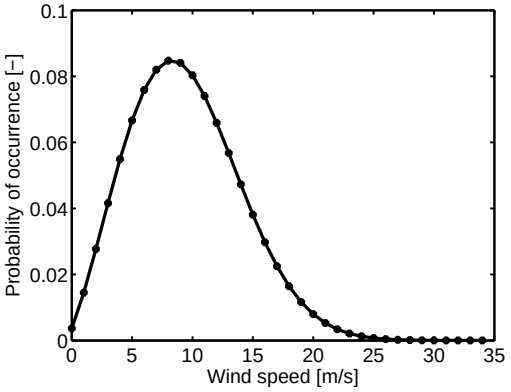

(b) Weibull distribution.

Figure 4.8: (a) Comparison of Class C and location-specific turbulence intensity based on Frandsen model including wake effects and (b) Weibull distribution of wind speeds.

Verification results for normalized EFLs at mudline and interface level are shown in Figure 4.9. The EFLs from the reference case with Class C turbulence were scaled to location-specific loads and then compared to the BHawC simulation. An almost exact match proves very good performance of the linear scaling approach. Slightly higher errors for very low or high wind speeds are due to the larger instability of these wind conditions. This effect is minor, since the absolute errors are still below 5%. Additionally, these wind speeds occur typically less during life of the OWT according to the wind speed Weibull distribution and thus contribute less to lifetime fatigue (cf. Figure 4.8b). Increased errors around rated wind speed ($V_W = 12m/s$) result from controller actions.

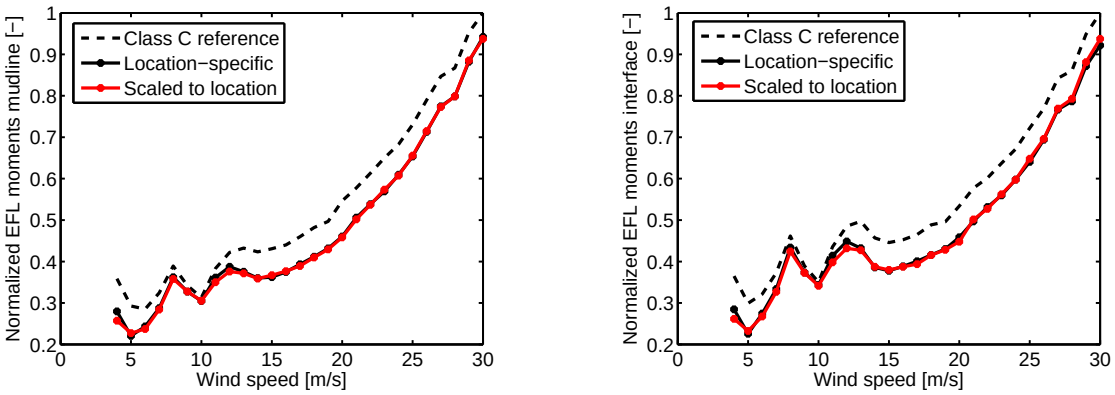

(a) Mudline. **(b)** Interface level.

Figure 4.9: Comparison of normalized wind-only EFLs from reference case, location estimates and aero-elastic computation at (a) mudline and (b) interface level.

The maximum error for all wind speeds and the lifetime error from combination with the Weibull distribution are stated in Table 4.5. The errors of the simplified turbulence intensity scaling are below the errors for wave load calculation, which makes it very suitable to use in the fatigue estimation method.

Location	Max. error	Lifetime error
Interface	3.9%	2.2%
Mudline	3.1%	1.8%

Table 4.5: Turbulence scaling errors for wind-only EFLs.

4.5 Comparison of wind-wave combined loads

The complete tool is verified by comparing estimated wind-wave combined EFLs to time domain aero-elastic simulations for all operational wind speeds. Wave properties corresponding to each wind speed were obtained from lumping scatter diagrams.
Figures 4.10-4.11 present the results of the verification study for EFLs at mudline and interface level: ideally load estimation values (red line) should match the BHawC results (black line). Additionally, the contribution of wind-only and wave-only estimates are visualized in the plot.
The load estimation tool gives the best results around rated wind speed of the turbine. Errors increase for higher wind speeds mainly due to an underestimation of wave loads. Higher inaccuracies of the wave load estimation for more severe sea states is in agreement with previous verification of the wave-only load estimation (cf. Section 4.3.2). Possible reasons are that for higher wind and waves non-linear effects in the wave load and also in the soil-structure interaction play more role which is not captured in the linear frequency domain wave model.
The errors made by quadratic superposition of wind and wave loads are expected to be

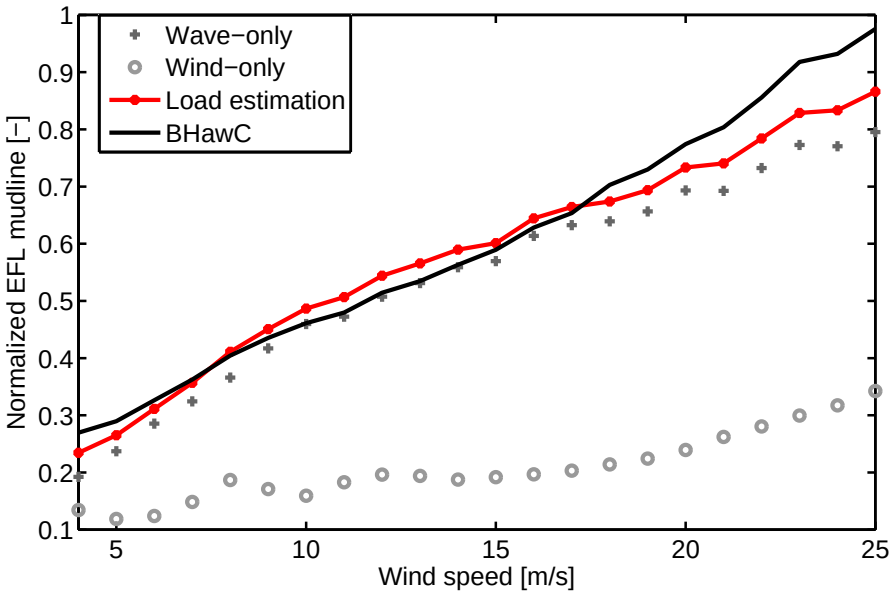

Figure 4.10: Comparison of wind-only, wave-only and wind-wave combined EFLs at mudline from the estimation tool with time domain aero-elastic simulations.

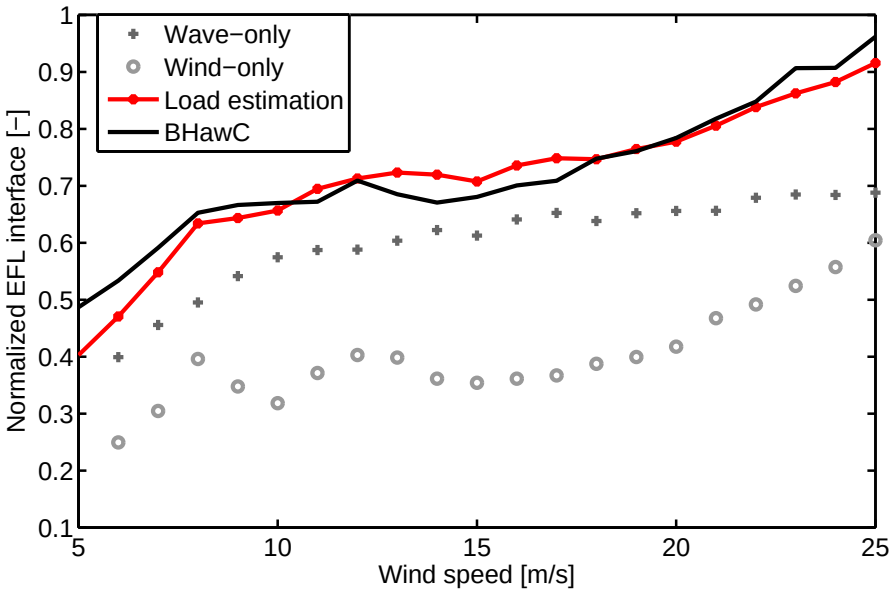

Figure 4.11: Comparison of wind-only, wave-only and wind-wave combined EFLs at interface from the estimation tool with time domain aero-elastic simulations.

higher, the more equal both load components are due to neglecting of the interference. This explains the better match of combined loads and BHawC simulations at mudline since here wave loads are clearly dominating. Since the importance of wind loads increases at interface, the quality of the match decreases. This can also be the reasons for higher errors at low wind speeds. Other possible error sources are the magnitude of assumed aerodynamic damping and small differences in the calculation models, e.g. discretization in structural model, C_M in Morison equation.

Table 4.6 states the maximum error of all wind speeds and the lifetime error from combination with the Weibull distribution (cf. Figure 4.8b). Maximum errors are unconservative due to underestimation of EFLs at high wind speeds. For weighted lifetime EFLs a total load estimation accuracy of 94% for interface and 95% for mudline bending moments (conservative error, EFLs are overestimated) is achieved.

Location	Max. error	Lifetime error
Interface	15.3%	6.0%
Mudline	13.6%	4.9%

Table 4.6: Errors of load estimation tool for wind-wave combined EFLs.

4.6 Discussion of verification study

From all three parts of the verification study (wave-only, wind-only, wind-wave combined), it appears that the fatigue load estimation method delivers results close to time domain simulations for internal bending moments at mudline and seabed. As a result, it is concluded that the developed method is appropriate to be used for site sensitivity assessments and uncertainty studies.

Limitations detected from verification study:

A major limitation of the developed method is that no consistent statement about conservatism is possible as required by industry. The total fatigue estimation method has a maximum conservative lifetime error of 6% (EFLs are overestimated). However, the tool underpredicts loads especially for low and high wind speeds. Thus, for application of the tool in industry projects contingency should be added.
Errors in the combined loads are introduced from wave-only loads, wind-only loads and load combination. Errors in the wave-only EFLs are larger for higher waves. Scaling of wind-only EFLs leads in general to unconservative results for turbulence factors <1. This is less critical since wind loads are of minor importance compared wave loads for deeper water sites and the scaling error is quite small. Combining wind and wave loads is expected to lead to higher errors when both load components are of comparable size. Further limitations are the insufficient estimation of shear forces by the wave tool. Force estimation can be improved if distributed wave loads along the monopile are transferred to internal loads directly instead of integration to equivalent forces. Nevertheless, the inaccuracy of the force estimation is judged less severe since design driving are internal bending moments. For this reason, the verification work of wind-only and wind-wave combined loads as well as the following sensitivity and uncertainty studies only consider bending moments (cf. Chapter 5 and appended papers).

Adequacy of verification study:

The verification study enables statements about the accuracy of the load estimation method compared to time domain simulations for a full set of load cases. A limitation hereby is that time domain simulations themselves contain potential errors and uncertainties. The aero-elastic simulation software used, BHawC, is so far only validated with measurements for onshore, but not for offshore conditions.
The verification study can be improved by eliminating remaining minor differences in calculation models, especially regarding choices of C_M and γ. Additionally, it is limited to one specific site, turbine and support structure. The following list indicates which important aspects have not been covered by the verification study:

- site conditions e.g. MSL or soil conditions,
- structural parameters e.g. eigenfrequency, geometry, mode shapes, elastic properties,
- turbine types,
- simplification of wind-wave directionality,
- lumping of sea states,
- wind-only: natural frequency correction and independence of turbulence and frequency scaling,
- accuracy of time domain simulation software, and
- accuracy of applied aerodynamic damping.

Chapter 5

Fatigue load modeling results

Wave-induced fatigue loads for three simulation cases are presented in this chapter. Special emphasis is placed on the effect of aerodynamic damping and wind-wave misalignment. Afterwards, statistical uncertainty in wave loads is analyzed using resampling methods. Finally, an overview of the content of the appended papers about wave load sensitivity and design clustering is given.

5.1 Wave load analysis

5.1.1 Simulation cases

Selected results of three simulation cases are shown in this chapter in order to demonstrate the functionality of the developed frequency domain method for wave loads. Furthermore, the result analysis illustrates the effect of some of the load influencing parameters defined in Chapter 2.2. The chosen simulation cases use the same structural model and sea states as defined for the verification study (cf. Chapter 4.1). In contrast to the verification study, aerodynamic damping is now included in the structural model.

5.1.2 Comparison of three sea states

According to Chapter 2.2, the wave climate is expected to be highly important for the load level. Therefore, the influence of different significant wave heights and peak periods on the structural response is presented in Figure 5.1. In this comparison wind and waves are modeled misaligned, the difference to fully aligned wind and waves is presented afterwards.
Figure 5.1 shows that the bending moments are higher for more severe sea states, as expected. However, this effect is larger for the response at mudline compared to the response at interface. The effect of larger bending moments is caused by two counteracting effects. Firstly, larger significant wave height leads to more wave excitation energy around wave peak frequency. Secondly, for sea states with larger significant wave heights the wave peak frequency typically shifts to lower values. Consequently, the eigenfrequency of the structure is further away from the wave peak frequency resulting in less dynamic amplification.

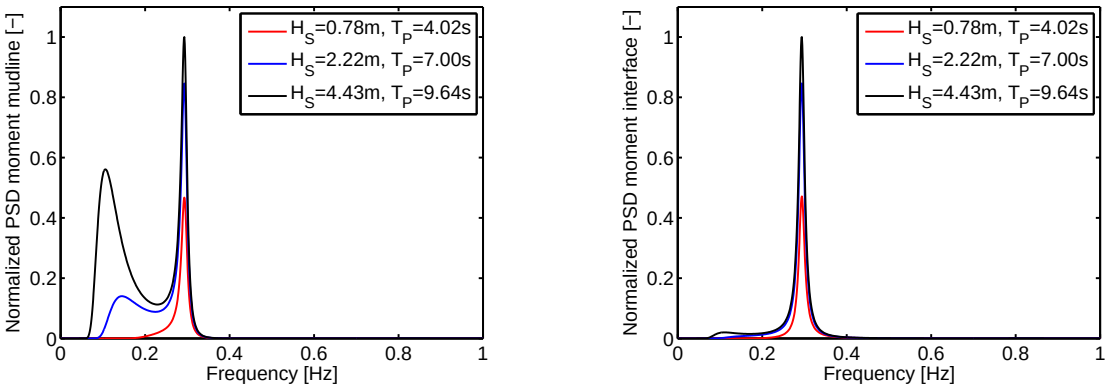

(a) Response moment mudline. **(b)** Response moment interface.

Figure 5.1: PSDs of response bending moment at (a) mudline and (b) interface level for three different sea states.

For the moment spectra at mudline, the response at wave peak frequency is larger for higher sea states. This impact is less visible in the spectra for interface level, which leads to the conclusion that bending moments at interface level are less effected by the severity of the fatigue sea state. These conclusions are also represented in the EFLs which are given in Table 5.1. The data is normalized by setting the lowest load to 1.
From this analysis the conclusion can be drawn that it is highly important for an accurate representation of fatigue loads to consider a sufficient number of sea states when lumping wave information from scatter diagrams during the design process of OWTs.

EFL for moments	**Sea State 1** $H_S = 0.78m$ $T_P = 4.02s$	**Sea State 2** $H_S = 2.22m$ $T_P = 7.0s$	**Sea State 3** $H_S = 4.43m$ $T_P = 9.64s$
Mudline [-]	2.29	3.80	5.02
Interface [-]	1.00	1.37	1.51

Table 5.1: Normalized EFLs of bending moment at mudline and interface for three different sea states.

5.1.3 Effect of wind-wave directionality

Directionality of wind and waves is of high importance for fatigue loads due to several reasons, such as aerodynamic damping and mode excitation [7]. In the following, it is distinguished between the effect of wind and wave directionality with respect to the coordinate system of the structure on the one hand. On the other hand, the direction of waves with respect to wind direction is considered, which is labeled with the term alignment.
Regarding the directionality of waves with respect to the support structure, it is industrial standard that during a time domain simulation waves are applied from a single direction [29]. Afterwards, the simulations for different wave directions,

which are typically lumped into bins of 30degrees, are combined. However, in a real sea environment the wave direction does not stay constant for the length of a time series (e.g. 600s). Consequently, the assumption of constant directionality leads to conservative results since the loads are applied at a single point instead of spread around the structure.
Wind and wave alignment is important, since it has a major effect on the magnitude of aerodynamic damping (cf. Chapter 3.2). Figure 5.2 presents the structural responses for sea state 2 with wind and waves aligned and misaligned.

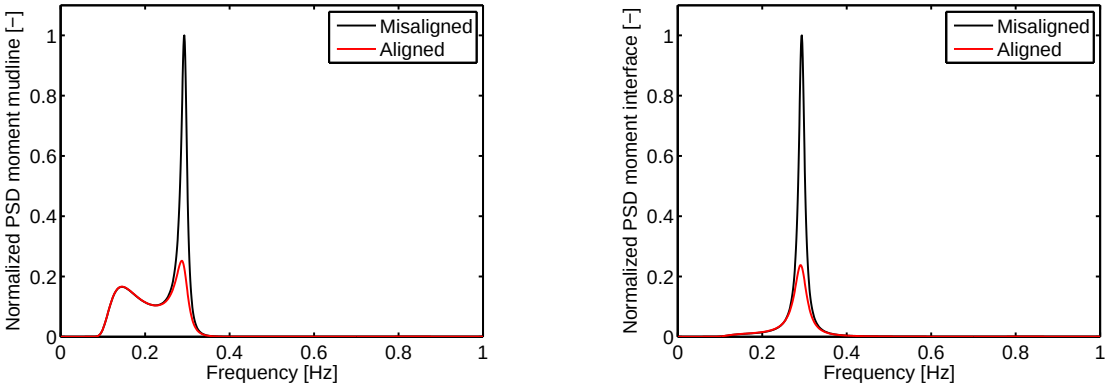

(a) Response moment mudline. **(b)** Response moment interface.

Figure 5.2: PSD of internal bending moments for wind-wave alignment and misalignment at (a) mudline and (b) interface level.

It can be seen that the response of the structure is lower for the case that wind and waves are aligned for mudline as well as for interface level, as expected (cf. Figure 5.2). This is due to the fact the direction of aerodynamic damping is determined by the wind direction. If the waves excite the structure in the same direction, i.e. wind and waves aligned, maximum aerodynamic damping applies also for wave excitation.

Explanation of aerodynamic damping:
The wind turbine oscillates due to wind and wave impact. In the first half-cycle of oscillation, the wind turbine moves with the wind direction. Thus, the rotor experiences a decrease in wind speed resulting in lower thrust force. Since the thrust force is acting in the wind direction, a decrease reduces the move of the turbine in the wind direction and therefore damps this oscillation. In the second half-cycle, the turbine moves against the wind direction. Consequently, the thrust force increases and acts against the turbine move once more. The change of thrust therefore reduced turbine oscillation and is described with aerodynamic damping.

The response peak at the first eigenfrequency is lower for the aligned case since aerodynamic damping is mainly applied on the first fore-aft bending mode of the structure. Consequently, there is less dynamic amplification. The response at wave peak frequency is identical for both cases. Table 5.2 quantifies EFL for the cases shown above. Additionally, EFLs are computed for the same sea state while neglecting aerodynamic damping. The data is normalized by setting the lowest load to 1.

EFL for Moments	Aligned	Misaligned	No Aerodamp
Mudline [-]	3.21	3.96	6.53
Interface [-]	1.00	1.42	2.35

Table 5.2: Normalized EFLs of bending moments at mudline and interface for wind and waves aligned, misaligned and neglecting aerodynamic damping.

As expected from the response spectra, EFLs are higher for the misaligned case. Furthermore, neglecting aerodynamic damping leads to much higher EFLs. This effect is stronger for the bending moment at interface level since the response is mainly in the range of the first eigenfrequency. As a consequence, implementation of aerodynamic damping and proper consideration of wind-wave alignment is essential for frequency domain calculations. This is consistent with the conclusions drawn by Kuehn [6], Salzmann [80] and van der Tempel [7] during their studies of frequency domain methods and aerodynamic damping for OWTs.

5.2 Statistical uncertainty in wave loads

Scatter diagrams contain statistical uncertainty since they are based on limited measurement times and hindcast data (cf. Chapter 2.5). The influence of this statistical uncertainty on wave fatigue loads is analyzed in the following. Therefore, a realistic scatter diagram was resampled with the bootstrapping method as explained in Chapter 3.6.
Figure 5.3a shows the original scatter diagram. The occurrences of H_S-T_P bins are indicated by colors - warmer colors represent higher occurrences. This scatter diagram is based on 30 years of hourly hindcast data, resulting in approximately 250000 observations in total.
The scatter diagram was resampled 10000 times. In the resampling, the number of observations was chosen as 10000, which represents approximately 1.5 years of hourly data. This resampling approach indicates, what variability can be expected in the scatter diagram, when it is based on only 10000 instead of 250000 observations. As an example, the variability of the bin $H_S = 1.125m$ and $T_P = 7.5s$ is presented in Figure 5.3b. The Figure shows the histogram of the probabilities of this bin for 10000 observations normalized to the probability in the original scatter diagram. The probabilities have a binomial distribution as predetermined by the bootstrapping approach of drawing from a sample space with replacement. The standard deviation of this H_S-T_P bin is 6.9%.

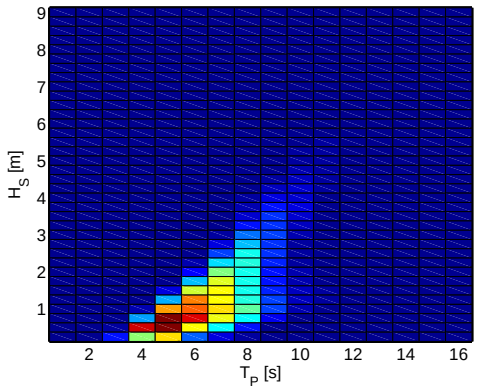

(a) Original scatter diagram.

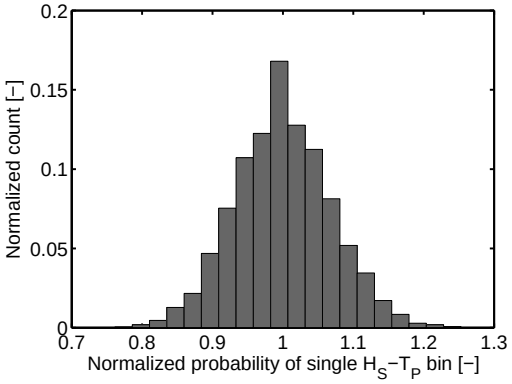

(b) Histogram of probabilities.

Figure 5.3: (a) Original scatter diagram. (b) Histogram of probabilities of the bin $H_S = 1.125m$ and $T_P = 7.5s$ for 10000 observations.

Since bootstrapping is a data-driven approach, standard deviations of more probable wave bins are higher. Figure 5.4a presents the standard deviations as color plot. The maximum standard deviation occurs in the most likely bin of $H_S = 0.875m$ and $T_P = 4.5s$. The bins that do not occur in the original scatter diagram can never occur in a resampled one and thus have zero standard deviation.
The effect of the scatter diagram variability on wave-induced EFLs was analyzed with MCS. EFLs were calculated for all H_S-T_P bins and weighted with the probability of occurrences of this bin in the scatter diagram. Accordingly, one equivalent lifetime fatigue value is obtained for each of the 10000 resampled scatter diagrams. This data set of lifetime EFLs was then analyzed statistically. In Figure 5.4b the histogram of lifetime EFLs is shown.

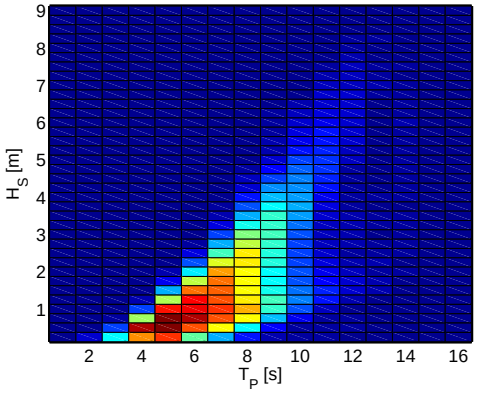

(a) Standard deviations in scatter diagram.

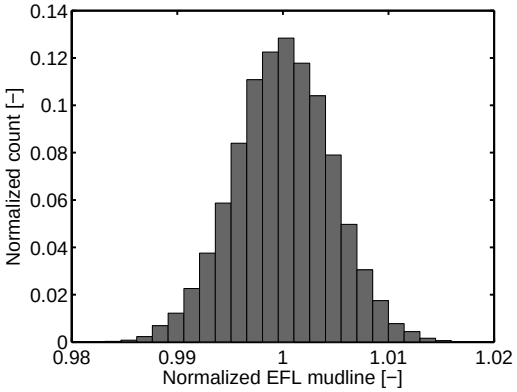

(b) Histogram of EFLs.

Figure 5.4: (a) Standard deviations in scatter diagram for 1.5 years hourly data. (b) Histogram of lifetime EFLs due to statistical uncertainty in scatter diagram.

The statistical properties of the EFL distribution are presented in Table 5.3. As expected, the mean value is identical to the original scatter diagram. A standard deviation of 0.5% shows minor variability in EFLs due to the determined statistical uncertainty in

scatter diagrams. A sensitivity study of wave fatigue loads to wave parameters has shown that the wave period T_P has a significant influence on loads (cf. appended paper B). Nevertheless, significant variabilities within the scatter diagram lead to only a minor variability in wave loads. The reason is the high number of bins in the scatter diagram (629 bins in total), which makes the difference of wave parameters to neighboring bins small ($\Delta H_S = 0.25m$, $\Delta T_P = 1s$). Thus, the effect of higher occurrences of single H_S-T_P bins is compensated by neighboring bins with respect to the lifetime EFLs.

Mean	STD	Skewness	Kurtosis
1.0	0.005	-0.033	2.982

Table 5.3: Statistical properties of EFLs due to scatter diagram variability.

5.3 Sensitivity of wave fatigue loads (Paper A)

The paper describes a sensitivity study of wave fatigue loads to changes in governing parameters such as water depth, soil stiffness, wave height, and wave period. A probabilistic assessment is performed with MCS.
Results show a significant influence of water depth and wave period on EFLs. Normal distributed input parameters in a probabilistic assessment yield a positively skewed probability distribution of EFLs.
This paper demonstrates that the developed probabilistic frequency domain method for wave fatigue loads is suitable for systematic studies on the influence of a variety of parameters on EFLs. Hence the paper is of highest relevance for a systematic concept of design optimization of offshore support structures and thus for the reduction of offshore wind energy costs.

5.4 Optimization of design clustering (Paper B)

The aim of this paper is to apply the probabilistic fatigue estimation method for design clustering in large offshore wind farms. Design clustering was formulated as an optimization problem by calculating site-specific EFLs for every turbine location in the wind farm. Brute-force and discrete optimization algorithm are used to solve the optimization problem. Additionally, the paper illustrates, how uncertainties in load calculation can alter allocation of turbines to clusters.
A study of an example wind farm of 150 turbines in 30-40m water depth shows a maximum EFL difference of 25% within the wind farm. Clustering gave a reduction of up to 13% of total design loads compared to standardized design, with the highest improvements through the first 6 clusters.
This paper suggests a novel approach to design clustering that improves nowadays industry practices. It demonstrates how design clustering can contribute to offshore wind energy cost reduction and is thus of highest relevance.
Further explanation on the discrete optimization algorithm is given in Appendix C.

Chapter 6

Discussion of fatigue estimation and its applications

This chapter assesses the probabilistic fatigue estimation method and its applications for sensitivity assessment and clustering optimization. Limitations are discussed followed by an evaluation of scientific value and potential applications of method and results in industry. In each section, first the fatigue estimation method, then the sensitivity study and finally the clustering approach is discussed.

6.1 Evaluation of estimation method and applications

Verification of the **fatigue load estimation method** confirms an total conservative error of 5–6% for EFLs of bending moments compared to time domain simulation, which indicates good load estimation. A computation time in the order of seconds per load case makes the tool in the order of 100 times faster than conventional time domain simulations. These properties make it suitable for systematic studies of sensitivity of wave loads through MCS and lead to a novel approach to design clustering in large offshore wind farms.
The efficiency and accuracy of the method enables broad application spectra, where fast results are needed, while load estimates are sufficient. However, the estimation tool simplifies many physical phenomena that a potential user has to bear in mind as discussed in the following chapter.
The **sensitivity studies** are suitable to reveal the importance of governing parameters, like water depth and soil stiffness, on EFLs. However, the results are only indicative for the specific problem setting and cannot be generalized. The main insight is gained from the global sensitivity studies, where parameter changes cover the full range of variability that can be expected in an example wind farm. The local sensitivity study quantifies the sensitivity of EFLs for a nominal value, but adds little value additional to the global sensitivity study.
Probabilistic assessments using MCS proved to give a good estimation of the output distribution of EFLs. In the two case studies presented in the scientific papers in Appendix B, the average MC errors for standard deviations of normalized EFLs were only $\pm 0.3\% - 0.4\%$. The drawback of MCS is the computational effort, which was 10–

48h computation time for the presented case studies.
For **design clustering**, the needs of industry are fast and robust tools, while nowadays larger wind farms typically have only 2–3 clusters. Brute-force optimization guarantees global optima at the expense of solution time, making it the best choice for up to 5 clusters for wind farms with 100–150 turbines. For more clusters, the local search algorithm showed very good performance for solution quality and computational efficiency in the order of seconds.
In the probabilistic clustering example shown in Appendix B, only few turbines change cluster since the distribution of STDs follows that of EFLs relatively closely. Thus STDs are only of importance near cluster-borders. It can be concluded that deterministic clustering has good stability for uniform sites.

6.2 Limitations

In order to be computational efficient and simple to use, the **fatigue load estimation tool** simplifies many physical contexts. Assumptions have been discussed in Chapter 3.2. Here, the focus is on critical simplifications concerning industry application and trends in offshore wind. The main aspects are stated in the following:

- The frequency domain model cannot depict non-linearity of waves and soil p-y-curves. This might be a reason that the combined tool underestimates loads for high wind speeds. Being conservative however, is indispensable in industry projects, thus contingency should be added in project applications.

- Diffraction is implemented simplified through the McCamy-Fuchs diffraction correction. Industry is moving to bigger turbines supported by XL-monopiles, thus wave diffraction becomes more important. This might reduce the accuracy of the estimation tool, since Morison equation and linear wave theory are less applicable.

- Wind-wave directionality is simplified into fully aligned and fully misaligned. Additionally, wind and waves are applied from a constant direction with respect to the support structure coordinate system during one simulation. This will lead to conservative results as it is standard in today's offshore wind industry. Due to its efficiency, the fatigue estimation tool offers an ideal starting point to investigate this conservatism in further studies.

- Equivalent loads at MSL and single transfer functions are used instead of distribution along the structure leading to a poor quality estimate of shear forces at mudline and interface level. This is unacceptable in industry projects and the tool should be adjusted to generate distributed transfer functions along the wave-action zone.

- Interaction between wind and wave loads is only accounted for with aerodynamic damping. All other effects are not modeled. This is of minor relevance when one load component is dominating. However, it might become a bottleneck for estimation accuracy for sites with equal magnitude of wind and wave loads.

- Clearly, this study provides an estimation tool for loads on OWT *monopiles*, which cannot be applied to other support structures one-to-one. Alternative support

structures for deeper water sites, especially jackets and floating structures, come into focus of research and industry. Nevertheless, there are still many projects nowadays with monopiles of the size considered in this study.

The limitations of the **verification study** were presented in detail in Chapter 4.6. Most important is here that the verification was conducted with BHawC which is only validated for onshore wind problems. In general, aero-hydro-servo-elastic tools do not reflect real loads exactly like measurement campaigns and code comparisons showed [81, 82]. For example, in a recent publication measured first tower bending frequencies are compared with design frequencies for 400 OWTs [82]. Results show that designs underpredict the natural frequencies in general, with a maximum difference of 20%. However, in the current design of the West of Duddon Sands Offshore Wind Farm a match of $\pm 2\%$ for the first natural frequency has been achieved using an automated design process and a tuned, site-specific pilesoil response formulation [82].
Since the wave load file for this verification study are provided externally, minor differences in parameter choices cannot be ruled out. A discussion with M. Seidel, who recently studied frequency domain methods for wave loads on monopiles as well [12], led to the conclusion that the true accuracy of the frequency domain method is expected to be even higher when eliminating remaining differences of models and calculation parameters in the verification study (personal communication, February 27, 2015).
Regarding applications in future projects, it is critical that the verification study is limited to only one specific site and geometry. Thus, there is no verification of the accuracy of the method for different structural and environmental settings.

The key limitation of the **sensitivity study and probabilistic assessment** is that results strongly depend on chosen input distributions and thus cannot be be generalized. For example, soil stiffness had in paper A only minor influence on EFLs due to high soil stiffness. For the study presented in paper B however, the influence of soil increased significantly for turbine locations with lower soil stiffness. Further limitations are:

- Input distributions were chosen based on publications and expert opinion, but they are not verified with data. The calculated distributions of EFLs have to be examined with reference to input choices and thus cannot be treated as validated.
- Only selected sources of uncertainties are considered which does not nearly cover all uncertainties in the load calculation. Some of the not covered uncertainties might have even higher influence on loads. This can be for example model uncertainties regarding directionality or diffraction correction.
- All parameters are assumed to be independent in the analyses which is questionable, e.g. for H_S and T_P.
- The validity of initial design across all parameter variations was only checked for the first natural frequency constraint and not for stresses and structural resistance.
- The study examines only load uncertainty and does not investigate uncertainty in structural resistances. Uncertainty in structural resistance can even be more significant for structural reliability than load uncertainty and needs to be added for use in reliability-based design.

The sensitivity studies and probabilistic assessments focus mainly on wave loads. The implemented wind load scaling method is comparatively unappealing for use in sensitivity study with MCS since (i) factor influence can be derived directly from the scaling approach and (ii) wind loads contribute less in combined fatigue loads for the chosen example wind farm so that uncertainty influence is barely visible in total EFLs. Accordingly, the results of the sensitivity studies presented in this thesis are mainly useful for deeper water sites, where wave loads are dominating.

A detailed description of the limitation for **design clustering** is given in paper B in Appendix B. The primary limitation for application in practice is the formulation of the optimization problem regarding "design loads" and not costs. Furthermore, possible constraints like maximum variation of MSL or load interpolation within clusters are not considered.

6.3 Industry application

The suggested **fatigue load estimation** approach has an efficiency that makes it very appealing for industry application. The essential question is: Is the method accurate enough for use in practice?
This question cannot be answered in this thesis, since it depends on application purposes and intentions of the user. The summary of limitations critical for application, as stated previously, should enable users to take their decisions fact-based. Assuming that the accuracy is sufficient for purpose, possible applications are:

1. clustering of turbines and design position optimization,
2. sensitivity and uncertainty analysis of load calculations,
3. interpolation of wave fatigue loads between design positions,
4. wind farm layout optimization, and
5. use in actual design process instead of time domain methods e.g. in preliminary design phase.

The first and second item were demonstrated in this thesis. Interpolation of fatigue loads between design position can either be based on the results of the sensitivity study, or on fatigue load estimates directly. Regarding item 4, wind farm layout is typically optimized for power output through wake modeling and cable costs [83]. Having this fast load estimation tool, support structure loads and costs can add a new dimension to layout optimization. The use of the method for preliminary design is of highest interest for industry. Additionally, the tool can help for proper lumping of sea states in preliminary design due to its efficiency. For detailed design and certification however, more elaborate tools are recommended.

Results from the **sensitivity study** can be applied to determine which parameters should be known with good accuracy already in an initial project phase. For this example case, MSL was confirmed to be one of the most influential site input parameter. Soil stiffness became an important parameter for poor quality soils. It was emphasized

before that the results of the sensitivity study cannot be generalized, however in every situation the first eigenfrequency of the structure showed high influence. If no detailed studies for a project exist, the first eigenfrequency is recommended as initial indicator for sensitivity.

The main message from the **probabilistic assessment** for industry is that uncertainties in input parameters can lead to a shifted mean value of EFLs compared to deterministic analysis. The distribution of EFLs depend highly on the range of input uncertainties, thus applying a general safety factor is not target-aiming for design optimization. A possible application of the probabilistic assessment approach is to perform the analysis for the highest loaded position of the wind farm, which is assumed to give a conservative variability for all other locations. This result combined with uncertainty in structural resistance can serve as suggestion for optimized safety factors for the specific wind farm and thus reduce design conservatism.

The **design clustering** tool is designed for immediate application in industry. It should be used in early project phases to improve decision-making on the optimal number of clusters and cluster configuration of a wind farm. Probabilistic clustering showed little effect on allocation of turbines to clusters and therefore is not recommended for daily engineering practice. It can be useful, however, for application with specific clustering problems, where only limited experience is available (e.g. large variations in site-specific uncertainties).

6.4 Scientific value

Frequency domain methods for wave load calculations have been applied to OWTs by several researchers before (cf. Chaper 2.3.4). Also the wind load scaling approach and the combination of wind and wave loads is based on existing knowledge and publications (cf. Chapter 3).
The main novelty of this work is the implementation of these tools for use in probabilistic assessments with MCS, sensitivity studies, and for design clustering in large offshore wind farms. Additionally, the definition and solution of design clustering of OWTs as a mathematical problem in discrete optimization is a novel approach.

Generalization of work:
For the offshore wind community, it is of particular interest to know how the results of this study can be generalized. The suggested **fatigue estimation tool** is made for monopile-based OWT and cannot be used directly for other support structures. However, the applied methodology and the idea, how to approach the problem of site variations, is very suitable for generalization to other foundation types. Published work exists that evaluates frequency domain analysis for other support structures, for example on semi-submersibles [45].
Once the estimation tool is extended, the **sensitivity and probabilistic assessments** can be performed with an identical methodology using MCS. The **clustering approach** is applicable directly for other support structure types. With load estimates available for all turbine locations, the suggested formulation of the optimization problem and solution algorithms can be applied generalized.

Chapter 7

Conclusions and recommendations

As cost reduction remains the most important challenge of offshore wind energy, conservatism of support structure designs has to be reduced. An important approach is the integration of variations of environmental site condition in the design process of large offshore wind farms, since they proved to have significant influence on support structure loading. In early design phases, OWTs are typically grouped into clusters, in which the support structure design is only performed once. A better understanding of load site variations and uncertainty in load calculations is needed to improve design clustering, and thus reduce design conservatism. As a result, the central research question of this thesis is (cf. Chapter 1):

How can probabilistic fatigue load estimation improve turbine clustering in large offshore wind farms to reduce costs of offshore wind energy?

In this thesis, a developed **probabilistic fatigue load estimation method** has proven to be suitable for site-specific EFL estimation. The method consists of four core elements:

1. frequency domain analysis to calculate wave loads,
2. turbulence and natural frequency scaling for wind loads,
3. combination of wind and wave loads with quadratic superposition, and
4. MCS to assess uncertainties.

A verified accuracy of 95% for lifetime EFLs of bending moments at mudline compared to time domain simulations with only seconds of computation time for one simulation case makes the estimation tool ideal for application in clustering optimization, load interpolation, uncertainty studies and preliminary design.
With the estimation tool, design clustering can now be formulated as an discrete optimization problem by calculating site-specific (probabilistic) EFLs for every turbine location in wind farms. A realistic case study with 150 OWTs in 30-40m water depth demonstrated the value of clustering optimization as it gave a reduction of up to 13% of total design loads compared to standardized design. Thus, a valuable design clustering approach was developed for use in offshore wind industry. It can, therefore, be concluded that the central research question of this master thesis has been answered. In the following, conclusions for the corresponding three research objectives are drawn.

Results of the **sensitivity study** show a significant influence of water depth and wave period on EFLs. The influence of soil stiffness on EFLs is minor for soils with high stiffness, but can increase significant for soils with low stiffness.
The computational efficiency of the fatigue estimation method allowed to assess uncertainties with MCS. Normal distributed input parameters in a **probabilistic assessment** yield a positively skewed probability distribution of EFLs. The variability of loads over a wind farm was shown to be quite similar with a maximum absolute difference of 4.5% for standard deviations. Turbines with higher EFLs featured higher variability. This is consistent with higher order sensitivity trends for larger MSL and lower soil stiffness.
For the exemplary wind farm, it was demonstrated that brute-force and discrete optimization algorithms are well suited to solve the formulated **clustering** optimization problem. Probabilistic clustering, which accounts for load variability by increasing the mean load level with 3*STD, proved to be only relevant at cluster borders leading to a difference in allocation for 12 out of 150 turbines.

To conclude, this project shows that it is essential to account for load differences in large offshore wind farms due to varying site conditions. Probabilistic load variability was shown to be highly dependent on input uncertainties. This questions the usefulness of generic safety factors in deterministic load calculations for design optimization. Design clustering proved to be an important approach for optimization of support structures and thus for cost reduction of offshore wind energy. As a key result, the suggested clustering approach is highly recommended for application in industry.

Recommendations:

For academics and industry, this work contributes to better understanding of load sensitivity to varying and uncertain site conditions, leading to enhanced turbine clustering. Further work is needed to improve the suggested fatigue estimation method and its verification and to extend sensitivity studies and design clustering. Therefore, five major recommendations are defined for future development:

1. **Improvement of estimation method**
   In order to increase estimation accuracy, the method should be extended to use distributed transfer functions in wave load calculations. Additionally, a detailed study of applicable aerodynamic damping values is recommended. The influence of support structure appurtenances on loads, for instance boat landing, should be investigated and accounted for in the estimation process. Since the estimation method proved to be valuable for a broad range of applications, further studies to develop load estimation tools for alternative support structures, e.g. jackets and floating foundations, are recommended.

2. **Extension of verification study**
   Further work is needed to extend the verification study to different structural, environmental and turbines settings. More precisely, focus of the studies should be to confirm the accuracy of the estimation method for (i) different eigenfrequencies of the support structure to validate results of sensitivity studies presented in the appended papers, (ii) shallow water depth where wind-loads have more influence, and (iii) larger turbines with bigger monopiles due to diffraction

effects. Additionally, the tool should be validated with other codes or ideally with experimental data in the future.

3. **Including uncertainty of structural resistance**
   The probabilistic assessment only accounts for load uncertainty, however uncertainty in structural resistance is also highly important for structural reliability. Thus an extension of the probabilistic approach to include uncertainty in resistance is recommended. Clustering can then be based on structural reliability instead of (probabilistic) design loads only.

4. **Clustering for cost optimization**
   Clustering optimization minimizes design loads which are assumed to be indicative for mass and costs of the support structure. Since this relation is not linear, further research is required to formulate the optimization problem regarding support structure costs. Finally, a study revealing the economic value of clustering optimization for cost of wind energy based on data from existing wind farm projects is desirable.

5. **Generalization of work**
   For generalization of the load estimation tool to alternative support structures, the methodology suggested in this thesis can provide a good development basis. Previous studies have shown that frequency domain analysis is suitable to calculate wave loads on various foundation types (cf. Chapter 6.4). New studies are needed to confirm the functionality of the wind load scaling approach for other support structures. It is expected to perform well for jackets due to small wave-induced support structure movements, however not be suitable for floating platforms. Finally, the relevance of site conditions and clustering for design optimization should be evaluated for alternative support structures.

Bibliography

[1] M. Bilgili, A. Yasar, and E. Simsek, "Offshore wind power development in europe and its comparison with onshore counterpart," *Renewable and Sustainable Energy Reviews*, vol. 15, no. 2, pp. 905–915, 2011.

[2] DNV GL Group, "Offshore wind: A manifesto for cost reduction," 2014. Retrieved from www.dnvgl.com on 12/12/2014.

[3] G. Corbetta, I. Pineda, J. Moccia, and J. Guillet, "The european offshore wind industry - key trends and statistics 2013," tech. rep., European Wind Energy Association, 2014.

[4] M. Seidel, "Integrated design approach for the material optimisation of steel monopiles," Presentation at 4th Annual Future Offshore Foundations Forum, Hamburg, Germany, 2014.

[5] F. Vorpahl, H. Schwarze, T. Fischer, M. Seidel, and J. Jonkman, "Offshore wind turbine environment, loads, simulation, and design," *Wiley Interdisciplinary Reviews: Energy and Environment*, vol. 2, no. 5, pp. 548–570, 2013.

[6] M. J. Kühn, *Dynamics and design optimisation of offshore wind energy conversion systems*. PhD thesis, TU Delft, The Netherlands, 2001.

[7] J. van der Tempel, *Design of support structures for offshore wind turbines*. PhD thesis, TU Delft, The Netherlands, 2006.

[8] L. Ziegler, S. Voormeeren, S. Schafhirt, and M. Muskulus, "Sensitivity of wave fatigue loads on offshore wind turbines under varying site conditions," *Energy Procedia*, in press.

[9] L. Arany, S. Bhattacharya, J. Macdonald, and S. J. Hogan, "Simplified critical mudline bending moment spectra of offshore wind turbine support structures," *Wind Energy*, 2014. (doi:10.1002/we.1812).

[10] M. Muskulus, "Simplified rotor load models and fatigue damage estimates for offshore wind turbines," *Philosophical Transactions of the Royal Society of London A: Mathematical, Physical and Engineering Sciences*, vol. 373, no. 2035, 2015.

[11] D. Zwick and M. Muskulus, "Simplified fatigue load assessment in offshore wind turbine structural analysis," *Wind Energy*, 2015. (doi: 10.1002/we.1831).

[12] M. Seidel, "Wave induced fatigue loads," *Stahlbau*, vol. 83, no. 8, pp. 535–541, 2014.

[13] B. Yeter, Y. Garbatov, and C. G. Soares, "Spectral fatigue assessment of an offshore wind turbine structure under wave and wind loading," *Developments in Maritime Transportation and Exploitation of Sea Resources*, vol. 1, pp. 425–433, 2013.

[14] P. Ragan and L. Manuel, "Comparing estimates of wind turbine fatigue loads using time-domain and spectral methods," *Wind engineering*, vol. 31, no. 2, pp. 83–99, 2007.

[15] M. Mršnik, J. Slavič, and M. Boltežar, "Frequency-domain methods for a vibration-fatigue-life estimation–application to real data," *International journal of fatigue*, vol. 47, pp. 8–17, 2013.

[16] L. Manuel, P. S. Veers, and S. R. Winterstein, "Parametric models for estimating wind turbine fatigue loads for design," *Journal of solar energy engineering*, vol. 123, no. 4, pp. 346–355, 2001.

[17] D. Zwick and M. Muskulus, "The simulation error caused by input loading variability in offshore wind turbine structural analysis," *Wind Energy*, 2014. (doi: 10.1002/we.1767).

[18] B. Yeter, Y. Garbatov, and C. Guedes Soares, "Fatigue reliability assessment of an offshore supporting structure," *The Maritime Technology and Engineering*, vol. 1, pp. 671–680, 2015.

[19] H. F. Veldkamp, *Chances in wind energy: a probalistic approach to wind turbine fatigue design*. PhD thesis, TU Delft, The Netherlands, 2006.

[20] M. Zaaijer, "Foundation modelling to assess dynamic behaviour of offshore wind turbines," *Applied Ocean Research*, vol. 28, no. 1, pp. 45–57, 2006.

[21] W. De Vries, N. K. Vemula, P. Passon, T. Fischer, D. Kaufer, D. Matha, *et al.*, "Final report WP 4.2: Support structure concepts for deep water sites," tech. rep., Upwind, 2011.

[22] M. Seidel, "Wave induced fatigue loads on monopiles - new approaches for lumping of scatter tables and site specific interpolation of fatigue loads," Conference Proceedings IWEC, Hannover, Germany, 2014.

[23] J. Twidell and G. Gaudiosi, *Offshore wind power*. Multi-Science Publishing Company, 2009.

[24] M. O. Hansen, *Aerodynamics of wind turbines*. Earthscan, 2nd ed., 2000.

[25] O. Faltinsen, *Sea loads on ships and offshore structures*. Cambridge University Press, 1990.

[26] International Electrotechnical Commission, "IEC 61400-3: Design requirements for offshore wind turbines," 2009.

[27] Det Norske Veritas, "DNV-OS-J101: Design of offshore wind turbine structures," 2014.

[28] F. Savenije and J. Peeringa, "Integral wind turbine design and analysis in the frequency domain," Conference Proceedings EWEA Offshore, Stockholm, Sweden, 2009.

[29] R. Haghi, "Loads and load cases," Lecture Notes OE5655-Offshore Wind Support Structures, TU Delft, The Netherlands, 2014.

[30] T. Camp, M. Morris, R. Van Rooij, J. Van Der Tempel, M. Zaaijer, A. Henderson, *et al.*, "Design methods for offshore wind turbines at exposed sites," tech. rep., OWTES Project, 2003.

[31] A. Henderson, M. Zaaijer, and T. Camp, "Hydrodynamic loading on offshore wind turbines," Conference Proceedings ISOPE, Toulon, France.

[32] E. Smid, "Offshore load calculations - load calculation process for sales projects," Presentation at Siemens Wind Power, Den Haag, The Netherlands, 2014.

[33] R. Haghi, T. Ashuri, P. L. van der Valk, and D. P. Molenaar, "Integrated multidisciplinary constrained optimization of offshore support structures," vol. 555, no. 1, 2014.

[34] T. Fischer, W. de Vries, P. Rainey, B. Schmidt, K. Argyriadis, and M. Kuehn, "Offshore support structure optimization by means of integrated design and controls," *Wind Energy*, vol. 15, no. 1, pp. 99–117, 2012.

[35] D. Kaufer, N. Cosack, C. Böker, M. Seidel, and M. Kühn, "Integrated analysis of the dynamics of offshore wind turbines with arbitrary support structures," Conference Proceedings EWEC, Marseille, France, 2009.

[36] T. Ashuri, *Beyond classical upscaling: integrated aeroservoelastic design and optimization of large offshore wind turbines*. PhD thesis, TU Delft, The Netherlands, 2012.

[37] P. S. Veers, "All wind farm uncertainty is not the same: the economics of common versus independent causes," Conference Proceedings AWEA Windpower'95, Washington, USA, 1995.

[38] P. S. Veers, "Fatigue reliability of wind turbine fleets: The effect of uncertainty on projected costs," *Journal of solar energy engineering*, vol. 118, no. 4, pp. 222–227, 1996.

[39] J. D. Sørensen and H. S. Toft, "Probabilistic design of wind turbines," *Energies*, vol. 3, no. 2, pp. 241–257, 2010.

[40] M. Hansen, L. Lohaus, T. Schlurmann, M. Achmus, P. Schaumann, R. Rolfes, *et al.*, "Probabilistic safety assessment of offshore wind turbines: Annual report 2010," tech. rep., PSA, 2013.

[41] W. Dong, T. Moan, and Z. Gao, "Long-term fatigue analysis of multi-planar tubular joints for jacket-type offshore wind turbine in time domain," *Engineering Structures*, vol. 33, no. 6, pp. 2002–2014, 2011.

[42] W. Dong, T. Moan, and Z. Gao, "Fatigue reliability analysis of the jacket support structure for offshore wind turbine considering the effect of corrosion and inspection," *Reliability Engineering & System Safety*, vol. 106, pp. 11–27, 2012.

[43] B. Ernst, H. Schmitt, and J. R. Seume, "Effect of geometric uncertainties on the aerodynamic characteristic of offshore wind turbine blades," *Journal of Physics: Conference Series*, vol. 555, no. 1, 2014.

[44] J. D. Sorensen and N. J. Tarp-Johansen, "Reliability-based optimization and optimal reliability level of offshore wind turbines," *International Journal of Offshore and Polar Engineering*, vol. 15, no. 2, pp. 141–146, 2005.

[45] M. I. Kvittem, *Modelling and response analysis for fatigue design of a semi-submersible wind turbine*. PhD thesis, NTNU, Norway, 2014.

[46] Det Norske Veritas, "DNVRP-C103: Column-stabilised units," 2010.

[47] T. Burton, D. Sharpe, N. Jenkins, and E. Bossanyi, *Wind energy handbook*. John Wiley & Sons, 2001.

[48] N. D. Barltrop and A. J. Adams, *Dynamics of fixed marine structures*. Butterworth-Heinemann, 3rd ed., 1991.

[49] S. K. Chakrabarti, *Hydrodynamics of offshore structures*. WIT press, 1987.

[50] J. Morison, J. Johnson, S. Schaaf, *et al.*, "The force exerted by surface waves on piles," *Journal of Petroleum Technology*, vol. 2, no. 5, pp. 149–154, 1950.

[51] Det Norske Veritas, "DNV-RP-C205: Environmental conditions and environmental loads," 2007.

[52] R. C. MacCamy and R. A. Fuchs, "Wave forces on piles: a diffraction theory," tech. rep., Beach Erosion Board, 1954.

[53] P. F. Skjoldan, *Aeroelastic modal dynamics of wind turbines including anisotropic effects*. PhD thesis, DTU, Denmark, 2011.

[54] S. Hirdaris, W. Bai, D. Dessi, A. Ergin, X. Gu, O. Hermundstad, *et al.*, "Loads for use in the design of ships and offshore structures," *Ocean Engineering*, vol. 78, pp. 131–174, 2014.

[55] C. G. Soares, "Effect of spectral shape uncertainty in the short term wave-induced ship responses," *Applied Ocean Research*, vol. 12, no. 2, pp. 54–69, 1990.

[56] E. Smid, "Load differences within offshore wind farms," tech. rep., Siemens Wind Power, 2014.

[57] T. Dirlik, *Application of computers in fatigue analysis*. PhD thesis, University of Warwick, England, 1985.

[58] American Petroleum Institute, "RP 2A-WSD: Recommended practice for planning, designing and constructing fixed offshore platforms-working stress design," 2005.

[59] P. Passon and M. Kühn, "State-of-the-art and development needs of simulation codes for offshore wind turbines," Conference Proceedings IEA Expert Meeting, Copenhagen, Denmark, 2005.

[60] L. E. Borgman, "The spectral density for ocean wave forces," Conference Proceedings Speciality Conference, Santa Barbara, USA, 1965.

[61] J. Wheeler *et al.*, "Method for calculating forces produced by irregular waves," *Journal of Petroleum Technology*, vol. 22, no. 3, pp. 359–367, 1970.

[62] S. Manenti and F. Petrini, "Dynamic analysis of an offshore wind turbine: Wind-waves nonlinear interaction," Conference Proceedings Earth and Space, Honolulu, USA, pp. 2014–2026, 2010.

[63] K. Hasselmann, T. Barnett, E. Bouws, H. Carlson, D. Cartwright, K. Enke, *et al.*, "Measurements of wind-wave growth and swell decay during the joint north sea wave project (JONSWAP)," tech. rep., Deutsches Hydrographisches Institut, 1973.

[64] S. Voormeeren, "Finite element model of offshore wind support structure," Internal Tool of Siemens Wind Power, Den Haag, The Netherlands, 2014.

[65] R. R. Craig and A. J. Kurdila, *Fundamentals of structural dynamics*. John Wiley & Sons, 2006.

[66] T. J. Hughes, *The finite element method: linear static and dynamic finite element analysis*. Courier Dover Publications, 2012.

[67] A. Naess and T. Moan, *Stochastic dynamics of marine structures*. Cambridge University Press, 2012.

[68] A. Carpinteri, *Handbook of fatigue crack: Propagation in metallic structures*. Elsevier, 1994.

[69] J. E. Shigley, *Shigley's mechanical engineering design*. McGraw-Hill, 2008.

[70] M. Matsuishi and T. Endo, "Fatigue of metals subjected to varying stress," *Japan Society of Mechanical Engineers, Fukuoka, Japan*, pp. 37–40, 1968.

[71] D. E. Newland, *An introduction to random vibrations, spectral & wavelet analysis*. Courier Corporation, 2012.

[72] E. Smid, "Influence of turbulence on fatigue loads," 2013. Internal Report ID: E W EN OEN DES TLS 4 2-50-0000-942401, Siemens Wind Power. Den Haag, The Netherlands.

[73] S. Frandsen, R. Barthelmie, S. Pryor, O. Rathmann, S. Larsen, J. Højstrup, *et al.*, "Analytical modelling of wind speed deficit in large offshore wind farms," *Wind energy*, vol. 9, no. 1-2, pp. 39–53, 2006.

[74] International Electrotechnical Commission, "IEC 61400-1: Design requirements," 2006.

[75] R. Kleiss and A. Lazopoulos, "Error in monte carlo, quasi-error in quasi-monte carlo," *Computer Physics Communications*, vol. 175, no. 2, pp. 93–115, 2006.

[76] W. Carswell, S. R. Arwade, D. J. DeGroot, and M. A. Lackner, "Soil–structure reliability of offshore wind turbine monopile foundations," *Wind Energy*, vol. 18, no. 3, pp. 483–498, 2015.

[77] B. Efron, *The jackknife, the bootstrap and other resampling plans*, vol. 38. Society for Industrial and Applied Mathematics, 1982.

[78] A. Nieslony, "Rainflow counting algorithm," 2003. MATLAB Central File Exchange. Retrieved from www.mathworks.com on 18/09/2014.

[79] P. D. Welch, "The use of fast fourier transform for the estimation of power spectra: a method based on time averaging over short, modified periodograms," *IEEE Transactions on audio and electroacoustics*, vol. 15, no. 2, pp. 70–73, 1967.

[80] D. Salzmann and J. Van der Tempel, "Aerodynamic damping in the design of support structures for offshore wind turbines," Conference Proceedings Copenhagen Offshore Wind, 2005.

[81] J. Jonkman and W. Musial, "Offshore code comparison collaboration (OC3) for IEA task 23 offshore wind technology and deployment," tech. rep., National Renewable Energy Laboratory, 2010.

[82] D. Kallehave, B. W. Byrne, C. L. Thilsted, and K. K. Mikkelsen, "Optimization of monopiles for offshore wind turbines," *Philosophical Transactions of the Royal Society of London A: Mathematical, Physical and Engineering Sciences*, vol. 373, no. 2035, 2015.

[83] C. N. Elkinton, J. F. Manwell, and J. G. McGowan, "Optimizing the layout of offshore wind energy systems," *Marine Technology Society Journal*, vol. 42, no. 2, pp. 19–27, 2008.

Appendix A

Properties of developed method

The following table presents the explicit values chosen for overall coefficients, discretization and other input parameters independent of specific simulation cases.

Component	Input	Description	Value	Unit
Discretization	f	frequency vector	0:0.001:1	[Hz]
	z	depth vector	0:0.5:d	[m]
Wave spectrum	γ	peak factor	$f(H_S, T_P)^{(1)}$	[-]
	g	gravitational acceleration	9.81	[m/s^2]
	d	water depth	30-40	[m]
Morison equation	ρ	water density	1025	[kg/m^3]
	C_D	drag coefficient	1	[-]
	C_M	inertia coefficient	$f(\lambda, D)$	[-]
Fatigue loads	m	Woehler slope	4	[-]
	T_{life}	structure lifetime	20	[years]
	N_k	equivalent cycle number	10^6	[-]

(1) Definition of peak enhancement factor γ according to IEC 61400-3 [26] if not defined in the text otherwise:

$$\gamma = \begin{cases} 5 & \text{for} \quad \frac{T_P}{\sqrt{H_S}} \leq 3.6 \\ exp(5.75 - 1.15\frac{T_P}{\sqrt{H_S}}) & \text{for} \quad 3.6 < \frac{T_P}{\sqrt{H_S}} \leq 5 \\ 1 & \text{for} \quad \frac{T_P}{\sqrt{H_S}} > 5 \end{cases} \tag{A.1}$$

Appendix B

Scientific papers

Paper A

Sensitivity of Wave Fatigue Loads on Offshore Wind Turbines under varying Site Conditions

L. Ziegler, S. Voormeeren, S. Schafhirt and M. Muskulus

05/01/2015: Submission for EERA DeepWind'2015
08/04/2015: Accepted with with minor editorial changes for publication in Elsevier Energy Procedia
20/04/2015: Submission of revised paper

Available online at www.sciencedirect.com

SciVerse ScienceDirect

Energy Procedia 00 (2015) 000–000

Energy Procedia

www.elsevier.com/locate/procedia

12th Deep Sea Offshore Wind R&D Conference, EERA DeepWind'2015

Sensitivity of Wave Fatigue Loads on Offshore Wind Turbines under varying Site Conditions

Lisa Ziegler[1,2]*, Sven Voormeeren[2], Sebastian Schafhirt[1], Michael Muskulus[1]

[1] *Department of Civil and Transport Engineering, NTNU, Høgskoleringen 7A, 7491 Trondheim, Norway*
[2] *Siemens Wind Power, Offshore Center of Competence, Prinses Beatrixlaan 800, 2595BN The Hague, Netherlands*

Abstract

Considerable variations in environmental site conditions can exist within large offshore wind farms leading to divergent fatigue loads on support structures. An efficient frequency-domain method to calculate wave-induced fatigue loads on offshore wind turbine monopile foundations was developed. A verification study with time-domain simulations for a 4MW offshore wind turbine showed result accuracies of more than 90% for equivalent bending moments at mudline and interface level. This accuracy and computation times in the order of seconds make the frequency-domain method ideal for preliminary design and support structure optimization. The model is applied in sensitivity analysis of fatigue loads using Monte-Carlo simulations. Local and global sensitivity studies and a probabilistic assessment give insight into the importance of site parameters like water depth, soil stiffness, wave height, and wave period on fatigue loads. Results show a significant influence of water depth and wave period. This provides a basis for design optimization, load interpolation and uncertainty analysis in large wind farms.

Selection and peer-review under responsibility of SINTEF Energi AS.

Offshore wind turbines; wave fatigue load; sensitivity analysis; frequency-domain; site variation

1. Introduction

Fatigue loads on offshore wind turbine (OWT) support structures vary in large wind farms due to changing environmental site conditions. Full load calculations, which are commonly done in the time-domain, are computationally demanding and cannot be performed for each turbine within the wind farm [1]. In practice, loads

* Corresponding author
E-mail address: lisa.ziegler@siemens.com

Selection and peer-review under responsibility of SINTEF Energi AS.

are evaluated for a limited number of design positions within the wind farm. Insight into the sensitivity of loads due to varying site conditions provides a basis for design position optimization during early design phases leading to more cost-effective support structures.

Previous studies investigated the influence of site parameters and foundation configuration on the natural frequency but emphasized the need for further work regarding sensitivity of fatigue damage [2, 3]. Large offshore wind farms are predominantly located in deeper water (25-40m) with monopile support structures. For this setup the design is typically governed by fatigue loads with a significant contribution coming from wave excitation [4].

Therefore, a computational model for efficient assessment of wave induced fatigue damage on monopiles was developed using frequency-domain analysis. For review of implementation and accuracy, a verification study was performed comparing time-domain simulation of a reference case to results obtained with the developed method. Due to its speed and accuracy, the developed method is ideal for sensitivity analysis. This paper aims at better insight into the sensitivity of fatigue loads to varying site conditions like mean sea level (MSL), soil properties, significant wave height (H_S) and wave peak period (T_P).

The remainder of this paper is organized as follows. First, Section 2 outlines the developed frequency-domain method (FDM), followed by a summary of the verification with time-domain simulations in Section 3. Thereafter, sensitivity analyses are addressed in Section 4, while Section 5 provides a discussion of the obtained results. Finally, the paper is ended with conclusions in Section 6.

2. Frequency-Domain Method for Wave Fatigue Loads

In current engineering practice fatigue loads on OWTs are typically assessed by extensive time-domain simulations of various load cases. The time-domain enables non-linear analysis with coupled simulations of wind, wave, and control system. Results of time-domain analysis are considered most accurate and are commonly used for certification. However, for preliminary support structure design less sophisticated models might be sufficient.

FDMs as an alternative have the potential to heavily decrease computational costs. Since frequency-domain analysis is linearized and wind and wave action decoupled, the method is considered less accurate than time-domain approaches. Frequency analysis has been applied to OWTs by several researchers [4, 5, 6, 7]. Kuehn [5] suggested a simplified method for fatigue analysis by superimposing time-domain simulations of aerodynamic loads with frequency-domain results of wave loads on the support structure. Later, van der Tempel [6] applied frequency-domain analysis to integrated support structure design. Both researchers treat wind and wave loads separately but emphasize the importance of dynamic interactions between turbine and support structure caused by coupled wind and wave excitation. The most important dynamic interaction is aerodynamic damping.

2.1. Approach

The developed FDM consists of three parts. Firstly, wave loading is obtained from a linearized Morison equation using wave kinematics power spectral densities (PSD) based on JONSWAP wave spectra. Secondly, structural transfer functions to determine the internal load response spectra are derived from a finite element (FE) model. After performing a modal analysis on this FE model, the transfer functions are synthesized using the modes in the frequency range of interest at the desired input and output degrees of freedom. In this synthesis, aerodynamic damping as a function of wind speed and wind-wave misalignment is taken into account. Finally, equivalent load ranges are obtained from the response spectra by use of Dirlik's method that provides information equivalent to rainflow-counting in the time-domain [8]. Output of the program are equivalent fatigue loads (EFL) for a specified number of cycles. The achieved computation time for one simulation case is approximately 10s.

2.2. Assumptions

To create a fast method, several assumptions are implemented simplifying full load calculations.

Assumptions for environmental data: Soil is modeled with distributed linear springs according to the Winkler model [9, 10]. Further effects like currents and sea ice are neglected, since the effects on the load level are

expected to be minor. Sea ice can have a major impact on loads but is assumed to not occur for the considered sites e.g. North Sea. It is assumed that scour protection is installed so that erosion and scour effects are not considered.

Assumptions for structural model: Foundation and tower are described with a linear FE model of Timoshenko beam elements. It is based on a realistic reference design, where outer diameter, wall thickness and elastic properties change over height of the support structure. The first ten modes of the structure are taken into account according to ten eigenfrequencies. The rotor-nacelle-assembly (RNA) is modeled as an equivalent concentrated mass on top of the tower. Damping consists of a contribution from combined structural, hydrodynamic and soil damping (damping ratio ca. 1%) and a contribution from aerodynamic damping (damping ratio ca. 1.5 - 8%). The latter is a function of wind speed, rotor speed, and mode shape and is superimposed to structural damping. It is determined turbine-specific with modal analysis from a non-linear aero-elastic model. Aerodynamic damping for the first mode (fore-aft) is increased for aligned wind and waves, while it is decreased for higher structure modes as well as for wind-wave misalignment. The term interface refers to the node at tower bottom.

Assumptions for calculation method: The absolute formulation of Morison's equation is used, since structural velocity is low compared to wave velocity. The drag term is linearized with a method developed by Borgman [11]. Constant stretching is used to stretch wave kinematics from mean sea level to wave crest [12]. Diffraction is accounted for by use of the empirical MacCamy-Fuchs diffraction correction [13]. Instead of using distributed transfer functions of the FE model along the monopile wave-action zone, only transfer functions for equivalent wave loads at mean sea level are generated in order to minimize the computational effort.

3. Verification

The frequency-domain approach is verified with time-domain simulations for a reference case using a non-linear aero-elastic tool, Bonus Energy Horizontal axis wind turbine Code (BHawC), for global dynamic analysis of wind turbines. The reference case consists of a 4MW OWT in several fatigue relevant sea states. The turbine is located in a water depth of approximately 35m. For each sea state wind and wave directionalities are simplified into fully aligned or misaligned. Fully aligned describes identical wind and wave directions while fully misaligned waves arrive with 90° offset to wind. Structural models for the support structures are identical in terms of structural dimensions, damping, and modal properties. Simulations are run wave-only, i.e., with aerodynamics turned off. The parameters for the time-domain simulation are summarized in Table 1a. Each simulation has a length of 600s with 0.04s time step. The use of 5 random realizations (seeds) minimizes statistical errors in the simulation.

Table 1a. Simulation parameters verification study.

Parameter	Value
Length of time series	600s
Time step	0.04s
Number of seeds	5

Table 1b. Parameter Welch's method.

Parameter	Value
Window type	Hamming
Number of sections	10
Overlap	50%

Simulation results are compared qualitatively in terms of response moment PSDs and quantitatively with EFLs. PSDs are generated from the load time series by applying Welch's method for which the choices are specified in Table 1b. The time series were multiplied with a Hamming window and divided into 10 sections with 50% overlap. Welch's method uses periodogram spectrum estimates to reduce noise in the estimated spectrum due to limited length of the time series. Rainflow-counting is applied to the load time series to obtain the number of cycles N_i per load range L_i from which the equivalent lifetime fatigue load EFL for a specified number of cycles N_k is computed with Equation 1 [14]. The material parameter $m=4$ is chosen for welded steel. T_{sim} is the simulation time and n equals the number of load ranges. Results of the verification study are presented in section 5.

$$EFL = \left(\sum_{i=1}^{n} \frac{N_i}{N_k} \cdot \frac{T_{life}}{T_{sim}} \cdot L_i^m \right)^{1/m} \tag{1}$$

4. Sensitivity Analysis

In the sensitivity analysis the verified FDM is used to study effects of the site variations of the parameters MSL, soil, $H_{S,}$ and T_P on EFLs. The structural properties are unchanged in the analyses, except for the length of the monopile, which is adjusted to keep hub height constant in terms of the absolute value to MSL. Tower properties are not modified, thus the distance between MSL and interface is constant in the analysis. Soil variations are represented by scaling of the soil stiffness which is obtained from nominal p-y curves with a factor that is constant over the full depth. Load sensitivity is analysed locally, globally, and in a probabilistic assessment. In every analysis all parameters are assumed to be independent. H_S and T_P are actually dependent but can be regarded independent for short-term consideration and small parameter variations. The local and global analyses consider variations in one variable at a time with the other three parameters remain unchanged, while the probabilistic assessment varies all four parameters simultaneously.

4.1. Local and global sensitivity

In the local approach the parameters are varied deterministically with a deviation of 1% around their nominal value. The relation of EFL to parameter is by definition linear in local sensitivity analysis. The local sensitivity *S* is defined as the relative change of *EFL* due to a change of the parameter *X* around its nominal value according to Equation 2.

$$S = \frac{\Delta EFL}{\Delta X} \tag{2}$$

In the global approach the parameter changes cover the full range of variability that can be expected within a wind farm. For each parameter 1000 deterministic simulations were run, stepping through the parameters with uniformly spaced increments. Table 2 states the chosen nominal values as well as global ranges of the parameters.

Table 2. Parameter variations.

Analysis	**Parameter**	**MSL [m]**	**Soil factor [-]**	**H_S [m]**	**T_P [s]**
Local sensitivity	Nominal value	35	1	2	7
Global sensitivity	Global range	20-40	0.1-1.9	0-6	2-12
Probabilistic assessment	Mean	31	1	2	7
	Standard deviation	3.5	0.2	0.25	1

4.2. Probabilistic assessment

The probabilistic assessment uses Monte Carlo sampling (MCS), where a normal probability distribution of the parameters is assumed based on their mean value and standard deviation (cf. Table 2). Random combinations of the four parameters are picked in 10000 MCS leading to an accuracy of ±0.4% for the estimate of normalized EFL. Parameter ranges were chosen to represent realistic variations within an exemplary wind farm site. In this frame the design is still valid concerning the natural frequency constraint. The choice is made based on wind farm data, existing publications of sensitivity studies [3, 15], and expert opinion. The standard deviations of MSL and soil over the wind farm are expected to be larger, while the wave properties vary less. The MSL mean value differs from the nominal value in the local sensitivity analysis since it is chosen as the average of an exemplary wind farm site, while the nominal MSL represents the design position with highest deterministic loads. Soil properties typically contain high uncertainties due to difficult measurement while the water depth is known with high accuracy.

5. Results and Discussion

5.1. Verification results

Results of the verification study are exemplarily presented for a sea state of $H_S=2.2m$ and $T_P=7.0s$. Figure 1a presents the time series of the response moment at mudline generated with BHawC. The comparison of normalized PSDs in Figure 1b shows that the developed method gives a very good estimate. A response at wave peak frequency $f_P=0.14Hz$ and the first eigenfrequency $f_1=0.29Hz$ due to dynamic amplification are predicted appropriately. The response of the FDM at eigenfrequency is slightly shifted to a higher frequency compared to the BHawC result which is due to the modelling of added mass in the FE model. The FDM represents accurately that no response is visible in the frequency range around the second bending eigenmode of the structure $f_2=0.85Hz$ for this example case.

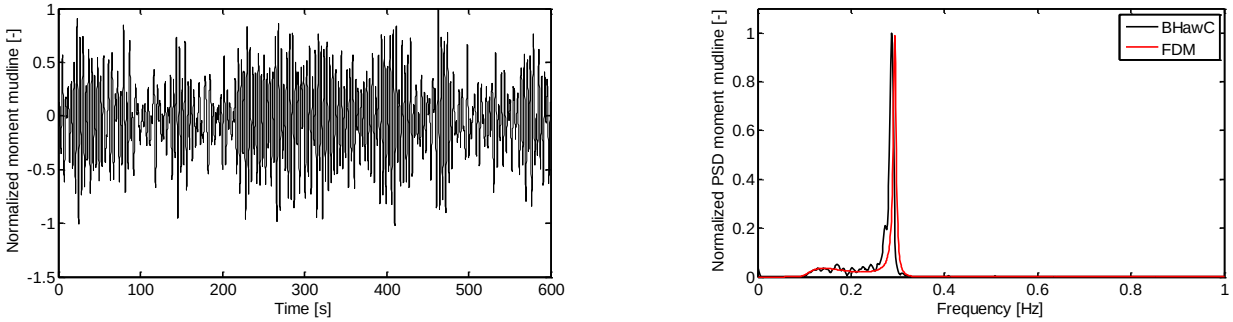

Fig. 1. (a) Time series response moment at mudline. (b) Comparison of normalized PSDs of response moment at mudline.

Figure 2 presents the results of rainflow-counting compared to PDFs obtained by Dirlik's method for the bending moment at mudline. From a qualitative perspective, the results of rainflow-counting are well-described by the PDF. This is likewise the case for response at interface level. Dirlik's formula combines and weights an exponential and two Rayleigh distributions. The closer the rainflow-count can be approximated by a weighted combination of these three distributions, the better will the results obtained by Dirlik's method match it.

The resulting EFL from rainflow-counting and Dirlik's method are given in Table 3. EFLs are normalized with the results of the time-domain simulations. Regarding the response moment estimation, the FDM leads to the closest results for sea states with lower wave heights where an accuracy of more than 95% is achieved. For higher fatigue relevant wave heights, the calculated equivalent fatigue moments differ less than 10% from the time-domain result.

From both qualitative and quantitative analysis, it appears that the developed FDM delivers results close to time-domain simulations for internal moments. However, the developed method is not suitable for detailed design and certification due to its accuracy. The influence of wind induced loads on the total fatigue loads should also be accounted for in relevant locations for design position optimizing and clustering. The developed model is mainly useful for deeper water locations (25-40m) where wave loads are dominating. Potential applications of the method are design position optimization, clustering of turbines, interpolation of wave fatigue loads between design positions, sensitivity and uncertainty analysis and also use in the actual design process e.g. preliminary design.

Table 3. Normalized EFL of time-domain simulations (BHawC) and frequency-domain method (FDM).

Sea State		**BHawC Mudline [-]**	**FDM Mudline [-]**	**BHawC Interface [-]**	**FDM Interface [-]**
H_S=0.78m	T_P=4.02s	1.0	0.97	1.0	0.99
H_S=2.40m	T_P=7.23s	1.0	0.96	1.0	0.96
H_S=4.34m	T_P=9.64s	1.0	1.08	1.0	0.94

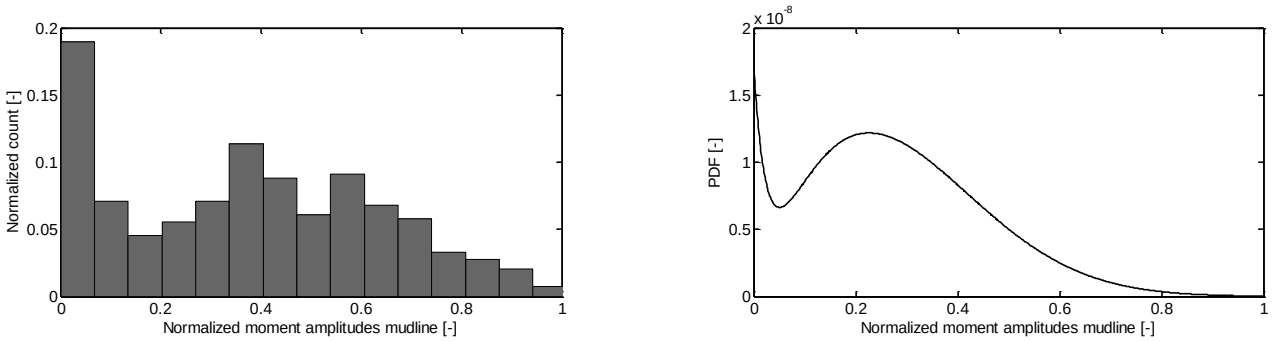

Fig. 2. (a) Histogram of rainflow-counts and (b) Dirlik's PDF. The number of load bins in (a) are reduced for visualization purpose.

5.2. Local and global sensitivity results

The sensitivities obtained from the local analysis are normalized with respect to relative changes of each parameter and offer insight into the influence of parameters on the load sensitivity (cf. Table 4).

Table 4. Normalized local sensitivities for EFL at mudline and interface level.

Location	**Soil**	**MSL**	**H_S**	**T_P**
Mudline [-]	-0.149	1.807	0.991	-1.297
Interface [-]	-0.203	1.533	0.991	-1.707

MSL and T_P influence EFLs most while scaling of soil stiffness only causes small variations of the load level locally around the nominal value. The strong dependency of loads with respect to MSL can be attributed to the combined effect of wave loads increasing with deeper water while the natural frequency of the structure decreases. The decreasing influence of MSL for the results from mudline to interface is due to the fact that the interface level is kept constant with respect to MSL. An increase in MSL thus extends the moment arm to mudline while not altering it to interface level. Soil and T_P sensitivity are higher for interface EFLs, since the relative deflections in the first mode shape are larger there which amplifies the impact of changing natural frequency. The wave height sensitivity is identical at interface and mudline, since all other parameters are kept constant while only the magnitude of the wave load scales linearly.

Soil properties and MSL are expected to have much higher variations within a wind farm compared to H_S and T_P. Since the uncertainty in soil is high [15], it is still a critical parameter in foundation design despite its low local sensitivity. The high sensitivity of loads to water depth makes optimization of design positions and clustering in large offshore wind farms crucial for cost-effective design.

In global analysis EFLs show a linear trend for H_S while T_P, soil, and MSL cause a higher order trend (cf. Figure 3a). The proportionality of EFLs to H_S is explained by the use of Airy wave theory.

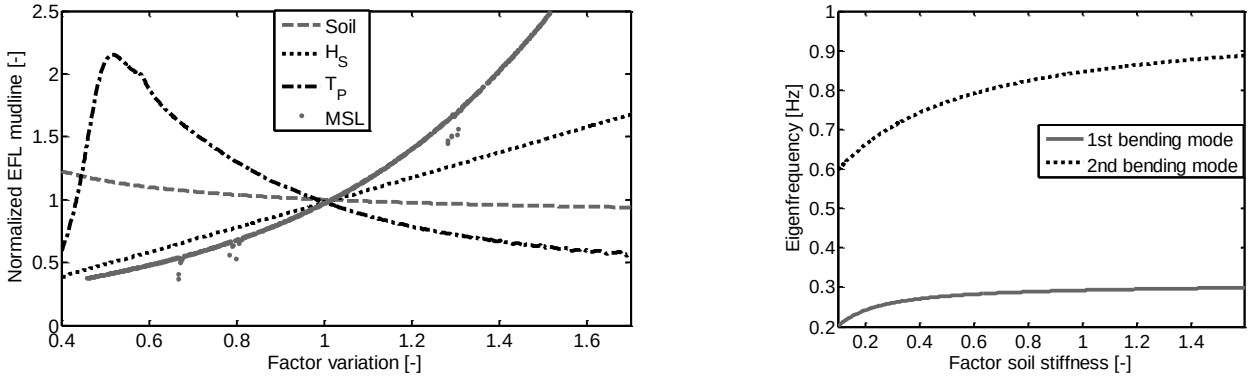

Fig. 3. (a) Normalized EFL (bending moment) at mudline as a function of parameter variation. (b) Change of eigenfrequency with soil stiffness.

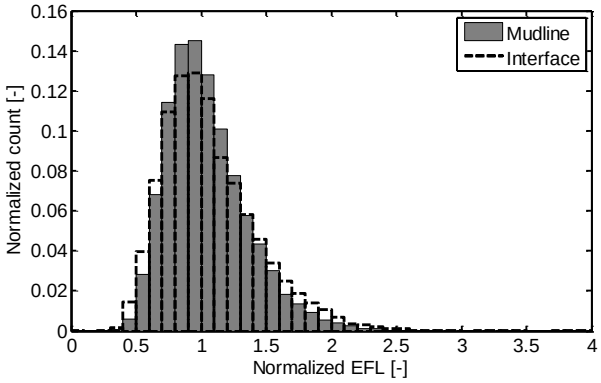

Table 5. Statistical properties of distribution of normalized EFL.

Property	Mudline [-]	Interface [-]
Mean	1.05	1.07
STD	0.38	0.38
Skewness	6.20	1.65
Kurtosis	114.55	13.57

Fig. 4. Histogram of EFL for probability assessment. EFLs are normalized to the result for all parameters at their mean value.

The analysed parameters either influence wave loads and/or the characteristics of the system, especially eigenfrequency and mode shape. Wave related parameters H_S and T_P change the wave load, soil changes the system characteristics, while MSL influences both. If the distance between natural frequency of the structure and wave peak frequency is decreased, higher dynamic amplification raises fatigue loads. This phenomenon is dominant for decreasing T_P, as for $T_P=3.4s$ the structure with an eigenfrequency of $f_1=0.29Hz$ is excited exactly in its first eigenmode (cf. Fig. 3a).

Decreasing soil stiffness causes lower eigenfrequencies with a square-root dependency as shown in Figure 3b. The second bending mode is affected more strongly, which is caused by larger deflections for the second mode shape at mudline. Decreasing soil stiffness shifts the natural frequency of the structure closer to load excitation frequencies which explains the increase of EFLs.

A sensitivity study of RNA mass variation proved a trend of EFLs that follow the change of natural frequency closely (not shown). The sensitivity of EFLs to RNA mass can be assumed to arise mainly from the effect of eigenfrequency change. This is in agreement with previous research which treats the natural frequencies of first and second bending mode as main indicator for dynamic response [3].

5.3. Probabilistic assessment results

The histogram of the computed EFLs in the probabilistic assessment with 10000 MC samples is shown in Figure 4 with the corresponding statistical properties stated in Table 5. All input parameters are Gaussian distributed leading to an EFL distribution that is positively skewed to higher loads (cf. Table 5). This is due to the high influence of T_P and MSL on the EFLs, as shown in the scatter plots in Figure 5. Hence, the skewness can be traced back to load sensitivity being of higher order regarding T_P for the considered variation. The stronger positive tail is also represented in the scatter plots where outliers to higher loads are more frequent.

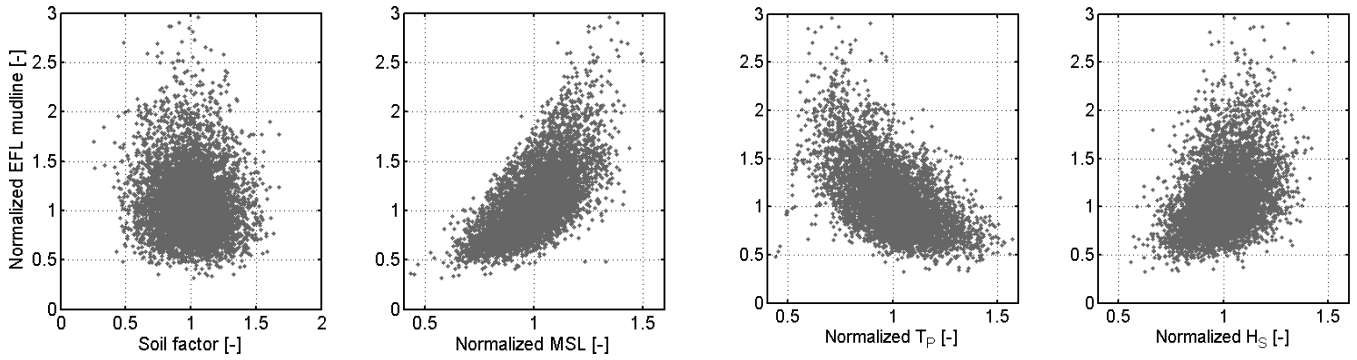

Fig. 5. Scatter plots of normalized EFL for all parameters at mudline for probabilistic assessment.

The scatter plots show the same trends as observed for the global sensitivity study. For this reference case soil has no significant influence on the mean EFL. This is consistent with the expectation based on the local sensitivity analysis. Sensitivity results are strongly influenced by the chosen parameter ranges of the reference case. Therefore, care must be taken for generalization of the results regarding assumptions and conditions in other cases.

6. Conclusion and Outlook

Increased insight into sensitivity of fatigue loads is needed in order to optimize support structures in large offshore wind farms, where considerable variations in environmental site conditions might occur. This paper uses frequency-domain load calculations to analyze the sensitivity of wave-induced fatigue loads to varying site conditions for OWT monopile foundations in deeper water locations. A FDM was created which calculates EFLs based on JONSWAP wave spectra, Morison equation, transfer functions from a FE model of the support structure, and Dirlik's method. This approach results in a computation time of approximately 10s for one simulation case.

Verification of the FDM using time-domain simulations from an aero-elastic code indicates an accuracy of more than 90% for fatigue bending moments at mudline and interface level. Additionally, a qualitative analysis of power spectral densities showed good agreement regarding responses at T_P and first eigenfrequency of the structure. The FDM is used in sensitivity analysis with MC sampling. Local and global analysis reveal high fatigue load sensitivity to changes in MSL and T_P. Normal distributed parameters in a probabilistic assessment yield a positively skewed probability distribution of EFLs.

Due to its accuracy and efficiency, the FDM is ideal for applications where fast simulations are needed, e.g. in design position optimization, clustering of turbines, interpolation of wave fatigue loads and in preliminary design. Further study is required to extend the developed method to include wind loads. Due to the identified importance of wave peak frequency and MSL on the results, further work should reveal the effect of uncertainty in wave loads on fatigue loads.

References

[1] Vorpahl, F., Schwarze, H., Fischer, T., Seidel, M., & Jonkman, J. (2013). Offshore wind turbine environment, loads, simulation, and design. *Wiley Interdisciplinary Reviews: Energy and Environment, 2(5),* 548-570.

[2] Zaaijer, M. B. (2006). Foundation modelling to assess dynamic behaviour of offshore wind turbines. *Applied Ocean Research*, *28*(1), 45-57.

[3] de Vries, W., et al. (2011). Final report WP 4.2: Support Structure Concepts for Deep Water Sites: Deliverable D4.2.8 (WP4: offshore foundations and support structures). *Upwind.*

[4] Seidel, M. (2014). Wave induced fatigue loads - Insights from frequency domain calculations. *Stahlbau*, *83*, 535–541.

[5] Kuehn, M. J (2001). *Dynamics and design optimisation of offshore wind energy conversion systems*. PhD diss. TU Delft, The Netherlands.

[6] Van der Tempel, J. (2006). *Design of support structures for offshore wind turbines*. PhD diss. TU Delft, The Netherlands.

[7] Ragan, P., & Manuel, L. (2007). Comparing estimates of wind turbine fatigue loads using time-domain and spectral methods. *Wind engineering*, *31*(2), 83-99.

[8] Dirlik, T. (1985). *Application of computers in fatigue analysis*. PhD thesis, University of Warwick, England.

[9] American Petroleum Institute (API). *Recommended Practice for Planning, Designing, and Constructing Fixed Offshore Platforms—Working Stress Design (2A-WSD).* American Petroleum Institute, Washington, D. C., 2005.

[10] Passon, P., & Kühn, M. (2005). State-of-the-art and development needs of simulation codes for offshore wind turbines. In *Copenhagen Offshore Wind 2005 Conference and Expedition Proceedings* (pp. 26-28).

[11] Borgman, L. E. (1965). The spectral density for ocean wave forces. *ASCE* .Santa Barbara speciality conference.

[12] Wheeler, J. D. (1970). Method for calculating forces produced by irregular waves. *Journal of Petroleum Technology*, *22*(03), 359-367.

[13] MacCamy, R. C., & Fuchs, R. A. (1954). *Wave forces on piles: a diffraction theory.* Tech. rep., DTIC Document (No. TM-69)

[14] Matsuishi, M., & Endo, T. (1968). Fatigue of metals subjected to varying stress. *Japan Society of Mechanical Engineers, Fukuoka, Japan*, 37-40.

[15] Carswell, W., Arwade, S. R., DeGroot, D. J. and Lackner, M. A. (2014). Soil–structure reliability of offshore wind turbine monopile foundations. *Wind Energy*.

Paper B

Design clustering of offshore wind turbines using probabilistic fatigue load estimation

L. Ziegler, S. Voormeeren, S. Schafhirt and M. Muskulus

12/05/2015: Submission to Renewable Energy

Design clustering of offshore wind turbines using probabilistic fatigue load estimation

Lisa Ziegler[a,b,*], Sven Voormeeren[a], Sebastian Schafhirt[b], Michael Muskulus[b]

[a] *Siemens Wind Power, Offshore Center of Competence, Prinses Beatrixlaan 800, 2595BN The Hague, Netherlands*
[b] *Department of Civil and Transport Engineering, NTNU, Høgskoleringen 7A, 7491 Trondheim, Norway*

Abstract

In large offshore wind farms fatigue loads on support structures can vary significantly due to differences and uncertainties in site conditions, making it necessary to optimize design clustering. An efficient probabilistic fatigue load estimation method for monopile foundations was implemented using Monte-Carlo simulations. Verification of frequency domain analysis for wave loads and scaling approaches for wind loads with time domain aero-elastic simulations lead to an accuracy of 95%. The computational speed is in the order of 100 times faster than typical time domain tools. The model is applied to calculate location specific fatigue loads that can be used in deterministic and probabilistic design clustering. Results for an example wind farm with 150 turbines in 30-40m water depth show a maximum load difference of 25%. Smart clustering using discrete optimization algorithms leads to a design load reduction of up to 13% compared to standardized design. The proposed tool improves industry-standard clustering and provides a basis for design optimization and uncertainty analysis in large wind farms.

Keywords: offshore wind turbine, fatigue, clustering, uncertainty, frequency domain, optimization, site condition, Monte-Carlo simulation

1. Introduction

Variations in site conditions, such as water depth, soil, and turbulence, lead to significant differences in fatigue loads on offshore wind turbine (OWT) support structures. Full load calculations are computationally demanding and can typically not be performed for each turbine within large wind farms [1]. In industry practice, loads are therefore often only evaluated for a limited number of design positions in the wind farm. OWTs are then grouped into design clusters according to the design positions. For each cluster the support structure design is only performed once. It is assumed that the resulting load levels and structural designs can safely be carried over to all positions in the associated cluster. In order for this to hold, the design position must be the highest loaded location in the cluster. Thus, optimization of design clustering is necessary to reduce design conservatism and the cost of offshore wind energy.
Industry practices base clustering decisions on variations of mean sea level (MSL) or expected

*Corresponding author
Email address: lisaziegler.mail@web.de (Lisa Ziegler)

first eigenfrequency of the support structures [2]. Recently, Seidel [2] suggested an improved approach of clustering using a site parameter that takes into account structural and hydrodynamic properties. This site parameter is however only suitable for wave load dominated designs. Thus, further work is needed to formulate turbine clustering as an optimization problem incorporating all important site specific information.
Since grouping of OWTs into design clusters must be performed in an early project phase, time-efficient approaches are essential. In this paper, a design clustering method for OWTs was developed using probabilistic fatigue load estimation. The fatigue load estimation method uses frequency domain analysis to calculate wave loads and a scaling approach for wind loads on monopile-based OWTs. Uncertainties in input data and model assumptions are analyzed through Monte-Carlo simulations (MCS). The deterministic estimation tool was verified with fully integrated, aero-elastic time domain simulations. Due to computational efficiency, fatigue loads can be calculated site specific for every turbine location within the wind farm. This makes turbine clustering a discrete optimization problem.
This paper provides a novel approach of optimization of turbine clustering. Additionally, probabilistic assessments give insight on how uncertainties in load calculation can alter allocation of turbines to clusters. This paper is organized as follows. Section 2 outlines the developed fatigue load estimation method, its model assumptions and verification. A summary of the probabilistic load assessment is presented in Section 3. Section 4 focuses on clustering optimization by discussing problem formulations and solution approaches using brute-force and discrete optimization algorithms. Section 5 demonstrates the established clustering optimization method for an exemplary wind farm of 150 monopile-based OWTs in a water depth range of 30-40m.

2. Method for Fatigue Load Estimation

Since a high number of load cases have to be performed for detailed design and certification of OWTs, computational effort for standard time domain fatigue load analysis is significant [3, 4]. Such simulations, although they are considered most accurate, are ill-suited for clustering optimization and probabilistic assessments. For these applications, load estimates are sufficient, as fast simulations are a necessity.
Several approaches exist in literature to decrease computational costs of OWT load analysis [6-16], either using integrated analysis or wind-wave separate assessment. In separate assessments, wave fatigue loads are mainly estimated from frequency domain analysis [6, 5, 7, 8, 9, 2, 13], which has also been applied to wind loads [7, 9, 13, 14, 16]. Other authors suggest simplified rotor load models or parametric models for fatigue damage estimation [10, 15]. For integrated methods, proposals exist for reducing the number of environmental conditions, number of simulation seeds or length [6, 11]. For example, Zwick and Muskulus [11] suggest simplified fatigue load assessment based on statistical regression models to reduce the number of load cases for damage estimation.

2.1. Approach

The developed estimation method calculates location specific equivalent fatigue loads (EFLs). The method is based on three core elements (cf. Figure 1): (1) calculation of wave-induced EFLs in the frequency domain using Dirlik's method, (2) scaling of wind-induced EFLs from a reference case, and (3) combination of wind-wave EFLs with direct quadratic superposition [6].
Wave loads are calculated based on JONSWAP wave spectra and Morison equation. To deter-

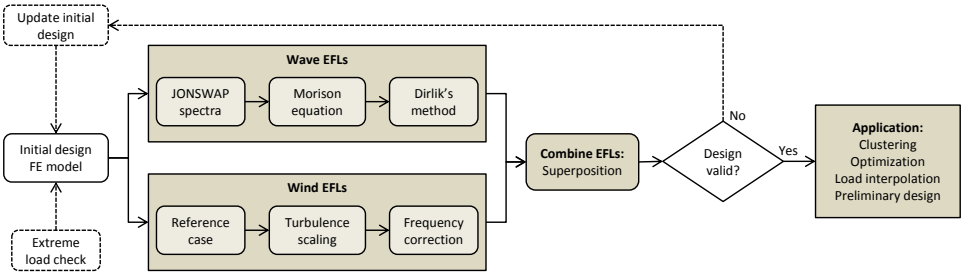

Figure 1: Flowchart of fatigue load estimation method.

mine internal load response spectra, transfer functions are derived from a finite element model of the support structure. In order to minimize the computational effort, transfer functions are generated for wave loads integrated to MSL only instead of using distributed transfer functions along the monopile wave-action zone. Wave-induced EFLs are obtained from the response spectra with Dirlik's method [17]. Aerodynamic damping as a function of wind speed and wind-wave misalignment is added to structural damping in order to account for dynamic interaction between wind and waves. Details of the wave-induced fatigue load estimation are described in [8].
The reference case for wind loads consists of EFLs from aero-elastic simulations in the time domain. This reference case is turbine type specific, but assumed generic regarding environmental conditions and support structure dimensions. For offshore wind turbines, the reference case $EFL_{wind,ref}$ consists typically of Class C turbulence intensity TI_{ref} [4]. Location specific wind loads $EFL_{wind,ls}$ are then approximated by applying linear scaling of the turbulence intensities and a natural frequency correction factor, f_{corr}, as shown in Equation (1). The location specific turbulence intensities, TI_{ls}, are calculated with the Frandsen wake model using input from measured, ambient TI [19]. The natural frequency correction is derived from interpolation of time domain simulations for four different turbines types with 3-7 frequency sets each.

$$EFL_{wind,ls} \approx EFL_{wind,ref} * \frac{TI_{ls}}{TI_{ref}} * f_{corr} \tag{1}$$

EFLs from wind and waves are combined using Equation 2 [6]. Direct quadratic superposition assumes that the zero-crossing period of wind and wave responses are identical which is usually not valid [6]. However, detailed verification studies by Kuehn [6] showed a good performance of the method. This approach is commonly assumed to be conservative; the neglected interference term is assumed to be negative [18].

$$EFL_{tot} \approx \sqrt{EFL^2_{wind,ls} + EFL^2_{wave,ls}} \tag{2}$$

The execution time for one simulation case is in the order of seconds.

2.2. Assumptions

To create a computationally efficient method, several assumptions are implemented to simplify the full load calculations. Detailed assumptions of the wave load estimation are outlined in [8]. Additionally, the following assumptions are important:

Assumptions for environmental data: Wind-wave scatter diagrams are lumped into 20 simulation cases consisting of mean wind speeds (V_W), significant wave heights (H_S), and wave peak periods (T_P). The lumping is performed in a damage equivalent way using a method suggested by Kuehn [6]. For each simulation case wind-wave directionality is simplified into fully aligned or fully misaligned. For this purpose, wind and wave roses are lumped in bins of 30degree. Fully aligned wind and waves occur in the same bin, where the aerodynamic damping is maximum. All other combination of wind and wave directions are treated as fully misaligned with reduced aerodynamic damping.
Assumptions for calculation method: The estimation approach for wind-induced EFLs only adjusts for TI and natural frequency. Differences in air density, wind shear, structural geometry or mode shapes are neglected since the effects on the load level are expected to either be minor or represented through the natural frequency correction.

2.3. Verification

The fatigue load estimation method is verified empirically against time domain simulations using the non-linear aero-elastic tool Bonus Horizontal axis wind turbine Code (BHawC), which allows for a global dynamic analysis of wind turbines. The verification was done for wave-only load cases (as described in [8]), as well as wind-only loads, and wind-wave combined loads for a 4MW OWT in 35m water depth. Results of this verification study are presented in Section 5.

3. Probabilistic Load Assessment

Fatigue load calculation processes contain significant uncertainties commonly addressed with safety factors in the design standards [4, 5]. Insight on the effect of uncertainties on EFLs improves the understanding of the actual structural reliability. A brief overview of existing work on probabilistic fatigue assessment of wind turbines is given by Yeter [20] and Veldkamp [21].
The novelty of this work is the use of frequency domain analysis with MCS to assess uncertainties in fatigue loads for application in probabilistic design clustering of OWTs. For every turbine location 1000 MCS were run with simultaneous, random variation of input parameters. As a result, the output distribution of EFLs can be estimated with a root-mean-square error of 0.3%.
Epistemic uncertainties in fatigue load calculations occur in the form of data, statistical and model uncertainty [22]. Previous work showed significant influence of data uncertainties in MSL and T_P on fatigue loads [8]. For the clustering problem, the probabilistic assessment is extended to include uncertainty in TI and model uncertainty. Model uncertainty is analyzed regarding the development of sea states, represented with the peak enhancement factor γ in the JONSWAP wave spectrum, and regarding diffraction, represented with the inertia coefficient C_M in the McCamy-Fuchs diffraction correction for Morison equation. All parameters in the probabilistic assessment are independent, normal distributed with mean value and standard deviation (STD) stated in Table 1.
Data uncertainty was given a constant STD over the wind farm. In practice, uncertainties can differ for some locations due to incomplete measurement data, for example soil measurements may not be available for every turbine position in early project phases.
Parameter ranges were chosen to represent realistic uncertainties for design clustering in large wind farms. The choice is made based on wind farm data, existing publications of sensitivity studies [21, 23, 24], and expert opinion. For example, the variation of MSL is chosen as tidal variation. Soil properties typically contain high uncertainties due to difficult measurement and

Table 1: Input distributions for probabilistic design clustering.

Uncertainties	**Data (factors)**			**Statistical**		**Model**	
Parameter	**TI [-]**	**MSL [-]**	**Soil [-]**	H_S **[m]**	T_P **[s]**	γ **[-]**	C_M **[-]**
Mean	1	1	1	1.6	6.9	1.5	1.7
STD	0.1	0.05	0.2	0.1	0.2	0.1	0.1

data interpretation while the water depth is known with better accuracy. Mean values of data inputs are location specific, thus the uncertainty is represented through a scaling factor. Soil variations are represented by scaling of the soil stiffness which is obtained from nominal p-y curves with a factor that is constant over the full depth. For probabilistic clustering only the sea state that contributes most to lifetime fatigue damage is analyzed. Mean values of γ and C_M are chosen based on exemplary wind farm and support structure data about fetch limitation and diffraction (cf. Table 1).

4. Clustering Optimization

The aim of design clustering is to find an optimum between number of clusters and the level of design conservatism. Clustering optimization here provides a solution to the question of cluster configurations: To which cluster should each OWT be assigned to?
Applying the developed (probabilistic) estimation method, fatigue loads are calculated site specific for all given turbine locations within the wind farm. The resulting set of discrete (deterministic or probabilistic) fatigue values is clustered regarding customized criteria.

4.1. Problem formulation

Clustering optimization has two dimensions: the decision on (i) number of clusters and (ii) cluster configuration. Regarding number of clusters, limiting cases are one cluster, meaning all turbines are designed for the highest load level in the wind farm, and individual support structure design, where cluster number equals number of OWTs. The number of clusters is typically restricted by resources in the engineering team and limited project time. Even if the industry moves towards faster tools and higher capacities making individual design feasible, clustering is still beneficial to implement for turbines with similar load level to optimize costs of manufacturing and installation.
Ideally, in clustering optimization the support structure costs should be minimized. In this study, the optimization problem is formulated to minimize design loads since accurate cost information is difficult to gather. Loads correlate to mass of the support structure which is commonly treated as cost indicator [6]. Thus, the unconstrained, non-linear objective function is the total design load TL calculated as the sum over all clusters n with Equation (3). N_i is the number of turbines in cluster i, while L_i equals the highest load level in cluster i.

$$TL = \sum_{i=1}^{n} N_i * L_i \tag{3}$$

The choice of number of clusters n can either be fixed prior to optimization or be included as a variable in optimization. If the clustering approach is extended for cost minimization, n will be

an optimization result.
Including uncertainties in fatigue load calculations results in a set of fatigue load distributions for all turbines. Probabilistic clustering is performed by increasing the mean load value with $k * STD$. Choice of k represents how much of the load variability is accounted for, for example $k = 3$ accounts for 99.7% of the sample population for a normal distribution. The higher k is chosen, the smaller is the chance of misgrouping turbines into clusters with too low load level.

4.2. Assumptions for clustering optimization

The formulation of the optimization problem reveals underlying assumptions for clustering:

- All turbines are designed for the highest load in the cluster, no design interpolation is done within clusters.
- Fatigue is design driving, extreme loads do not influence clustering. This is typically valid for monopiles in deeper water, where the design is often dominated by wave induced fatigue loads. A check should be performed for every project to confirm fatigue as a design driver.
- Location specific loads are calculated with the same initial design for all positions. Thus, the validity of the design for all positions has to be confirmed which can be done through the frequency constraint. Alternatively, the initial design can be updated in an iterative procedure of clustering and renewed load calculation.

4.3. Solution approaches

The pattern of the optimization problem is explained for an example of 150 turbines equally divided into five clusters with cluster 1 ($T_1 - T_{30}$) containing the highest loaded turbines and cluster 5 the lowest loaded turbines ($T_{120} - T_{150}$). Thus, 30 turbines are in each cluster ($N = 30$). Moving one turbine T_{60} from cluster n_2 to cluster n_3 causes:

1. $(N - 1)$ turbines in cluster n_2,
2. $(N + 1)$ turbines in cluster n_3 and
3. Increase of maximum load in cluster n_3 to L_{60}.

The formulated problem is addressable with algorithms of combinatorial optimization [25]. The discrete solution approaches brute-force and local search were compared in terms of efficiency and robustness. In **brute-force** the number of recombination are reduced by using pre-knowledge of the solution that (i) clusters are filled with turbines sorted in load descending order making optimization only a cluster-border decision and (ii) when adding a cluster, the number of turbines in every cluster is less or equal to the maximum number of turbines in the previous n clusters. Problems with 150 OWTs and up to 6 clusters can be solved with brute-force giving the global minimum in a computation time of less than 1 hour.
An approximate algorithm using **local search** starts from an initial cluster guess, selects a random cluster-border, and optimizes it in terms of decreasing the objective function, while keeping all remaining positions constant. The optimization of the single cluster-border is performed by selecting the position with the minimum cost of all possible border positions. This procedure is repeated in every iteration step. With a chance of 5%, the previously optimized cluster-border is replaced by a random border to ensure that the algorithm does not become trapped in a local minimum with poor quality. In the tested example for 150 OWTs, 100 iterations were sufficient

for the algorithm to reach the global minimum or local minima with good quality. The quality of local minima depends on the shape of the solution space and the initial guess. In order to avoid poor local minima, the optimization algorithm is repeated for several initial positions selected randomly. In a fast check, the quality of the computed local minima is compared against a linear distribution of load levels in the offshore wind farm and results for individual design. For a linear distribution of loads, the optimal solution is an equal number of turbines in each cluster.

5. Results and Discussion

5.1. Probabilistic fatigue load estimation results

Results of the verification study for the load estimation method are presented in Figure 2. EFLs were calculated based on seven wind and wave realizations for all operational wind speeds. The load estimation tool gives the best results around rated wind speed of the turbine. Errors increase for higher wind speeds mainly due to an underestimation of wave loads. This is in agreement with previous study of the wave-only load estimation tool [8]. Possible reasons are that for higher wind and waves non-linear effects in the wave load and also in the soil-structure interaction play a larger role which is not captured in the linear frequency domain wave model. Additionally, aerodynamic damping magnitude and small differences in the calculation models (e.g. discretization in structural model, C_M coefficients in Morison equation) are further error sources. Combining the simulation cases to weighted lifetime EFLs using a Weibull distribution for wind speed occurrences, a total load estimation accuracy of 95% (conservative error, EFLs are overestimated) is achieved.

Figure 3a presents the location specific EFLs for 150 turbines calculated with the load estimation tool for a realistic wind farm example in 30-40m water depth leading to a maximum load difference of 25% in the wind farm. MSL, soil properties, and TI are varied site specifically, while all remaining parameters are constant, e.g. identical lumped sea states or wind-wave alignment. Sorting the turbines for ascending mudline EFLs does not result in interface loads sorted correctly. This is due to the higher local sensitivity of wave-induced EFLs at mudline nodes to changes in MSL as shown in [8]. Thus, a critical decision in clustering optimization is the position of interest, since clustering regarding mudline EFLs might result in interface EFLs being in a suboptimal cluster. In this study, optimization of mudline EFLs was performed since these are typically the highest loaded nodes on the support structure. Alternatively, multi-objective optimization or an optimization based on the "integrated load from interface-mudline-pile tip"

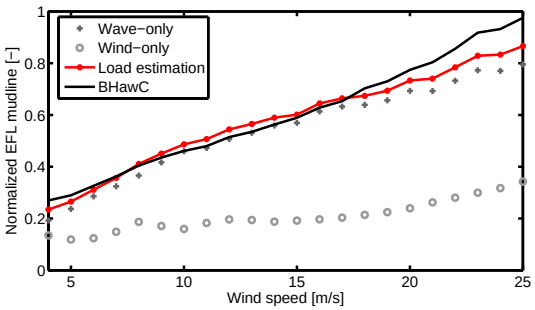

Figure 2: Comparison of normalized EFLs of response moment at mudline.

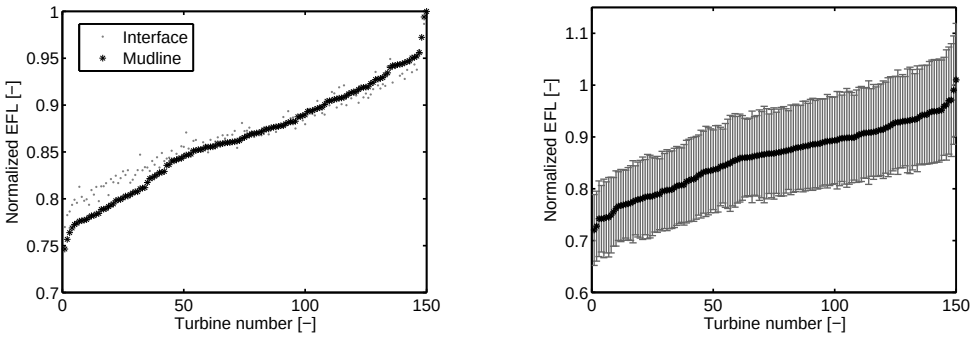

(a) Location specific EFLs mudline and interface.

(b) Mean value and STD of EFLs.

Figure 3: (a) Location specific EFLs at mudline and interface level for 150 turbines normalized to the maximum load in the wind farm. The EFLs are sorted ascending for mudline location. (b) Mean value and STD of probabilistic, location specific EFLs at mudline.

might be suitable.

Figure 3b shows the normalized mean load values with an error bar for STDs of all turbines resulting from the probabilistic load assessment. Mean load values are normalized to the maximum mean load value in the wind farm. In general, STDs between the turbines are quite similar; the maximum absolute difference is 4.5%.

A reason for the relatively small variation between location specific STDs is the choice of input distributions. In this example case, only the data factors for MSL, soil, and TI introduce location specific uncertainties, while the remaining uncertain parameters are identical for all turbines (cf. Table 1). Scatter plots of EFLs for the input parameters reveal that MSL, soil stiffness, T_P, H_S, and C_M uncertainties influence the loads equally while γ and TI have no relevant influence (not shown). Higher location specific uncertainties may increase variability differences within wind farms.

Figure 4 shows STDs of EFLs as scatter plots for natural frequency, MSL, and load level. The following two trends regarding the load variability are observed:

1. STDs of EFLs increase with higher load level and accordingly also with deeper water or lower eigenfrequency. This result matches previous analysis that showed a higher sensitivity of EFLs for increasing water depth and decreasing soil stiffness [8].
2. For turbines on a similar load level, differences in STD up to 2% exist. This variability can be attributed mainly to location specific uncertainties since the effect of model and statistical uncertainty is constant for the same load level.

5.2. Clustering results

Standard clustering approaches based on eigenfrequency and MSL give an indication but do not fully capture the variation of EFLs as Figure 5a shows. The representation of EFL change through eigenfrequencies is of higher quality than for MSL. A better match was achieved by Seidel [2] with his suggested load site parameter. Using the developed load estimation tool, clustering can now be performed based on complete site specific fatigue load information.

Figure 5b shows the total design loads (TLs) of all possible recombinations for grouping 150

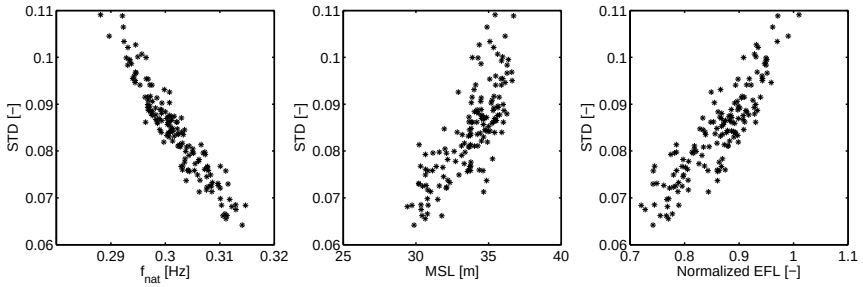

Figure 4: Scatter plots of normalized STD for the natural frequency, MSL, and normalized EFLs.

turbines into three clusters using brute-force. Cluster 1 is the highest loaded, cluster 3 the lowest loaded cluster. The solution space of the optimization problem has a convex pattern with a rather flat bottom with good quality local minima (cf. Figure 5b). This shape and the relative smoothness of the problem enable local search algorithms to achieve good results.
The local search algorithm for optimizing 10 clusters is applied for 20 random initial positions as shown in Figure 6a. This confirms that the local search algorithm leads to a very good local minimum with only minor influence of initial positions. The maximum difference between the different local minima is 0.4% for this example which is negligible.
Figure 6b presents TLs minima as a function of the number of clusters. The clusters 1-6 are calculated with the brute-force method resulting in the global minimum, while higher number of clusters are solved with the local search algorithm. One cluster means all turbines are designed for the highest load in this wind farm, while 150 clusters represent individual design. This emphasizes the necessity to implement a sufficient number of clusters in large offshore wind farm since designing all support structures to the highest loaded position leads to 13% larger TLs compared to individual design for this example case. On the contrary, the marginal gain adding more clusters reduces significantly after 6 clusters. TLs approach individual design results quickly after 10 clusters already, where more designs add little value.

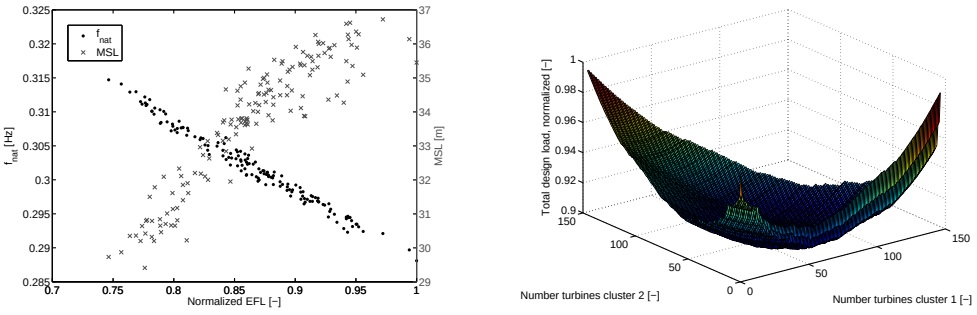

(a) Site specific EFLs.

(b) Brute-force optimization.

Figure 5: (a) Scatter plots of site specific EFLs for eigenfrequencies of the structures fnat and MSL variation. (b) Brute-Force optimization of 150 turbines in 3 clusters.

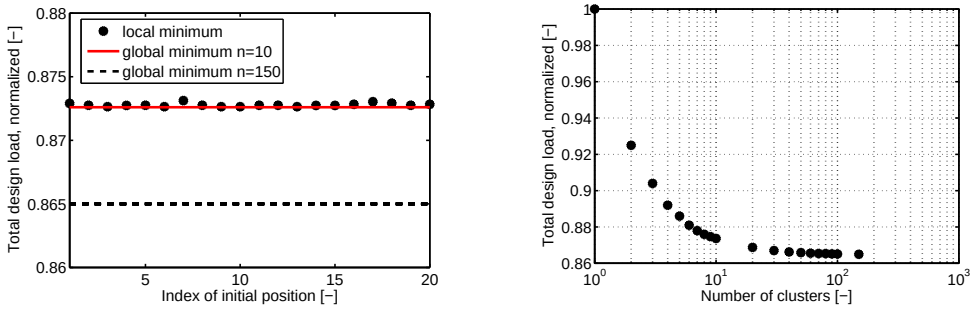

(a) Local minima.

(b) Cluster minima.

Figure 6: (a) Local minima obtained with discrete optimization algorithm for different random initial positions. (b) Minima of TLs for 150 turbines as a function of number of clusters.

The optimal cluster configurations are shown in Table 2. Optimization has to be performed for the number of turbines in each cluster N_i only; the maximum load in the cluster L_i results from ascending turbine sorting (cf. Figure 3a). This setup based on brute-force solving can also be used for interpolation to higher number of clusters instead of applying optimization algorithms. Next, based on the calculated load distributions (cf. Figure 3b), clustering is now performed probabilistically by allocating turbines based on their mean load level increased with 3*STD. Figure 7a presents the rearrangement of turbines compared to deterministic clustering based on only mean values for the case with three clusters. In this example, the number of turbines in cluster 1 increased by one while cluster 3 has one turbine less. In Figure 7a, the numbers indicate turbine IDs, grey stating the turbines in the cluster for deterministic clustering and the red

Table 2: Optimal cluster configurations.

Number of clusters		**1**	**2**	**3**	**4**	**5**	**6**	**150**
Cluster 1	N_1	150	54	24	18	4	4	1
	L_1	1	1	1	1	1	1	1
Cluster 2	N_2	-	96	53	41	30	20	1
	L_2	-	0.883	0.919	0.929	0.952	0.952	0.994
Cluster 3	N_3	-	-	73	57	43	30	1
	L_3	-	-	0.862	0.878	0.908	0.919	0.972
Cluster 4	N_4	-	-	-	34	39	25	1
	L_4	-	-	-	0.812	0.862	0.883	0.956
Cluster 5	N_5	-	-	-	-	34	37	1
	L_5	-	-	-	-	0.812	0.861	0.952
Cluster 6	N_6	-	-	-	-	-	34	1
	L_6	-	-	-	-	-	0.812	0.951
Cluster 150	N_{150}	-	-	-	-	-	-	1
	L_{150}	-	-	-	-	-	-	0.746
Normalized TL		1	0.925	0.904	0.892	0.886	0.881	0.865

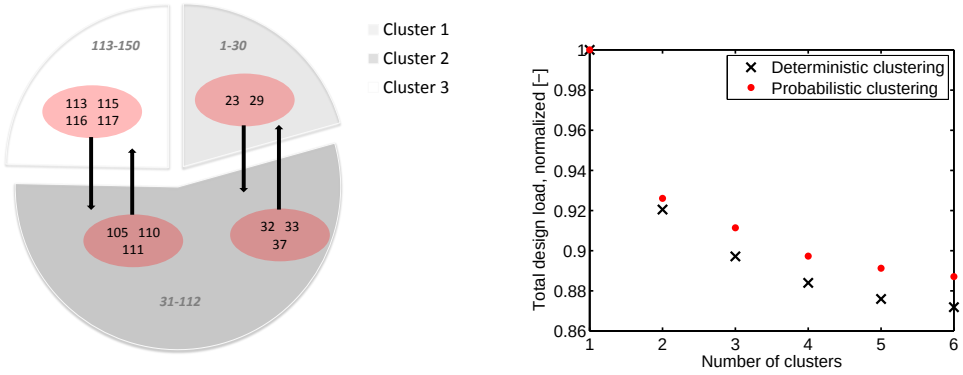

(a) Turbines changing clusters.

(b) Design loads.

Figure 7: (a) Turbines changing clusters in probabilistic compared to deterministic optimization. (b) Total design loads for deterministic and probabilistic clustering.

boxes referring to turbine moving due to probabilistic clustering. In total, twelve turbines change clusters as indicated by the arrows. These are often turbines located close to the cluster-borders but can also be turbines that have a higher STD than load neighbouring turbines (e.g. ID23). Turbines changing clusters leads to an increase of the highest mean EFL in the clusters. Therefore, the total design loads are higher for probabilistic clustering compared to deterministic clustering as shown in Figure 7b.

5.3. Evaluation of load estimation and clustering methods

Limitations of the current estimation tools are the simplification of many physical phenomena, for example non-linearity of waves and soil, wind-wave directionality and interaction between wind and wave loads. Moving to bigger turbines supported by XL-monopiles with diameters above 7m, wave diffraction becomes more important, making use of Morison equation in linear wave theory only applicable when diffraction corrections are included. Immediate improvement of the method can be achieved through the use of distributed transfer functions in the wave load tool and detailed study of suitable aerodynamic damping values.
Verification of the fatigue estimation method confirms a total conservative error of 5% indicating good load estimation. However, since some results of the estimation tool are non-conservative for high wind speeds (cf. Figure 2), contingency should be added in project applications.
Probabilistic assessment of all turbines within an example wind farm gave only 5% differences in STD over the wind farm. For design practice, it is suggested to perform a single probabilistic assessment for the highest loaded position in uniform wind farms to indicate the variability of loads due to uncertain input parameters for all turbine locations. With some contingency, this approach is conservative as it was shown that STDs increase with higher loads.
A main limitation of the probabilistic assessment is that results strongly depend on chosen input distributions. For example, soil stiffness had only minor influence on EFLs compared to parameters like MSL and T_P in previous studies [8]. This was due to high soil stiffness for the example site. Soil stiffness became in this study a more important parameter for turbine locations with poorer soil stiffness. This emphasizes that probabilistic assessments are problem specific and cannot be generalized. Consequently, applying a general safety factor in the design process is

not expedient for design optimization. Probabilistic load assessment can, combined with uncertainty in structural resistance, form a good decision-making basis for optimizing safety factors.
For design clustering, the needs of industry are fast and robust tools, while nowadays larger wind farms typically have only 2-3 clusters. Brute-force optimization guarantees global optima at the expense of solution time making it the best choice for up to 5 clusters for wind farms with 100-150 turbines. For more clusters, the local search algorithm is recommended which showed very good performance for solution quality and computational efficiency. For practice, a possible constraint in the optimization routine can be a limit on MSL difference within clusters so that monopile lengths can be kept constant for all cluster positions.
In the probabilistic clustering example, only few turbines change cluster since the distribution of STDs follows that of EFLs relatively closely. Thus STDs are only of importance near cluster-borders. It can be concluded that deterministic clustering has good stability for uniform sites.

6. Conclusion and Recommendations

6.1. Conclusion

Fatigue load differences of 25% for 150 OWTs in 30-40m water depth showed the importance of site condition variations, making design clustering necessary. A developed probabilistic fatigue load estimation method proved to be suitable for site specific EFL estimation. A verified accuracy of 95% with only seconds of computation time for one simulation case makes the estimation tool ideal for application in clustering optimization, load interpolation, uncertainty studies and preliminary design. Based on EFL estimates, optimization of design clustering gave a reduction of up to 13% of total design loads compared to standardized design. This makes clustering an important approach in support structure cost reduction.
By investigation of the marginal gain of adding additional clusters (cf. Figure 6b), the clustering tool can improve decision-making on the optimal number of clusters of a wind farm in early project phases and is strongly recommended for use in industry. An alternative application of the combined load estimation and clustering tool is wind farm layout design. The layout is typically optimized for power output through wake modeling and cable costs. Having this fast load estimation tool, support structure loads and costs can add a new dimension to layout optimization.

6.2. Recommendations

Two main recommendations for the load estimation tool are: firstly, the verification study should be extended to different structural and environmental settings. More precisely, studies should confirm the accuracy of the estimation method for different support structure eigenfrequencies and in shallow water depths where wind loads have more influence. Ideally, the tool should be validated on experimental data in the future. Secondly, resistance uncertainty should be included in the probabilistic approach making it applicable for reliability-based design. Clustering can then be based on structural reliability instead of (probabilistic) design loads only.
For clustering optimization the following recommendations are made:

- Extend the clustering algorithms for costs optimization.
- Test the local search algorithm for load distributions that feature significant local minima.
- Include load interpolation by formulating the objective function for minimum load difference within clusters. Multi-objective optimization should be implemented to consider EFLs at multiple support structure levels.

REFERENCES

[1] Vorpahl, F., Schwarze, H., Fischer, T., Seidel, M. and Jonkman, J. (2013). Offshore wind turbine environment, loads, simulation, and design. *Wiley Interdisciplinary Reviews: Energy and Environment, 2(5)*, 548-570.

[2] Seidel, M. (2014). Wave induced fatigue loads on monopiles - New approaches for lumping of scatter tables and site specific interpolation of fatigue loads. *Conference Proceedings IWEC 2014*, Hannover, Germany.

[3] Fischer, T., De Vries, W. E. and Schmidt, B. (2010). *Upwind design basis (WP4: offshore foundations and support structures)*. Upwind.

[4] International Electrotechnical Commission (2009). *IEC 61400-3: Design requirements for offshore wind turbines*.

[5] Det Norske Veritas (2010). *DNV-OS-J101: Design of offshore wind turbine structures*.

[6] Kuehn, M. J. (2001). *Dynamics and design optimisation of offshore wind energy conversion systems.* PhD thesis, TU Delft, The Netherlands.

[7] Van der Tempel, J. (2006). *Design of support structures for offshore wind turbines.* PhD thesis, TU Delft, The Netherlands.

[8] Ziegler, L., Voormeeren, S., Schafhirt, S. and Muskulus, M. (in press). Sensitivity of wave fatigue loads on offshore wind turbines under varying site conditions. *Energy Procedia.*

[9] Arany L., Bhattacharya S., Macdonald J. and Hogan S. J. (2014). Simplified critical mudline bending moment spectra of offshore wind turbine support structures, *Wind Energy*. doi: 10.1002/we.1812.

[10] Muskulus, M. (2015). Simplified rotor load models and fatigue damage estimates for offshore wind turbines. *Philosophical Transactions of the Royal Society of London A: Mathematical, Physical and Engineering Sciences, 373(2035)*. doi: 10.1098/rsta.2014.0347.

[11] Zwick, D. and Muskulus, M. (2015). Simplified fatigue load assessment in offshore wind turbine structural analysis. *Wind Energy*. doi: 10.1002/we.1831.

[12] Seidel, M. (2014). Wave induced fatigue loads - Insights from frequency domain calculations. *Stahlbau, 83,* 535-541.

[13] Yeter, B., Garbatov, Y. and Soares, C. G. (2013). Spectral fatigue assessment of an offshore wind turbine structure under wave and wind loading. *Developments in Maritime Transportation and Exploitation of Sea Resources*, 425-433. doi: 10.1201/b15813-52.

[14] Ragan, P. and Manuel, L. (2007). Comparing estimates of wind turbine fatigue loads using time-domain and spectral methods. *Wind engineering, 31(2)*, 83-99.

[15] Manuel, L., Veers, P. S. and Winterstein, S. R. (2001). Parametric models for estimating wind turbine fatigue loads for design. *Journal of solar energy engineering, 123(4)*, 346-355.

[16] Mršnik, M., Slavič, J. and Boltežar, M. (2013). Frequency-domain methods for a vibration-fatigue-life estimation-Application to real data. *International journal of fatigue, 47*, 8-17.

[17] Dirlik, T. (1985). *Application of computers in fatigue analysis.* PhD thesis, University of Warwick, England.

[18] Manenti, S. and Petrini, F. (2010). Dynamic analysis of an offshore wind turbine: wind-waves nonlinear interaction. *Earth and Space*, 2014-2026.

[19] Frandsen, S., Barthelmie, R., Pryor, S., Rathmann, O., Larsen, S., Hjstrup, J. et al. (2006). Analytical modelling of wind speed deficit in large offshore wind farms. *Wind Energy, 9*, 39-53. doi: 10.1002/we.189

[20] Yeter, B., Garbatov, Y. and Guedes Soares, C. (2015). Fatigue reliability assessment of an offshore supporting structure. *The Maritime Technology and Engineering.* Taylor & Francis Group, 671-680.

[21] Veldkamp, H. F. (2006). *Chances in Wind energy: a Probabilistic Approach to Wind Turbine Fatigue Design.* PhD thesis, TU Delft, The Netherlands.

[22] Soares, C. G. (1990). Effect of spectral shape uncertainty in the short term wave-induced ship responses. *Applied Ocean Research, 12(2)*, 54-69.

[23] De Vries, W. E., Vemula, N. K., Passon, P., Fischer, T., Kaufer, D., Matha, D. et al. (2011). *Final report WP 4.2: Support Structure Concepts for Deep Water Sites*, tech. rep., Upwind.

[24] Carswell, W., Arwade, S. R., DeGroot, D. J. and Lackner, M. A. (2014). Soil–structure reliability of offshore wind turbine monopile foundations. *Wind Energy*, 18, 483-498. doi: 10.1002/we.1710.

[25] Wolsey, L. A. and Nemhauser, G. L. (2014). *Integer and combinatorial optimization.* John Wiley & Sons.

Appendix C

Local search optimization

This appendix extends the explanation of the local search algorithm for solving the clustering optimization problem that is introduced in the paper "Design clustering of offshore wind turbines using probabilistic fatigue load estimation" in Appendix B. The local search algorithm is implemented in the software environment R for statistical computing.

Figure C.1 presents the flowchart of the local search algorithm. The algorithm starts with the choice of number of clusters n. Secondly, a random initial guess about the number of turbines T_i in each cluster i is made. According to the initial guess, turbines are sorted to clusters in load descending order. Afterwards, a random cluster-border b_i with $i = \{1...(n-1)\}$is selected. The total design loads TL are calculated for all possible positions of the selected cluster-border, while keeping the remaining borders constant. For the selected border, $(T_i+T_{(i+1)}-1)$ possible positions exist between the two neighboring, constant cluster-borders. Finally, the cluster-border is put on the position with the smallest TL value. The steps from selection of a cluster-boarder to putting it on the local optimum position form one iteration loop. After the local optimum cluster-border position is chosen, this border position is replaced by a random position with a chance of 5% before the start of the next iteration. This avoids that the optimization algorithm is trapped in a local minimum with poor quality. The local search algorithm stops after a defined number of iterations.

For the example case in paper B with 150 turbines, 100 iterations were sufficient for the algorithm to reach the global minimum of the solution space or local minima with good quality. Alternatively, a stopping criteria could be defined, when the solution converges to a local minimum.

An alternative solution approach to the clustering problem based on site-specific EFLs is the application of standard continuous optimization solvers for nonlinear functions, for example "fminsearch" in MATLAB®. For this case, the discrete distribution of fatigue loads has to be approximated by a continuous function through interpolation. The obtained solution must then be rounded to the nearest discrete value. This approach is comparable efficient, in terms of computation time, as the local search algorithm. However, for the example case of 150 turbines, it leads to a local optimum that is less good compared to results obtained with the discrete local search algorithm due to the continuous approximation and rounding.

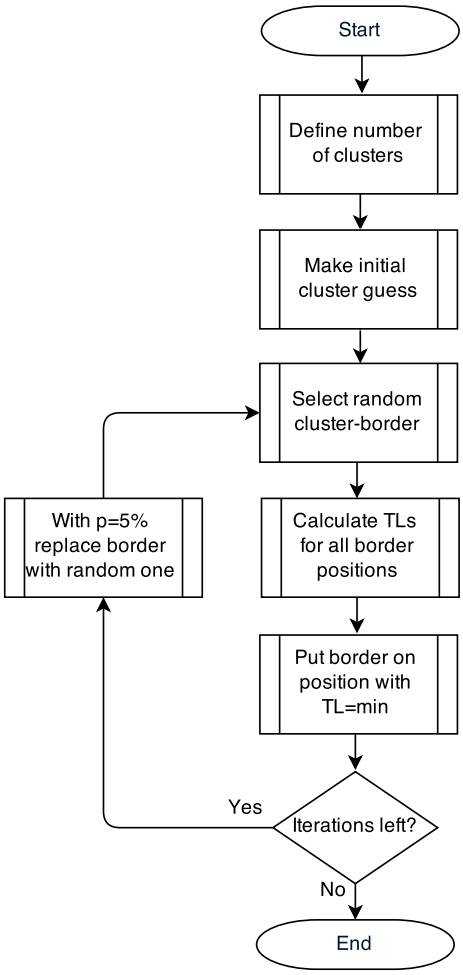

Figure C.1: Flowchart of local search algorithm for clustering optimization.